Direct Observation of Oil Consumption Mechanisms In a Production Spark Ignition Engine Using Fluorenscence Techniques

by

Roderick M. Lusted

B. A., Chemistry; Saint Olaf College, 1977

Submitted to the Departments of
Ocean Engineering and Mechanical Engineering
in Partial Fulfillment of the Requirements for the Degrees of

NAVAL ENGINEER
and
MASTER OF SCIENCE IN MECHANICAL ENGINEERING

at the
Massachusetts Institute of Technology
May 1994

A. A. Sonin, Chairman
Departmental Committee on Graduate Studies
Department of Mechanical Engineering

This Page Intentionally Blank

Direct Observation of Oil Consumption Mechanisms In a

Production Spark Ignition Engine

Using Fluorescence Techniques

by
Roderick M. Lusted

Submitted to the Departments of
Ocean Engineering and Mechanical Engineering
in Partial Fulfillment of the Requirements for the Degrees of

NAVAL ENGINEER

and

MASTER OF SCIENCE IN MECHANICAL ENGINEERING

ABSTRACT

The oil consumption characteristics of a four cylinder, normally aspirated spark-ignition engine were investigated for different piston ring end-gap configurations. A radiotracer was used to perform direct measurement of the oil consumption while Laser-induced Fluorescence (LIF) was used to perform the oil film thickness measurements for consumption predictions using the "Puddle Theory of Oil Consumption," which relates oil consumption to second land film thickness and reverse flow through top ring gap. The consumption data was evaluated to determine the impact of top ring end-gap azimuthal location on oil consumption. The film thickness data was used to evaluate the extent to which the Oil Puddle Theory predicts variations seen in the actual oil consumption.

A tritium radiotracer oil consumption measurement system with an accuracy of 94.6% was designed and constructed. This was used to perform direct measurements of the test engine oil consumption in two different test matrices. The first evaluated a piston ring configuration with the rings free to rotate. The second evaluated configurations with the top ring and second piston rings pinned to fix the azimuthal location of the end-gap; the azimuth of the top ring was varied. In the second test matrix, the oil film thickness on the piston's second land was measured, and predictions were made on the basis of that measurement.

The first test matrix results indicated only a weak speed dependence and a large amount of variability in the oil consumption measurements.

The second test matrix results showed an oil consumption speed dependence that was a function of top gap azimuth. Speed normalized results showed that the oil consumption was larger when the end-gap was on the thrust side of the test engine than when on the anti-thrust side.

3

Measured oil consumption differed substantially from that predicted. This was found to be due to difficulties in determining effective ring gap flow areas **and** due to a previously un-documented azimuthal variation in second land oil film thickness. However, analysis of the results also indicates that the Puddle Theory is still a plausible oil consumption mechanism.

Thesis Supervisor: Dr. Victor W. Wong
Title: Lecturer, Department of Mechanical Engineering

Dedication

This thesis is dedicated to the three people who have paid the highest price for its successful completion: my wife, Patricia, and my two sons, Ethan and Kevin.

To the three of you, thank you for your unwavering love and support.

This Page Intentionally Blank

Acknowledgements

Dr. Victor Wong, my thesis advisor, has provided a special kind of freedom and support in this project. He has accommodated the idiosyncracies of my Navy schedule with understanding and flexibility.

CAPT Alan Brown provided the initial inspiration to begin the project.

Dave Fiedler, of the Dana Corporation, provided inspiration throughout the project with his keen interest and practical advice.

Dr. David Hoult provided shrewd experimental insight at several critical junctures in the project.

Don Fitzgerald and Brian Corkum each provided practical insight and guidance to overcome many of the technical hurdles. Very few projects would ever "get off the ground" in the Sloan Automotive Engine Laboratory without them. If I had spent more time actively seeking their advise, I would have wasted a lot less time.

LCDR Greg Thomas whose personal sacrifice of family time as the Submarine Design Project leader allowed me the flexibility to complete this project.

F. D. Tamai and Tian Tian gave selflessly of their time whenever I need their help; you both proved to be "shipmates" in the finest sense of the word! A special thanks to Tian for patching me up when I did foolish things to myself.

LT R. B. Lawrence, Janice Dearlove, Mike Norris each provided friendship and encouragement in just the right measure to make the lab a fun and exciting place to work.

The U. S. Navy allowed me the "time-off from work" to complete this thesis and the course work that formed the basis for it.

To all of you my most sincere gratitude. I wish you all "fair winds and following seas" in what ever endeavors you put your hands and minds to in the future.

R. Mark Lusted
CDR,   USN
6 May 1994

This Page Intentionally Blank

Table of Contents

List of Abbreviations

a	Absorptivity $(1/[gm*cm])$
A	Area; used to indicate orifice cross-sectional area in general <u>and</u> the area of the effective oil puddle under the top ring gap $(mm)^2$
A_p	Area of the oil puddle $(mm)^2$.
A_{ref}	Reference area in the Shaw Model $(mm)^2$.
A^*	Non-dimensionalized oil puddle radius.
b	optical sample path length (cm).
bmep	Brake Mean Effective Pressure (kPa).
c	Speed of sound (m/s) or sample concentration (gm/liter).
C_d	Coefficient of Drag.
D	Piston to cylinder wall clearance (mm).
DAS	Data Acquisition System
d_2	Diameter of the second land (cm or m).
f	Coefficient of Friction (N/N).
g	Top piston ring end-gap (mm).
h_i	Initial oil film thickness in the oil puddle (mm).
HC	Total Unburned Hydrocarbons; normally measured in ppm C_1.
HCA	Total Hydrocarbon Analyzer
HDD	Heavy Duty Diesels
h^*	Non-dimensionalized Δh.
k	Proportionality constant for surface tension

	(N/[m°K]).
Kpa	kilo-Pascal
LIF	Laser Induced Fluorescence System
l_2	Length of the second land (mm).
LDV	Light Duty Vehicles
LSC	Liquid Scintillation Counter
m	Walther's viscosity correlation negative slope.
mV	milli-Volt
N	Walther's viscosity correlation intercept.
OC	Lubricating Oil Consumption rate; the units vary through out.
OU	DAS output unit (4.88 mV)
P	Used in Section 2.5 to mean luminous power of a fluorescence transmitted light; elsewhere, pressure in kPa.
PMT	Photomultiplier Tube
P_o	Luminous power of a light source.
PCV	Positive Crankcase Ventillation
PM	Exhaust Particulate Matter; normally measured in grams.
Q	Volumetric flow rate of RBB gases through the top ring gap.
R,r	Oil puddle radius: maximum and general respectively.
RBB	Reverse Blowby: The gases traveling through

the top ring gap into the crown land region.

RF	Radio Fluorescence.
ROCS	Radiotracer Oil Consumption System
Shaw Model	Shaw Puddle Theory of Oil Consumption
SI	"Spark Ignition" gasoline engine (as opposed to a diesel or "compression ignition".)
T_a	"Taylor number" = $(\mu * U)/\sigma$
T_1	Temperature of the second land (°K)
T_o	Reference temperature for surface tension (°K)
t_{max}	The time duration between top ring transition from the bottom to the top of the ring groove until peak RBB.
U	Average gas velocity over the oil puddle.
v(r)	Gas velocity over the oil puddle.
WCS	Exhaust Water Collection System (a subsystem of the ROCS)
WOT	Wide Open Throttle
z	Axial piston coordinate measured down from the crown (mm).

GREEK CHARACTERS

Δh	Change in oil film thickness in the oil puddle under the top ring gap due to oil removed by reverse blowby.
η	Compressibility factor for gases.
θ	Azimuthal piston coordinate measured form the

13

	from of the piston (degrees)
λ	Wavelength (nm).
μ	Low shear dynamic viscosity.
μ_a	Dynamic viscosity of air.
ν	Kinematic viscosity (mm^2/sec in Walther's equantion; m^2/sec elsewhere).
ρ	Density (the specific substance for which it is. used varies throughout the thesis.
ρ_o	The density of the lubricating oil at a reference temperature.
σ	Low shear surface tension.
ϕ	Equivalence ratio ($[fuel:air]/[fuel:air]_{stoich}$)

Chapter 1: Introduction and Background

1.1 Motivation

Lubricating oil consumption (OC) in internal combustion engines has historically been of concern from an economic basis; the oil consumed in an hour of operation has to be replaced at some cost and with some impact on engine operating profile. The magnitude of the problem varies from a spark-ignition automobile engine consuming approximately four grams of oil per operating hour (0.43 g/bhp-hr)[1] to large marine diesels consuming approximately three kilograms of oil per operating hour (0.37 g/bhp-hr)[2].

More recently concern has been raised over the part OC plays in engine emissions. Lubricating oil admitted to the combustion chamber contributes to Total Unburned Hydrocarbons (HC) and other gases in engine exhaust streams. In the case of diesel engines, oil consumption has also been found to contribute to exhaust particulate matter (PM).

Unburned Hydrocarbons are composed of a variety of polar and non-polar organic compounds ranging from simple alkanes to substituted cyclo-alkenes and aliphatic ketones.[3] Depending

---

[1]Experimentally determined data for a Chrysler 2.2 liter engine.

[2]**PHONECON** with Hal Furlucci, Caterpiller, Inc. dtd 11 April 1994.

[3]Reference 1, pg. 598.

15

on their reactivity, these compounds contribute to the formation of photochemical smog. Analysis of diesel engine PM indicates that the adsorbed HC contain carcinogenic compounds.[4] Growing public concern over the environment has given rise to legislation that provides aggressive emissions standards for such varied internal combustion engine applications as onroad vehicles (automobiles and trucks) and large ships (both U. S. Navy and civilian) operating within waters contiguous to the United States. Table 1-1 is a partial listing of some of the standards for Light Duty Vehicles (LDV).

Table 1-1: Regulatory Standards for HC and PM[5]			
Exhaust Constituent	CAA Standard 1996	CAA Standard 2003 (Projected)	Typical Emission for Light Duty Vehicle
HC	0.31 grams/mile	0.125 grams/mile	1.3[6] grams/mile
PM	0.10 grams/mile	0.10 grams/mile	0.3 to 1.0[7] grams/mile

For both HC and PM, current LDV emissions must be reduced significantly to meet even 1996 standards. Exhaust catalysis

---

[4]Reference 1, pg. 597.

[5]Section 202, Federal Clean Air Act (CAA)

[6]Based upon **Road Load** calculated for an SI powered economy car using Equation 2.18c from Reference 1, exhaust HC concentration of 750 ppm (low end of the expected band) and stoichiometric operation; 95% catalyst efficiency is assumed.

[7]Reference 1, pg. 626.

provides only a partial solution to the challenge of meeting the current and future HC standards. Typical automotive catalysts operate at a maximum of 95 percent efficiency for oxidation of HC. This indicates that methods must be found to reduce exhaust port HC levels.

Heavy-duty diesel (HDD) standards differ from those applied to LDV's because they are written on a grams per brake horsepower hour basis. Table 1-2[8] shows the PM standards for HDD by model year.

Table 1-2: Regulatory PM Standards for HDD	
Model Year	Standard (g/bhp-hr)
1990	0.60
1991	0.25
1994	0.10
1996*	0.05

* New urban buses only

With the current aggressive standards and the potential for more stringent standards in the future, all potential methods for reducing emissions have to be examined.

As engine designs are refined to allow for more efficient fuel combustion, the relative contribution of oil consumption to total hydrocarbon and particulate emissions becomes increasingly important. Tests conducted by Wentworth on a spark ignition engine in 1982 indicate that approximately 30 percent of total HC concentration in a spark ignition engine

---

[8]Reference 2, pg. 1.

exhaust comes from oil consumption.[9] Current HDD emissions reduction schemes require the reduction of the lubricating oil contribution to exhaust port emissions by 30%.[10] To the extent that lubricating oil plays a part in emissions, it is of benefit to understand the OC mechanisms to allow engine and lubricant designs to include OC in their optimization scheme.

1.2 Mechanisms

Lubricating Oil is consumed by an internal combustion engine via three basic paths:

a. Valve stem leakage (Overhead),

b. Positive Crankcase Vacuum (PCV) flow, and

c. Piston ring leakage.

Table 1-3[11] shows the relative contributions of the three sources; the largest contributor is the latter.

Table 1-3: Relative Contribution OC Paths	
Path	% of Total (Range Reported)
Overhead	15.6 to 55.2
PCV	7.3 to 10.1
Piston Ring Leakage	38.7 to 77.1

Piston ring leakage can be broken down into two broad

---

[9]Reference 3.

[10]Reference 2, Figure 2.

[11]Reference 4.

18

mechanisms:

    a. Flow past the ring face, and

    b. Flow through the ring gap.

The contribution of the first mechanism is relatively minor; Wahiduzzaman et al. estimated that evaporative consumption of oil on the cylinder wall accounted for between two and five percent of total oil consumption[12], and piston oil film thickness studies have shown that the crown land runs consistently dry indicating the inertial introduction of oil into the combustion process is negligible. The dominant mechanism for OC is flow through the compression ring (top ring) end-gap.

    Shaw advanced the "Puddle Theory of Oil Consumption" (Shaw Model) via flow through the end-gap.[13] The Shaw Model states that the oil admitted to the combustion chamber through the top ring end-gap is governed by the velocity of the reverse blow-by (RBB) gases[14] over the "puddle" of oil under the top ring end-gap (the geometry is shown in Figure 1-1), by the depth of the puddle and by the surface tension and viscosity of the oil in that puddle. The peak RBB velocity is governed by the cylinder pressure profile, the piston geometry

---

[12]Reference 5.

[13]Reference 6.

[14]Gases flowing from the second land, through the top ring gap and into the crown land area.

19
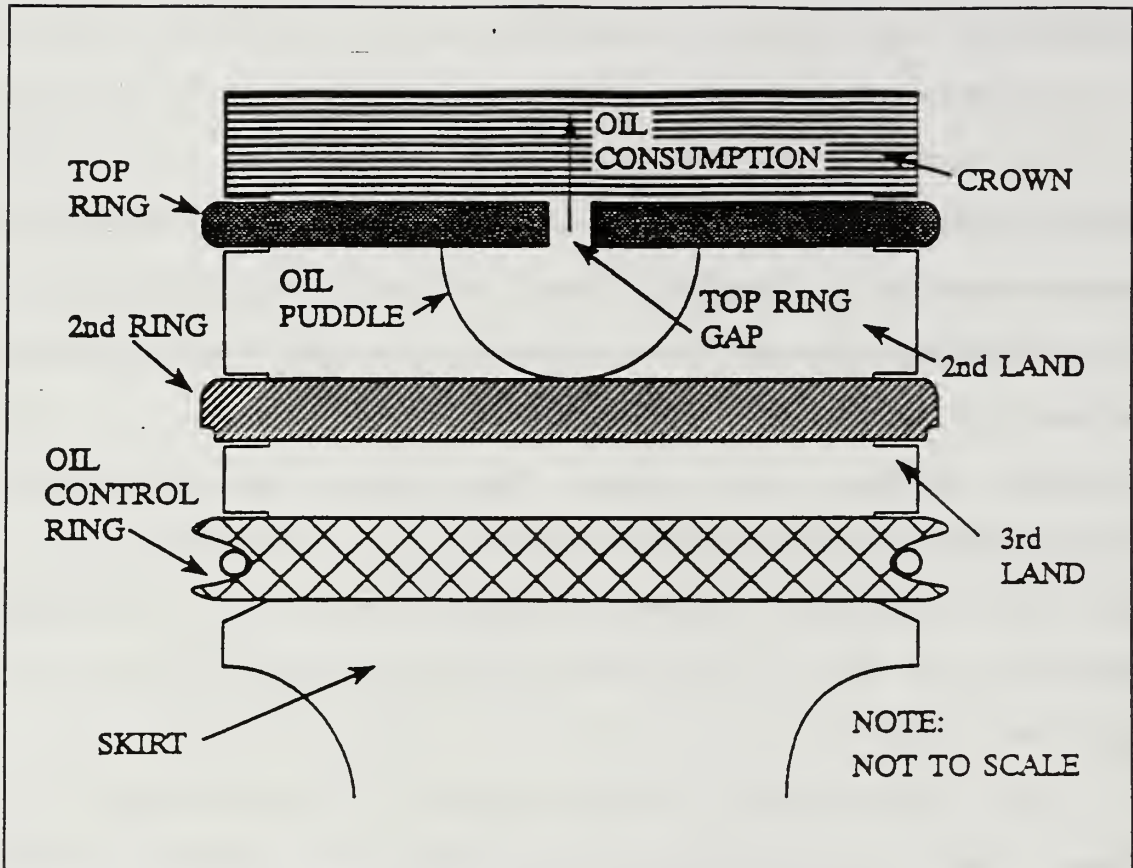
Figure 1-1: Geometry of the Oil Puddle Model

and cylinder geometry.[15]

1.3 Previous Work

In 1990 Hartman investigated oil consumption in a single cylinder Kubota diesel engine with unpinned rings[16]; he found considerable variability in the data. In 1991, Shaw conducted experiments designed to validate the Puddle Theory using direct oil consumption measurements and Laser Induced Fluorescence measurement of oil film thickness on the same

---

[15]Reference 7.

[16]Reference 8.

single cylinder Kubota engine with pinned rings[17]; he was
able to achieve a reduced variability in the data and an 84
percent correlation between experimentally determined and
calculated oil consumption. Figure 1-2[18] shows a comparison
between Hartman's results and those of Shaw.
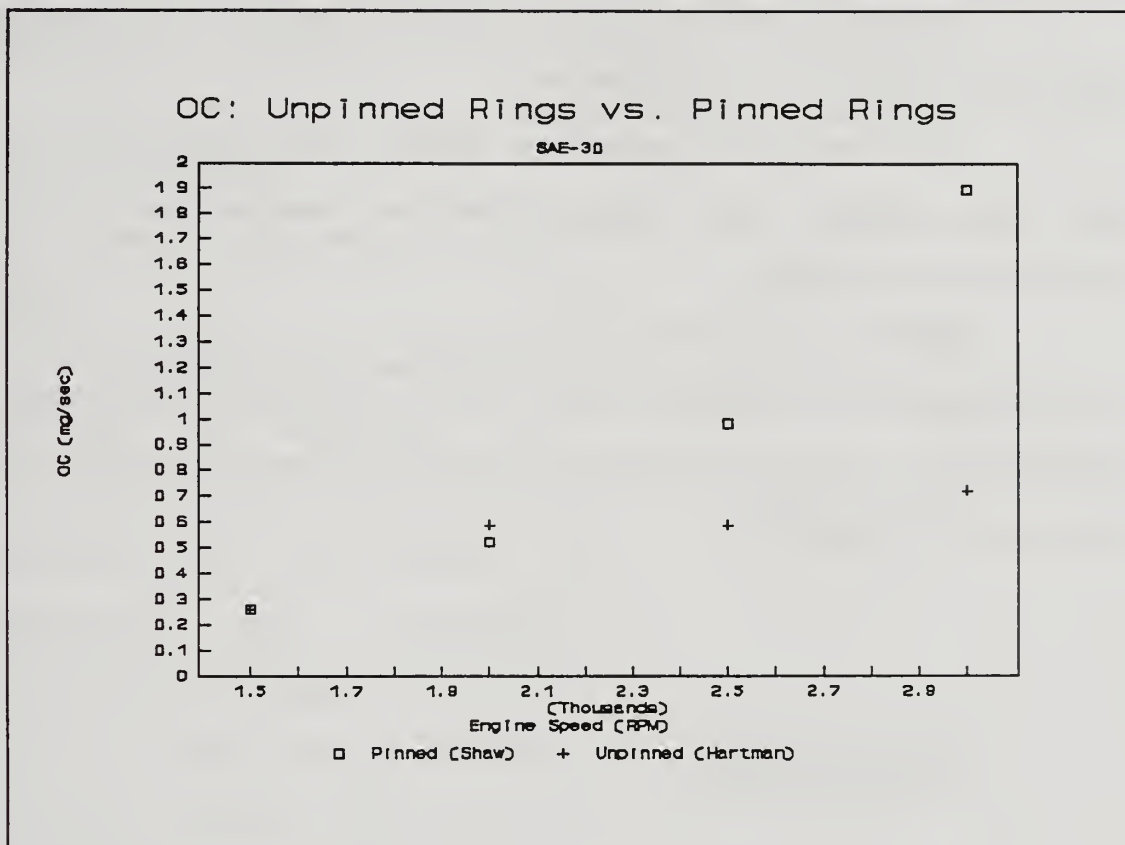
Figure 1-2

Both the Heywood-Namazian model for gas flow and the Shaw
Model initially assume a constant end-gap/second land
geometry. However, factors like bore distortion, ring

---

[17]Reference 9.

[18]Transcription of Figure 4-1, Reference 9.

rotation[19] and piston secondary[20] motion are factors that may cause that geometry to vary cycle-to-cycle and within a cycle.

1.4 Objectives

The objectives of this research are three fold:

a. Establish and validate a reliable method of directly measuring engine oil consumption.

b. Use the above method to observe the effect of top ring gap azimuth on oil consumption mechanisms in a production, SI engine.

c. Combine the results of Objective b with simultaneous LIF measurements to observe the correlation between Shaw Model predictions of OC via ring-gap and actual OC for different top ring gap orientations.

_____

[19]Reference 10.

[20]Reference 11.

Chapter 2: Theory

2.1 General

The theory presented in this chapter covers both the basic mechanisms and measurements involved in this project. Additional theories and hypotheses used in the analysis of the experimental results will be presented in Chapter 5.

The piston coordinate system used in this paper is shown in Figure 2-1.

2.2 Piston Ring End-gap Gas Flow

To predict an engine's OC, it is necessary to calculate the gas velocities in the piston ring region. Namazian and Heywood presented a model for gas flow in the piston ring crevice regions[21] that uses a one-dimensional (z dimension) descriptions of the continuity equation for
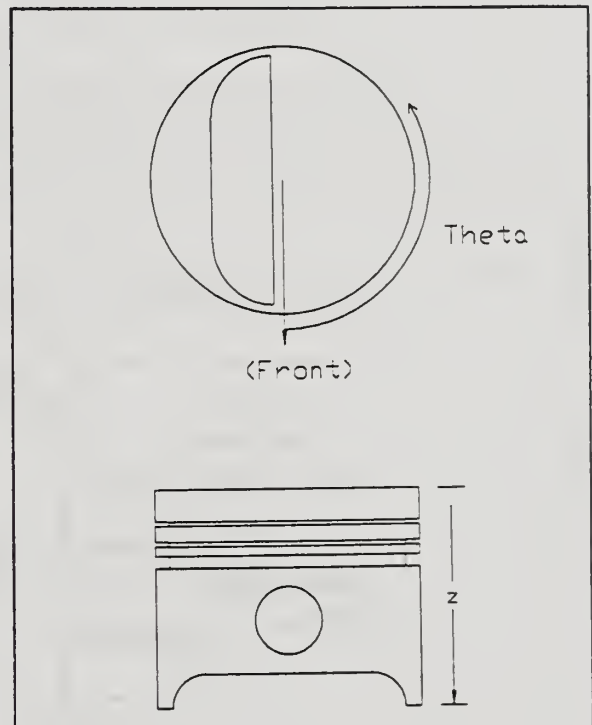
Figure 2-1: Piston Coordinate System

each crevice (Figure 2-2[22]) and the ring motion.

---

[21]Reference 7, pp 10-13.

[22]Reference 7, Figure 15.

23

a. Continuity (assuming isothermal conditions):

$$m_{o_i}(\frac{dP_i/p_{o_i}}{dt}) = \dot{m}_{i-1,i} - \dot{m}_{i,i+1} \qquad (2.1)$$

where: region index, i = 1 to 5 (See Fig. 2-2),

m_{oi} is the initial mass in the ith region and

P_{oi} is the initial pressure in the ith region.
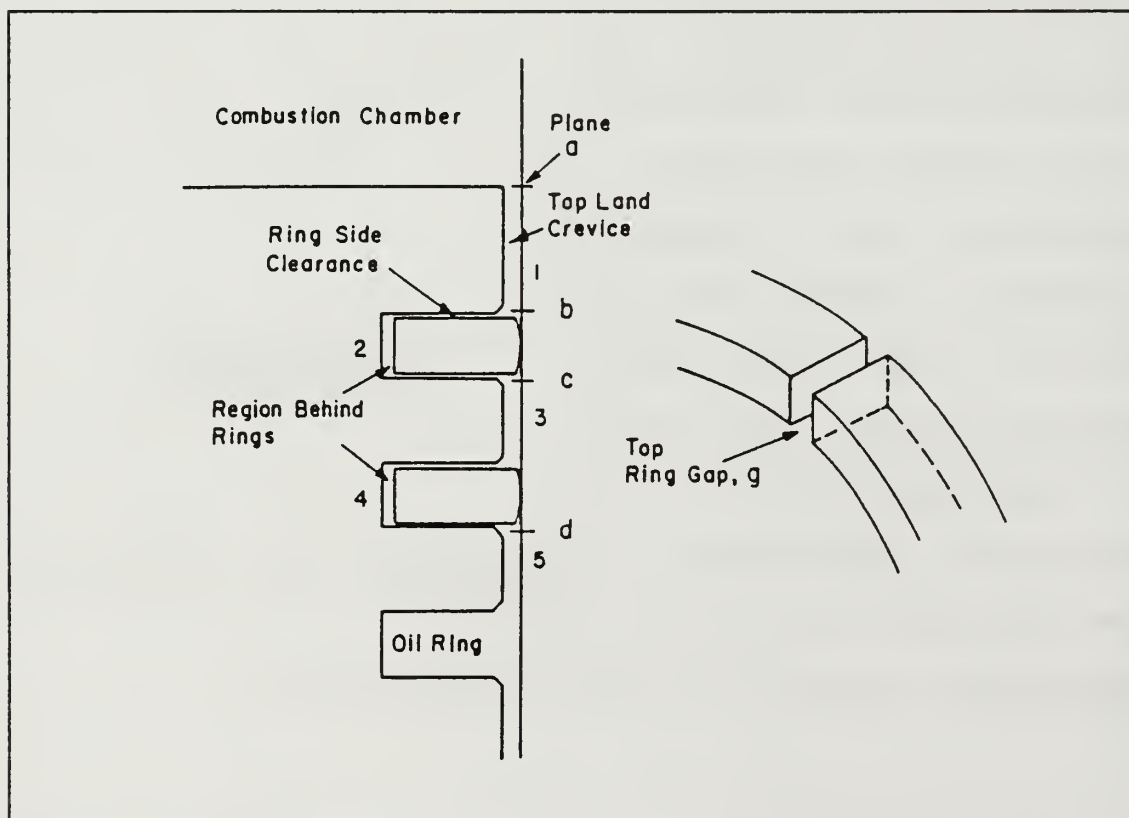
Figure 2-2: Piston Ring Crevice Regions

b. 1-D equation of motion for the ring:

24

$$M_{I}\left(\frac{d^2h}{dt^2}\right) = F_p + F_f + F_1 - F_s \qquad (2.2)$$

where the variables are those shown in Figure 2-3.

Additionally, flow between regions is described as orficial flow and the mass flow rate is given by:

$$\dot{m} = fC_d A \rho c \eta \qquad (2.3)$$

where: fC_d = 0.6

A   is the orfice area

ρ is the gas density

c   is the speed of sound

η is the compressiblity factor of the gas.
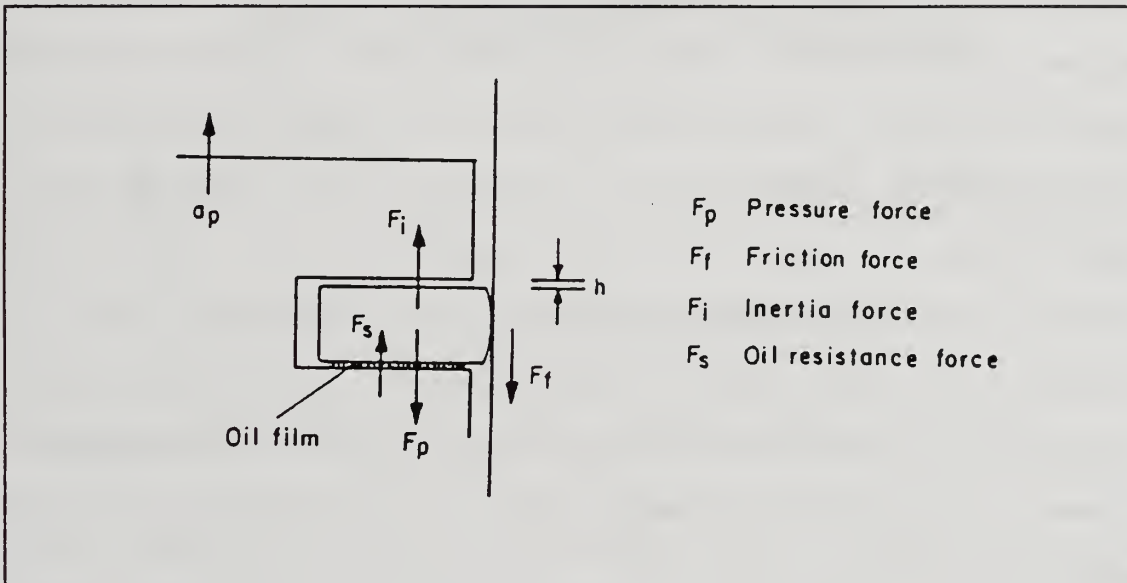
Figure 2-3:   Piston Ring Force Diagram

25

The program GASFLOW[23] uses the Namazian-Heywood model described above with a cylinder pressure profile to iteratively calculate the gas flow rates and ring positions for an input engine geometry. The outputs of the program used to predict OC in this study were the top ring gap volume flowrate for reverse blowby and the top ring axial position profile.

2.3 The Puddle Theory of Oil Consumption

Shaw hypothesized that, during engine operation, it is primarily the lubricating oil which accumulates on the second land immediately under the top ring gap which contributes to oil consumption.[24] This hypothesis is born out in the observations made by Namazian and Heywood in transparent engine experiments[25]. These indicate that a portion of the second land oil film is blown into the crown land region and the combustion chamber by the reverse blowby (RBB) during a short burst or "jet" of high velocity flow. This high velocity flow coincides with the top ring transition from the bottom of the ring groove to the top of the ring groove and is driven by the change in the sign of the pressure differential between the combustion chamber and the second land during the expansion stroke.

---

[23]Copyright (C) by Hoult and Company, September 1990.

[24]Reference 9, Chapter 5.

[25]Reference 7, pg. 11.

26

Geometry

The region of second land oil film effected by the gas flow can be thought of as a semi-circular puddle. The Puddle

Piston Dimensions used in Oil Consumption Model.
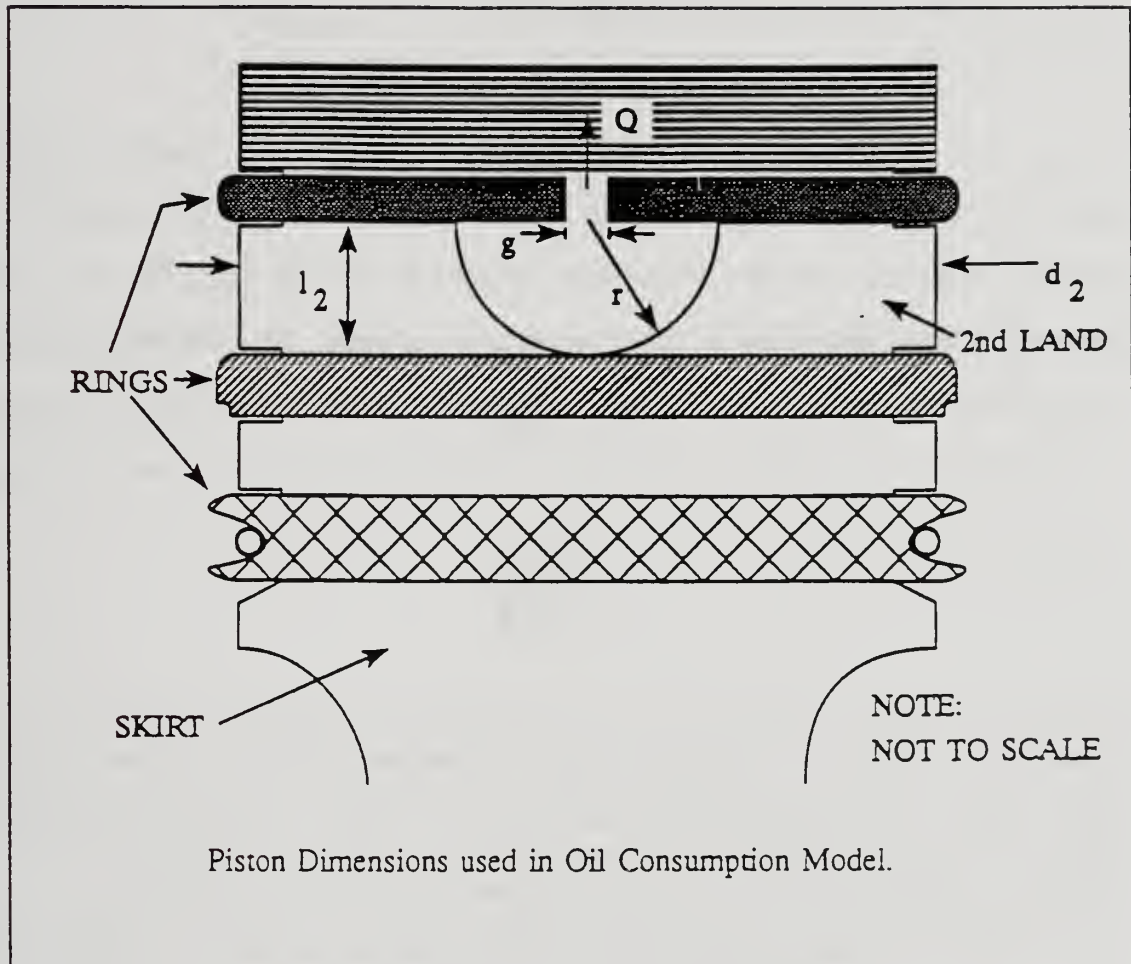
Figure 2-4

Theory geometry is shown in Figure 2-4.[26] Where Q is the volume flow rate of the RBB gases, g is the top ring gap, d_2 is the piston diameter at the second land, l_2 is the length of the second land and r is the puddle radius. Figure 2-4 shows

---

[26]Reference 9, 5-1.

27

the limiting puddle size which is used as the reference area (A_{ref}). The puddle area and reference area are given by equations 2.4 and 2.5.

$$A_p = \frac{\pi r^2}{2} \qquad (2.4)$$

and

$$A_{ref} = \frac{\pi (l_2)^2}{2} \qquad (2.5)$$

The oil transfered in this process is given by the equation:

$$OC = \rho \Delta h A_p \qquad (2.6)$$

or

$$A_p = \frac{OC}{\rho \Delta h} \qquad (2.7)$$

where ρ is the oil density at the temperature of the second land, Δh is the change in the depth of the oil puddle during the oil transfer and A_p is the area of the oil puddle.

Shaw non-dimensionalized the puddle area (A^*) and the change in puddle depth (h^*) as follows[27]:

$$A^* = \frac{A_p}{A_{ref}} = \frac{r^2}{(l_2)^2} = \frac{2OC}{\pi \rho \Delta h l_2^2} \qquad (2.8)$$

---

[27]The definitions for h^* differs between Reference 6 and Reference 9; the definition shown here is that given in Reference 6.

28

and

$$h^* = \frac{\Delta h}{h_i}$$ (2.9)

where: h_i is the second land oil film prior
to top ring transition.

Motive Force

The mass fraction of liquid expelled from a tube with gas
flowing through it was shown by Taylor to be a function of the
viscosity of the liquid, the velocity of the gas and the
surface tension of the liquid[28].   He formed a non-dimensional
quantity which will be called the Taylor number in this paper.

$$T_a = \frac{\mu U}{\sigma}$$ (2.10)

Treating the second land geometry like a tube terminating in
the top and second ring gaps, Shaw used the volume flow rate
of the gas through the top ring gap to determine the average
gas velocity over the oil puddle as follows. The gas velocity
as a function of puddle radius may be expressed:

$$v(r) = \frac{Q}{\pi r D}$$ (2.11)

where: D is the clearance between the
second land and the liner.

The velocity is then radially averaged:

---

[28]Reference 12, pg. 161.

$$\overline{v} = (\frac{1}{R-\frac{g}{2}}) \int_{g/2}^{R} (\frac{Q}{\pi r D}) \, dr \qquad (2.12)$$

or

$$\overline{v} = \frac{Q}{\pi D(R-g/2)} \ln(\frac{R}{g/2}) \qquad (2.13)$$

and

$$U = \overline{v} \qquad (2.14)$$

Non-dimensional Parameters

Shaw showed empirically that A^* and h^* are functions of the Taylor number according to the relationships shown below.[29]

$$A^* = 15.28 (T_a)^{-2/3} \qquad (2.15)$$

and

$$h^* = \frac{1.3 U(t_{max}) T_a^{1/3} (\frac{\mu_a}{\mu})}{4 l_2} + 0.61 \qquad (2.16)$$

where: U is the average gas flow velocity over the puddle,

μ_a is the dynamic viscosity of air,

μ is the dynamic viscosity of

---

[29]Reference 6, pg. 82.

oil,

t_{max} is the time (in seconds) from
top ring transition until
maximum RBB, and

l_2 in the length (z dimension) of
the second land.

Fluid Properties

The physical properties of the lubricating oil used were
obtained from the following empirical relationships:

a. Density (in kg/m³):

$$\rho = \rho_o - 0.63(T_1 - T_o) \qquad (2.17)$$

b. Low shear surface tension (σ) (in N/m):

$$\sigma = k(T_1 - T_o) + \sigma_o \qquad (2.18)$$

where: T_1 is the second land temperature
in degrees K

σ_o is the surface tension at the
reference temperature T_o.

k is the surface tension
proportionality constant that
is lubricant specific.

c. Low shear kinematic viscosity (ν) (in mm²/sec):

$$\log_{10}\log_{10}(\nu + 0.6) = -m\log_{10}(T_1) + N \qquad (2.19)$$

where: m and N are empirically derived
constants supplied by the

31

manufacturer.

d. Low shear dynamic viscosity (μ):

$$\mu = \nu\rho \qquad (2.20)$$

Oil Consumption

Using the above relationships, the oil consumption in grams per hour can be calculated:

$$OC = (0.03)\,RPM\rho\,h_i h^* A_{ref} A^* \qquad (2.21)$$

where: h_i and A_{ref} are in mm and mm^2 respectively, and

ρ is in g/ml.

where initial film thickness and must be input from experimentally determined data.

Inspection of the above scheme for determining the OC reveals that the calculation is not closed-form: the non-dimensional parameters and the Taylor number must be iteratively calculated to achieve an internally consistent solution. In practice, it is beneficial to determine as many of the physical parameters as possible to limit the degrees of freedom involved in the solution.

2.4 Radiotracer Oil Consumption Measurement

In this research, measurement of the actual engine oil consumption is done using a radiotracer technique. In this technique, lubricating oil is doped through a catalytic

32

exchange process where a fraction of the atomic hydrogen in the lubricant sample is exchanged for tritium which is a low energy beta emitter. Lubricant involved in a combustion event in the cylinder is exhausted as water, carbon dioxide, carbon monoxide, unburned/partially burned hydrocarbons and compounds of sulfur in various degrees of oxidation. If all the compounds in the exhaust are subsequently completely oxidized through catalysis or other means, all exhaust stream constituents will be converted to oxides; the consequence of this fully oxidized state is that all the hydrogen and tritium atoms will be included in the exhaust water. The specific activity of the water can be stoichiometricly related by equation 2.22 to the specific activity of the oil to give the fraction of all engine water that comes from the oil.

$$CH_n + (\frac{n}{4})(O_2 + 3.773N_2) \rightarrow CO_2 + (\frac{n}{2})H_2O + (\frac{n}{4})N_2 \qquad (2.22)$$
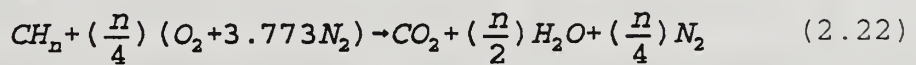
where: n is the Hydrogen to Carbon ration
for the fuel (typically 1.87 for
gasoline)

The only non-organic source of exhaust water vapor is the humidity in the air; this can be compensated for by including the air in the calculation. If the fuel and air flow rates and the specific humidity are known, the oil total consumption rate can then be calculated from the stoichiometry of combustion.

For a spark ignition engine **not** operating at a wide open

33

throttle (WOT) condition, stoichiometric operation (equivalence ratio, ϕ = 1) may be assumed. This assumption was made for this study and the air flow was not measured. If, however, the engine is not operating at a stoichiometric mixture, the air flow or the equivalence ratio must be known. The chemical equation then becomes:

$$CH_n + \frac{1}{\phi} [1 + \frac{n}{4}] (O_2 + 3.773 N_2) \rightarrow CO_2 + \frac{n}{2} H_2O + 3.773 (\frac{4+n}{4\phi}) N_2 \quad (2.23)$$
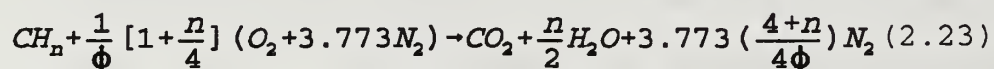
As the equivalence ratio decreases, the specific humidity increases in relative importance. The equations used for OC calculation are detailed by Warrick and Dykehouse.[30] A typical radiotracer OC calculation can be found in Appendix A.

As discussed in Chapter One, soot is a much larger exhaust constituent for diesel engines than for Spark-ignition (SI) engines. Since soot contains a significant fraction of the HC emitted from a diesel engine, it must be taken into account when performing OC measurements on diesels. Since the test engine for this study was a SI engine, it was not necessary to consider soot; however, the measurements and assumptions necessary to account for lubricating oil combustion products adsorbed on the soot particles were

---

[30]Reference 14, Appendix A.

34

discussed by Hartman.[31]

2.5 Fluorescence Measurements

Since this study makes use of both Laser Induced Fluorescence (LIF) and Radio Fluorescence (RF), it is worthwhile to review the fundamentals of fluorescence. Some chemical species absorb excitation energy (light, ionizing radiation, etc.) and dissipate the absorbed energy by emitting

A, Diagram showing isotropic luminescence produced by absorption of radiation from incident beam of power P_0. Radiant power (L) of luminescence is some fraction of the radiant power absorbed $(P_0 - P)$.

B, Changes in energy of a chemical species during absorption (A) and resonance fluorescence (F). Resonance fluorescence is a special luminescence process.
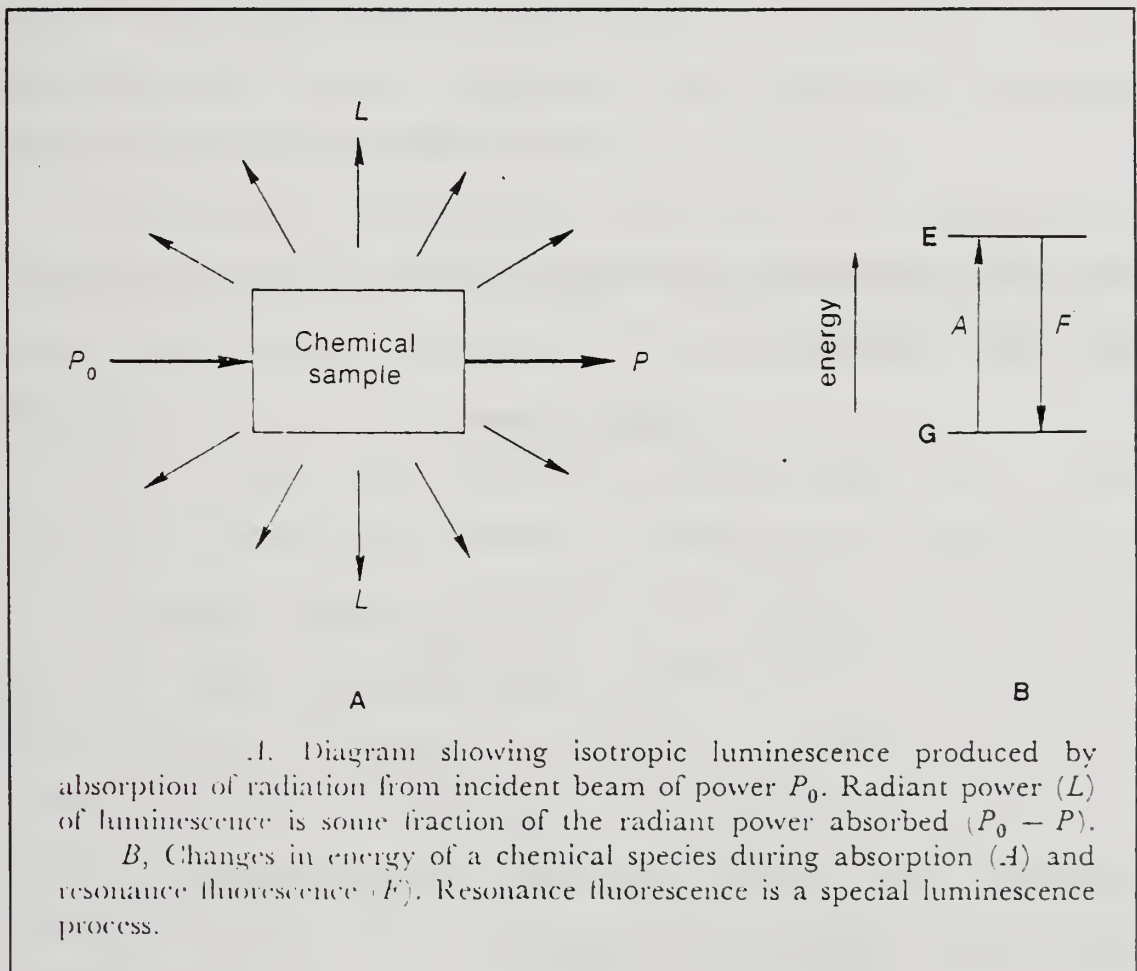
Figure 2-5: Luminescence Process

---

[31]Reference 8, pg. 11.

light.[32]   This property is called luminescence.   Figure 2-5
shows that while the incident and transmitted light are
directional, the emitted light is isotropic; this feature
proves useful in some detector geometries.

The power of the emitted light (L) is given by:

$$L=k(P_o-P) \tag{2.24}$$

where: P_o is the incident light power,

           P is the transmitted light power,

           k is the proportionality constant
                  related   to   the   quantum
                  efficiency for luminescence of
                  the species.

This relationship can be restated substituting the Lambert-
Beer relationship:

$$L=kP_o(1-10^{abc}) \tag{2.25}$$

where: a is absorptivity ($gm^{-1}cm^{-1}$),

           b is sample path length (cm) and

           c is   sample   concentration
                  (gm/liter).

Using the first term of the Taylor series expansion of an
exponential, equation 2.25 becomes:

---

[32]Reference 15, pg. 606.

$$L = 2.3kP_oabc = k'P_oabc \qquad (2.26)$$

where: k' is a proportionality constant modified to include the conversion factor from base 10 to base e.

This provides a linear relationship that can be used over a **limited** range of concentration.[33] The relationship is analytically useful because the emitted light can be measured using a photomultiplier tube (PMT) which generates a current proportional to concentration and/or path length.

Luminescence can be broken down into two categories: fluorescence and phosphorescence. The different electron energy state changes involved in luminescence are shown in Figure 2-6.

On a basic level, the difference between these two is the relaxation process time constant. Fluorescent processes have a time constant between 10^9 and 10^6 sec^{-1} while phosphorescent processes have time constants between 10^6 and 10^{-1} sec^{-1}. Because of the short time constant, fluorescence can be thought of as "real time" which is an advantage, but also can present difficulties. The advantage is that it can be used as an in-line, point measurement technique since the response time is short; it is perfect for real-time data acquisition

---

[33]This demonstrates why fluorimetry must be calibrated close to the path length and concentration measured.

Electronic energy-level diagram for a molecule with ground state (**G**) and excited singlet (**S**) and triplet (**T**) states. Radiationless transitions between states are represented by wavy arrows; *A* is absorption, *F* is fluorescence, *P* is phosphorescence, VR is vibrational relaxation. IX is intersystem crossing, and IC is internal conversion. (See text for discussion.)
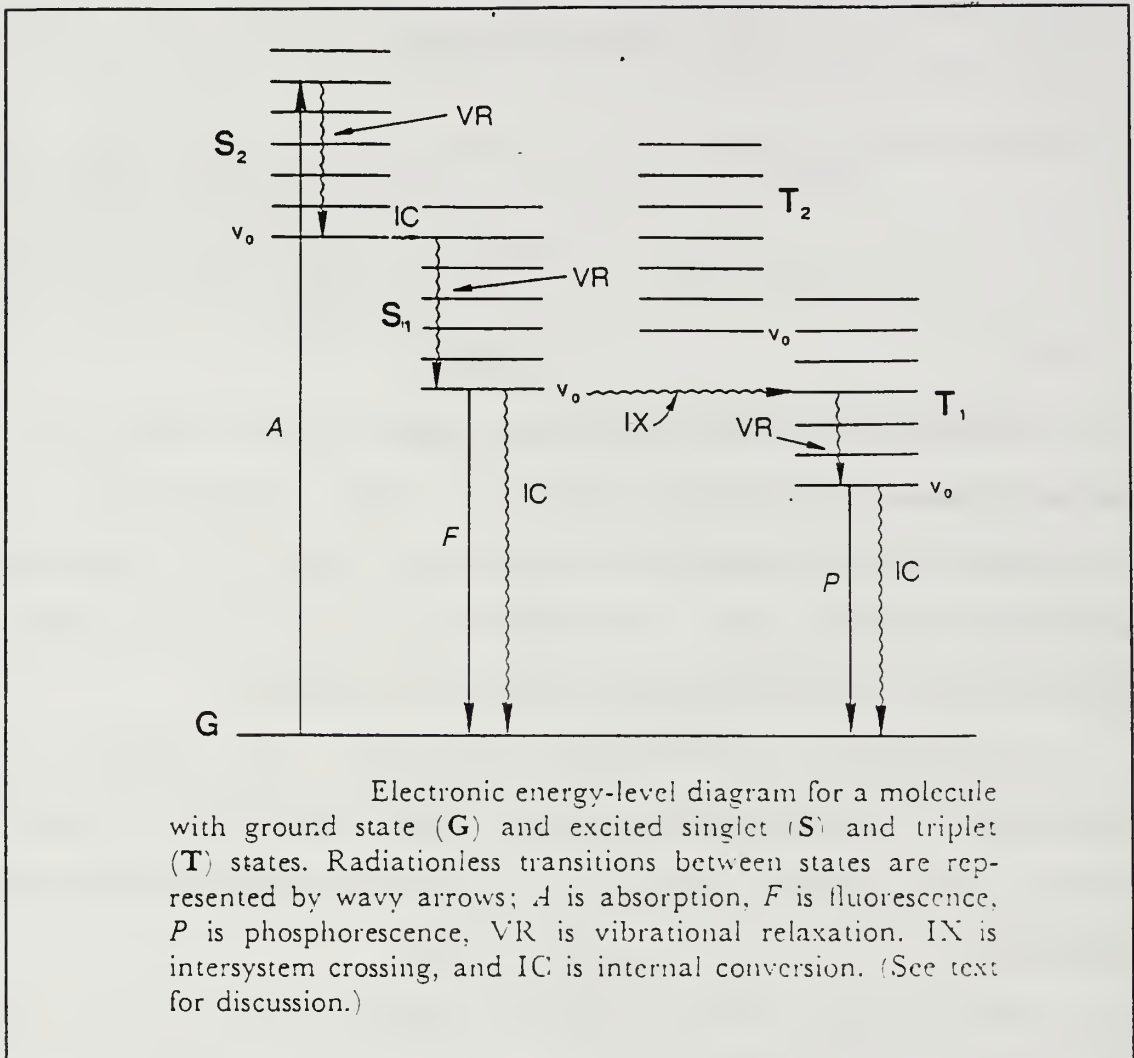
Figure 2-6: Electron Transitions for Luminescent Processes

systems. The difficulties arise in separating the simultaneous fluorescent contributions of varing species and contribution of the incident light to the signal presented to the PMT. An additional complication in both types of luminescence is "quenching." Quenching refers to the self absorption of the luminescent light by the sample itself.

Laser Induced Fluorescence

Laser Induced Fluorescence, as used in this application,
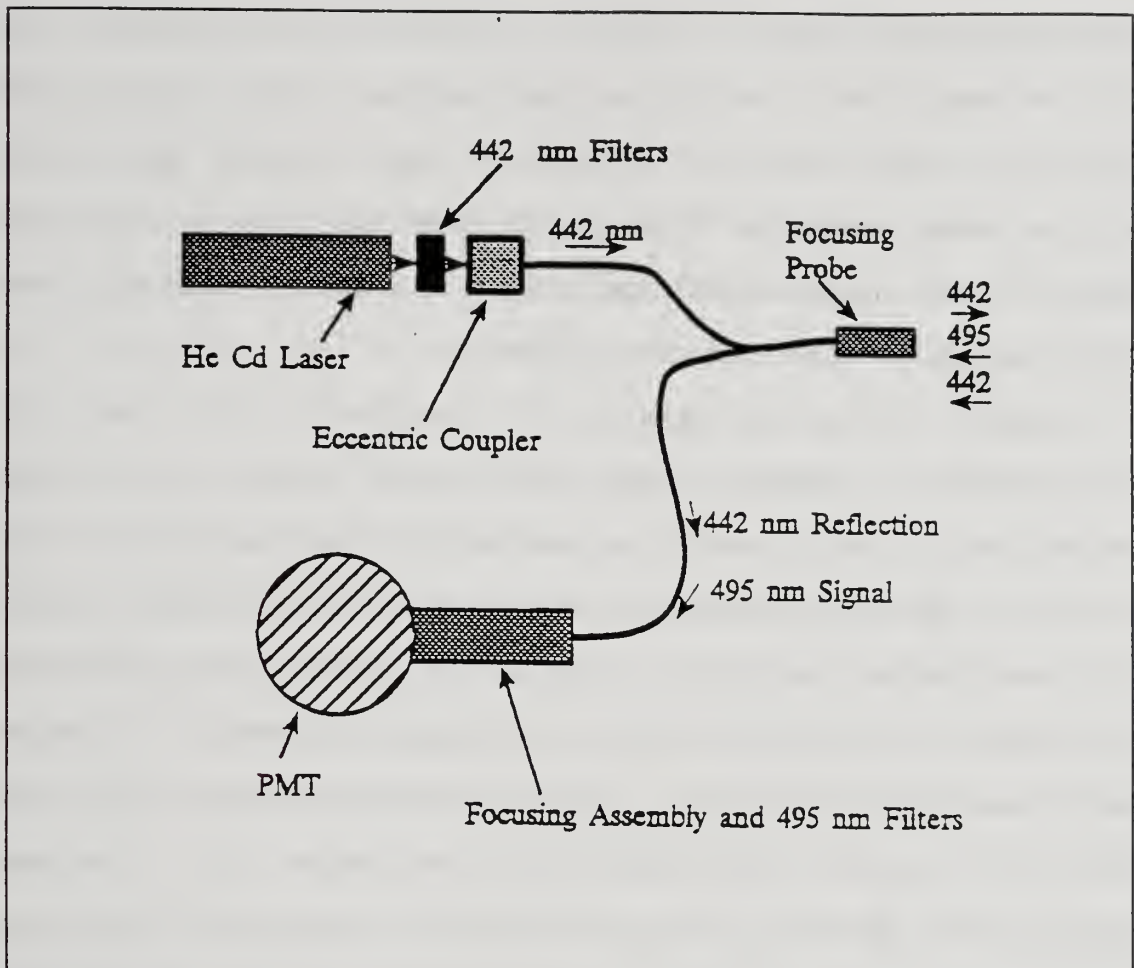
Figure 2-7: LIF Schematic

uses visible light (λ = 442nm) to stimulate a fluorescent dye
at a constant concentration in the lubricating oil to measure
the "sample path length" and thereby determine the oil film
thickness. Shaw gives a detailed description of the
instrumentation involved in this technique[34], and Lee
provides a detailed description of the specific geometry used
in the test engine[35]. Figure 2-7[36] shows schematically the

---

[34]Reference 9, Appendices A and B.

[35]Reference 16, pp 13-23.

LIF sampling geometry. In practice the incident light and the fluorescent light travel the same optical path through the focusing probe; there is a 53nm difference in the wavelength of the laser and the fluorescent spectral peak of the dye which allows bandpass filtration to be used to eliminate the contribution of the incident light.

Other factors impact the accuracy of the LIF technique[37]. Among these are PMT power stability, temperature effects on dye concentration and on quenching, and precision in focussing probe positioning. The impact of all of these factors is that LIF film thickness traces require calibration. LIF calibration uses a salient feature of known measurement on the piston (such as tooling marks or a ring profile) that is observable on the trace. A constant calibration factor is then applied to the entire trace to adjust the feature to the correct dimensional measurement. The calibration features selected for this study were the tooling marks on the piston skirt.

Radio Fluorescence

The Radiotracer method for determining oil consumption relies on the use of radio fluorescence for determining the concentration of tritium in the oil and water samples. The samples are mixed with a solution containing an excess of a compound that fluoresces when subjected to beta radiation.

---

[36]Reference 17, Figure 4.

[37]Reference 18.

The individual fluorescent events (scintillations) are detected in a Liquid Scintillation Counter which reads out in Decays per Minute (dpm). The beta radiation flux (the equivalent of the P_o or incident power) is determined with the species concentration and sample path length (discussed above) held constant. P_o is then used to determine the specific activity[38] of the tritium which is measured in dpm per gram of sample. Correctly determining the amount of quenching is crucial in liquid scintillation counting and each sample must be analyzed for absorption at the measured wavelength. Figure 2-8 shows a typical quench curve for tritium analysis. The parameter "tSIE" is a measure of the transmittance (P/P_o) of the sample and is dependent on the color and clarity of the sample. The counting efficiency is a measure of the percentage of actual scintillations detected by the liquid scintillation counter. The lower the efficiency the poorer the statistical sample of scintillations and the greater the error in sample activity for a given counting time. However, the results achieved from highly quenched samples can be improved by extended counting times. In this study, quenching became a problem in oil samples. If undiluted, the oil samples gave counting efficiencies of approximately **five percent** with the corresponding specific activities varying by

---

[38]The specific activity is a measure of the tritium concentration; however, it is most convenient to work strictly in specific activity units (dpm/gram or μCi/gram) as long as only one radionuclide is involved.

41

as much as ±100%. Oil' sample dilution improved the
reliability of the results without extending the counting
times.
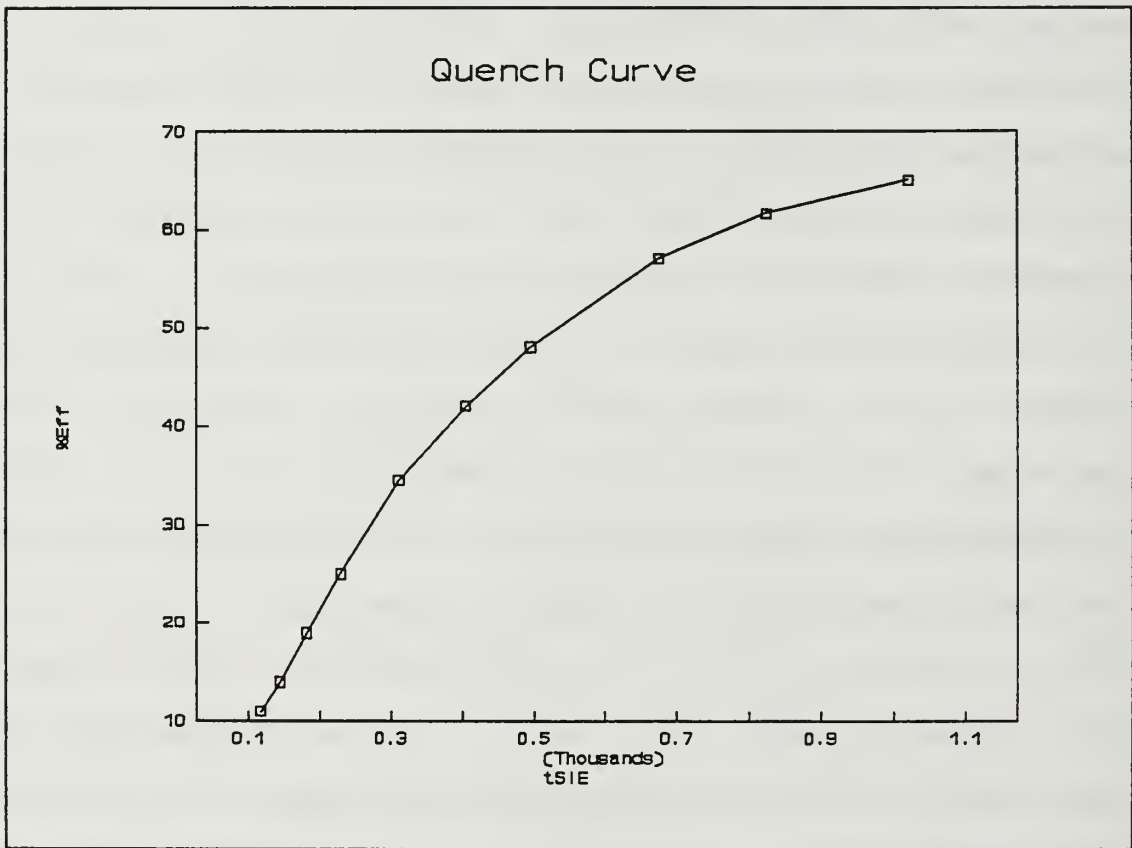
Figure 2-8: Quench Curve

Chapter 3:   Equipment Setup and Instrumentation

3.1 General

This section contains a general description of the engine, Laser Induced Fluorescence (LIF), radiometric and Data Acquisition (DAS) systems. A detailed equipment breakdown is contained in Appendix B.

3.2 Engine Description

The test engine was a production, naturally aspirated Chrysler 2.2 liter, four cylinder engine originally available in the Dodge Daytona. The cylinder head for the engine had been modified to accept piezo-electric pressure transducers for cylinder pressure monitoring. Table 3-1 shows the installed engine instrumentation.

Table 3-1: Engine Instrumentation	
Parameter	Indication
Temperatures	
Coolant into Engine	Type K Thermocouple
Coolant out of Engine	Type K Thermocouple
Oil Sump	Type K Thermocouple
Fuel into Throttle Block	Type K Thermocouple
Intake Air	Type K Thermocouple
Coolant, Cylinder 2	Type K Thermocouple
Liner, Cylinder 4	Type K Thermocouple
Pressures	

Table 3-1: Engine Instrumentation	
Parameter	Indication
Cylinder #4 Pressure	Piezo-electric Transducer w/Charge Amplifier
Intake Manifold	Mercury Manometer
Oil Pump Discharge	Gauge
Fuel Pump Discharge	Gauge
Coolant Head Tank	Gauge
Miscellaneous	
Shaft Position	Optical Encoder
Load	Strain Gauge Load Cell
Speed	Magnetic Pulse

The exhaust system was modified to allow separate exhaust sampling of cylinder number four. The number four cylinder exhaust line was insulated to reduce heat loss prior to the Water Collection System (described below) connection; the insulation caused higher exhaust line temperatures which required the use of welded flexible fittings instead of the pre-existing brass fittings. Test Matrices D and F (Chapter 4) required that the top and second piston ring end-gaps be pinned to restrict gap azimuthal motion to $\pm 1°$; this was accomplished with notched rings and a brass pin inserted **radially** into the piston ring groove. Figures 3-1 and 3-2 show relevant pinning geometries.

The engine was further modified by the installation of a quartz window in the number four cylinder wall at the cylinder coordinates z = 40mm and $\theta = 90°$, referenced respectively from

44

the fire deck of the engine and from the forward wrist-pin axis. Lee provides and an excellent discussion of the window
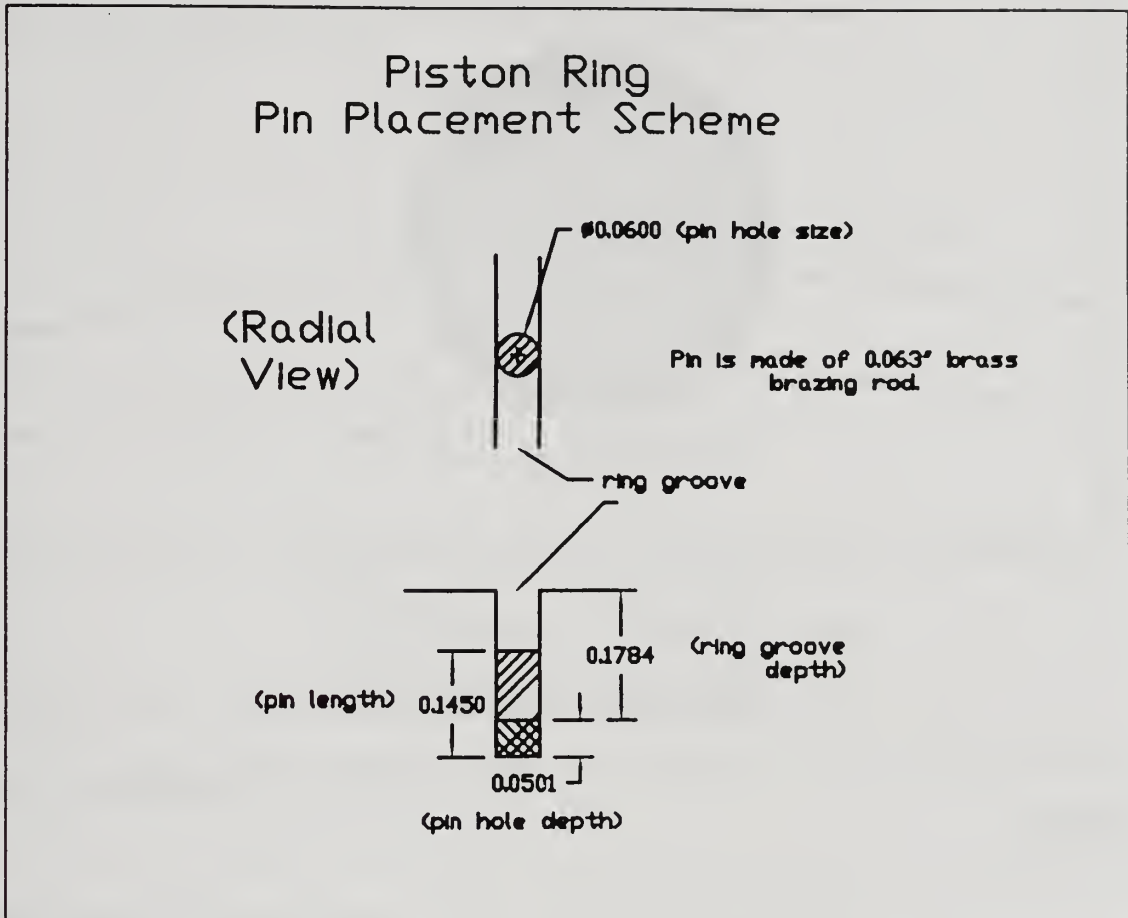
Figure 3-1: Pin Schematic

installation in the test engine[39]. Figures 3-2[40] and 3-3[41] show the window geometry in detail.

3.3 Laser Induced Fluorescence System (LIF)

The LIF system used in this research was the same as that

---

[39]Reference 16, pp 13 - 23.

[40]Reference 16, Figure 2-1.

[41]Reference 16, Figure 2-2.

described by Shaw, Hoult ·and Wong[42]. It consists of two major subsystems:

Ring Notch Scheme
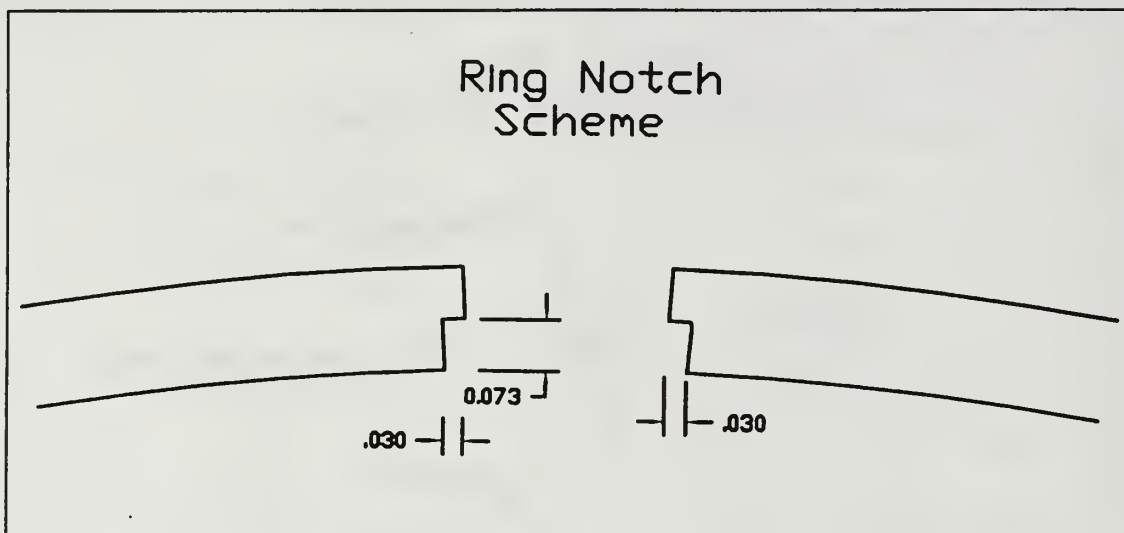
Figure 3-2:   Ring End-gap Notching Scheme

     a. the excitation subsystem and

     b. the fluorescence subsystem.

The dividing point for the two subsystems is the side of the piston.

Excitation Subsystem

The excitation subsystem consists of a He-Cd laser radiating at 442 nm, a fiber optic coupling, and a focusing probe. This subsystem delivers excitation energy to the oil in front of the number four cylinder optical window. A fluorescent dye[43] is dissolved in the oil at a concentration of 0.15 grams per liter. Upon excitation, the dye fluoresces

---

[42]Reference 17.

[43]Coumarin 523 available from the Exciton Chemical Company, Inc.
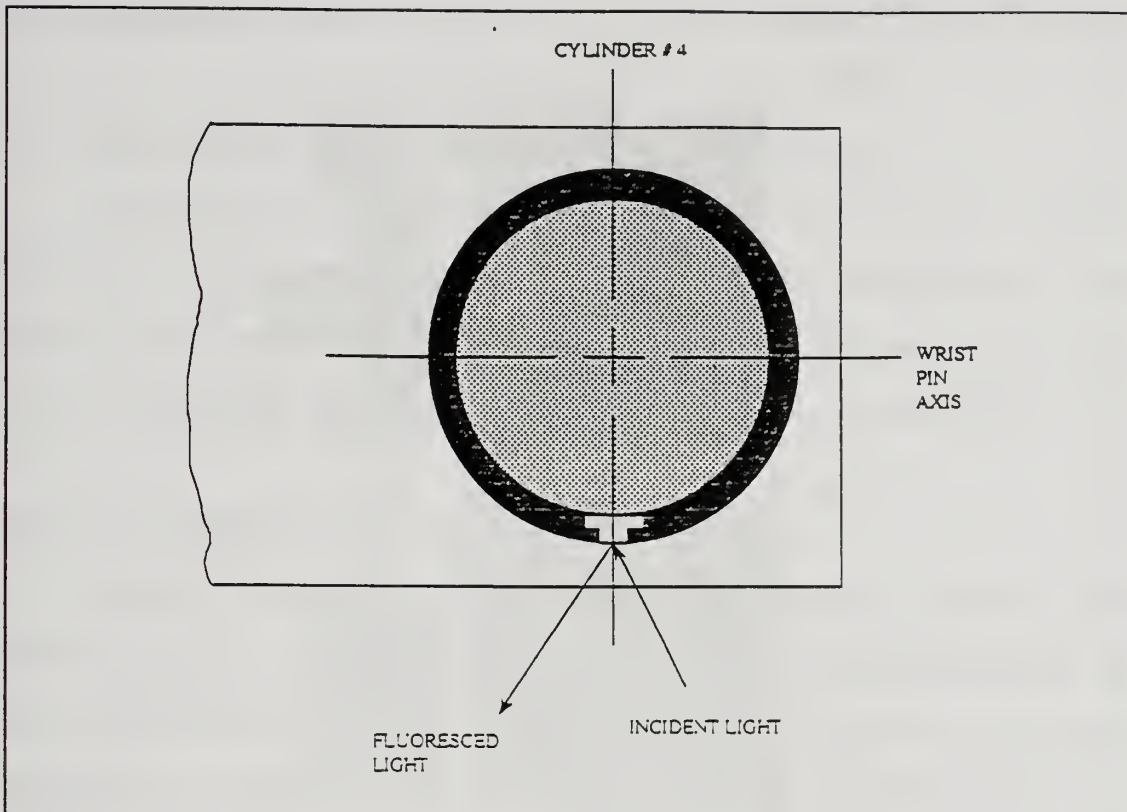
Figure 3-3: Quartz LIF Window (Top View)

at a wavelength of 495 nm.

Fluorescence Subsystem

The fluorescence subsystem consists of the focussing probe (shared with the excitation subsystem), a fiber optic coupling which is coaxial with the excitation fiber optic cable, a high voltage power supply, a focusing/filtration unit, a photomultiplier tube (PMT) and a high gain output amplifier.

The LIF system outputs a voltage proportional to the oil film thickness in front of the optical window. As discussed in section 2.5, the output is also affected by laser strength,

47
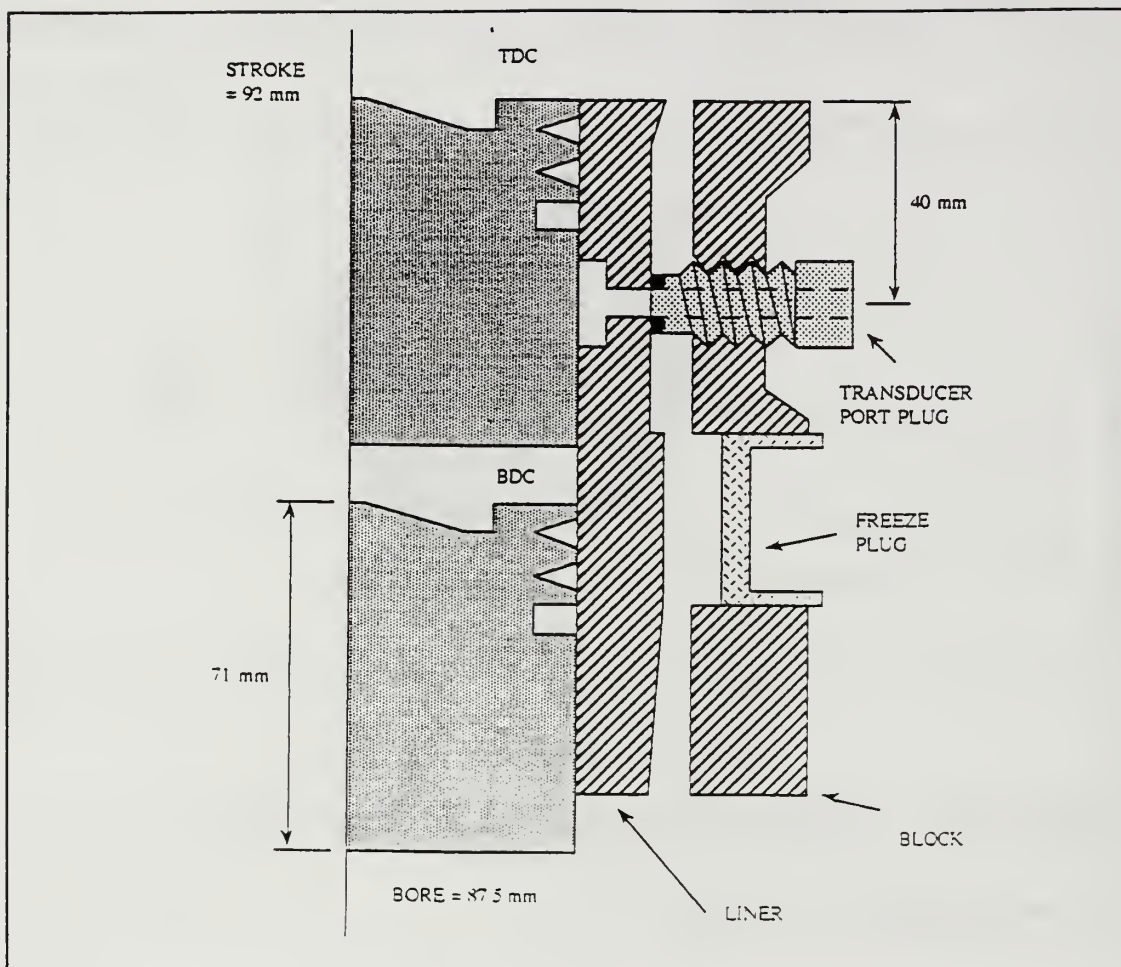
Figure 3-4: Quartz Window Installation (Side View)

focussing probe position, PMT high voltage supply and dye concentration; output trace calibration is required and is discussed in Chapter 5. A schematic of the LIF system was shown in Figure 2-7.

The PMT output is a nano-amp current that requires amplification to be usable. A high gain, low-noise two-stage amplifier with a sensitivity of 0.667 V/μA[44] is used to accomplish the desired output. A low pass filter with a cut-

---

[44]Reference 8, pg. 53.

48

off frequency of 100 kHz is used to reduce the system noise.

3.4 Radiotracer Oil Consumption System (ROCS)

The radiotracer system is a tritium ($^3H_1$) tracer system similar to that reported on by Warrick and Dykehouse[45]. Its major components are the Water Collection System (WCS) and Liquid Scintillation Counter (LSC), and the Tracer Oil.

Water Collection System

The WCS is piped to the number four cylinder exhaust and consists of a quartz glass catalytic oxidation tube mounted in an thermostatically controlled oxidation furnace, a coiled condenser, a sample receiver and an oil-free sample pump. A schematic of the WCS system is shown as Figure 3-5. The piping in the system is either laboratory glass or stainless steel to allow the effective use of heating tape to maintain sample gas temperature. The system requires three stainless steel-to-glass transitions; these are accomplished with graded seals. A beaded catalyst is used instead of a honeycomb catalyst to facilitate installation in the furnace tube.

---

[45]Reference 14.
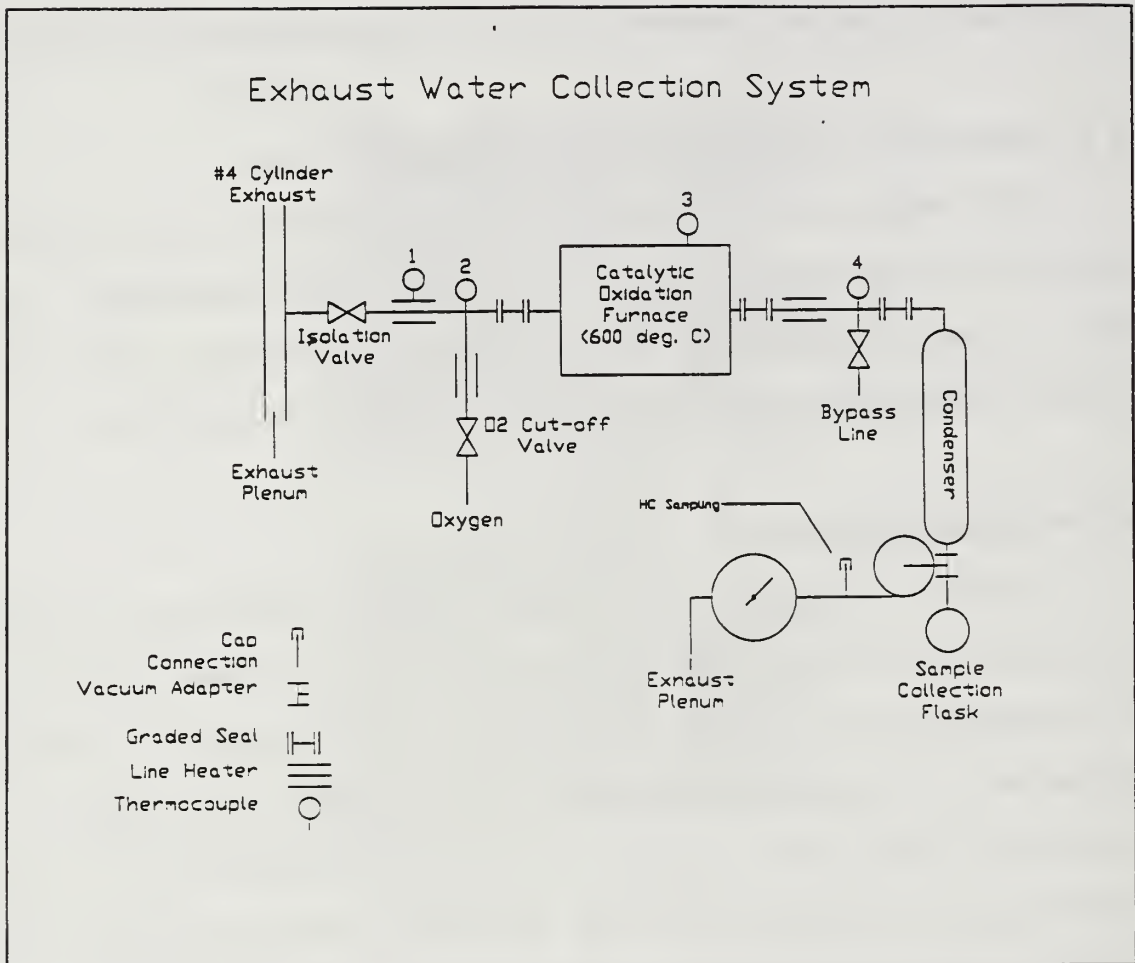
Figure 3-5: WCS Schematic

Thermocouples are installed to monitor gas and heating tape[46]
temperatures; a variac is supplied for line heat control.
Supplemental oxygen is supplied to the system just prior to
the furnace entrance. The oxygen line is heated to reduce

---

[46]The installed heating tapes are "Fibrox" and a temperature
limitation of 482° C. Several heating tapes must be operated close
to the limit to maintain the exhaust gases entering the furnace at
as high a temperature as possible (500°C would be ideal) and
require regular monitoring to prevent burnout. In the future, the
system performance may be improved by replacing the Fibrox tapes
with Samox tapes (760°C limit). This would allow higher operating
temperatures and less monitoring.

50

sample cooling by the oxygen[47]. A purge valve and an isolation valve are supplied to reduce system stabilization times subsequent to changes in operating conditions.

The use of glass in the furnace, condenser and collection flasks allows visual monitoring of gross engine performance[48], catalyst performance and sample line contamination. Appendix B contains photographs of various WCS details.

Liquid Scintillation Counter (LSC)

The LSC system consists of an automatic liquid scintillation analyzer and an analytical balance. The various pieces of volumetric chemistry equipment are discussed in appropriate sampling procedures.

Tracer Oil

The tracer oil used is SAE-30W. Only a small volume of oil is subjected to the catalytic proton exchange process, but resulting tracer oil has an extremely high specific activity. In order to safely handle the tracer oil, it is subjected to two dilutions. The tracer stock is stored by the Radiation Protection Office. The specific activities of the catalysis

---

[47]If sample cooling occurs prior to the oxidation furnace, the catalyst efficiency falls; if the cooling occurs between the oxidation furnace and the condenser, premature condensation can occur contaminating the sample lines and increasing purge times.

[48]Gross problems in engine operation/performance can be detected by periodically observing the point where bulk oxidation (cherry-red glow) is occurring in the catalyst. Experience showed that during proper operation of the test engine, oxidation started 80% of the way down the furnace tube.

sample and the two dilutions are shown in Table 3-3.

Table 3-3: Tracer Oil Specific Activities	
Dilution	Approximate Specific Activity (μCi/gram)
Catalysis Sample	7×10^5
Tracer Stock	700
Operating Oil	2 - 5

3.5 Data Acquisition System (DAS)

An automatic data acquisition system is used to sample the pressure in cylinder number four and LIF system output. The system consists of an IBM 80486 clone with an analogue to digital conversion card. The shaft encoder attached to the forward end of the engine allows 2000 data points to be taken per crank shaft revolution. Data acquisition is clocked by a Top Dead Center (TDC) pulse from the shaft encoder. Each data point consists of sample sets (bursts) of up to four parameters (only the two mentioned above were used in this experiment).

Chapter 4: Experimental Procedures

4.1 General

This section contains a general description of the test matrix and of the experimental and support procedures used in this study that were not extant in sufficient detail elsewhere. The detailed operating procedures and logs may be found in Appendix C. The areas covered by this chapter are:

a. WCS design procedure,

b. test matrices,

c. radiotracer system validation procedures,

d. engine/dynamometer operating procedure,

e. LIF/DAS procedure,

f. piston exchange procedures and

g. radiological safety practices and procedures.

4.2 Water Collection System Design

As discussed in Chapter Three, a Radiotracer Oil Consumption System (ROCS) comprises a Water Collection (WCS) subsystem and a Liquid Scintillation Counter (LSC) subsystem. Sloan Automotive Engine Laboratory has access to an adequate LSC at the Radiation Protection Office (RPO), but construction of a WCS was required. The WCS was constructed on a portable lab bench which allowed relatively rapid configuration changes for system evaluation in much the same way that bread-boarding functions in electronic design.

53

Design Objectives: The basic design for the system is that developed by Warrick and Dykehouse[49]. The specific design objectives imposed by this project are shown in Table 4-1.

Table 4-1: WCS Design Objectives	
Objective	Priority
Provide Sample Precision of 85%	1
Provide a Maximum Sample Period: 9.4 Minutes/Sample[50]	2
Minimize Cost	3

Materials: Design proceeded based upon the assumption that it would be unrealistic to perform an independent verification of the oil consumption measurements obtained from the system. For this reason the material selected for the majority of the WCS was various grades of laboratory glass; this allowed visual detection of sample line contamination. The remainder of the system piping and connections was constructed of stainless steel to allow minimal piping corrosion under typical exhaust gas conditions and to provide maximum heat transfer where that was necessary.

---

[49]Reference 14.

[50]This sample period is based upon achieving 9 samples in a two hour engine operating period (pinned piston ring operating time limit) with a 20 minute engine warm-up period and a total of 15 minutes of stabilization time between engine operating conditions. The implicit assumption of this period is that only steady-state engine conditions (as indicated by temperatures) would be evaluated.

54

Internal Connections: All system internal connections up to the condenser assembly were made with metal-to-metal compression fittings to allow operation at and above 600° Celsius. Since the gas flow path was through three different materials (quartz glass, Pyrex® glass and stainless steel) it was necessary to accommodate differing thermal expansion coefficients with Kovar-to-glass graded seals.

Oxidation: Exhaust gas oxidation was achieved with a single thermostated oxidation furnace with a quartz glass oxidation tube filled with beaded 3-way truck catalyst[51]. Satisfactory oxidation efficiency was achieved when the catalyst and exhaust gases are above 500° Celsius. Due to thermal line losses, 80 to 90 percent of the catalyst bed length was used to reheat the exhaust gas to this temperature reducing the length of catalyst bed available for oxidation; heating tapes were added to the sampling lines and to the supplemental oxygen line to reduce the amount of reheating necessary in the oxidation furnace.

Flow Control: The number of valves in the flow path was

---

[51]The use of this type of catalyst was based upon availability. Beaded catalysts are being phased out in passenger car applications, but are still available in some truck catalytic converters. Use of a beaded catalyst allows creation of catalysis bed in a variety of geometries without specifically designing the catalyst element to each geometry. Put another way, the catalyst could be poured directly into whatever shape tube the oxidation furnace geometry dictated.

minimized to reduce the system head loss. However, it was necessary to provide the following valves for flow control:

    a. a system isolation valve and

    b. a condenser purge valve.

The system isolation valve became necessary because exhaust system pressure pulses moved exhaust gases through the WCS even when the sample pump (WCS pump) and line heaters were turned off creating a high degree of WCS sample line contamination during such operations as oil flushes and WCS system heatup with the engine operating. The condenser purge valve allows purging the tritiated water from the condenser system with ambient air during changes in engine operating conditions reducing WCS system stabilization times at the new condition.[52]

Carry-over Control: Carry-over of liquid from the condenser assembly to WCS pump has the following undesirable consequences:

    a. pump damage,

    b. reduced sample collection rates and

    c. increased pump internal contamination levels.

---

[52]The alternative is to allow the condensers to be "purged" with tritiated water vapor at the specific activity of the new operating condition. The difference between these two methods of purging the condensers (although the analogy is rather rough) can be thought of as the difference between a fluid system "drain and fill procedure" and a "feed and bleed procedure". The air purge provides a much faster and more thorough removal of activated sample water from the condenser heat transfer surfaces.

High gas velocities in the area of the vacuum adapter initially created a carry-over rate of approximately 75% of the condensate. To prevent this, the vacuum adapter throat was extended by 12 cm (Figure B-1) and a water trap added between the vacuum adapter and the WCS pump. Operating experience shows that the throat extension reduces carry-over to zero percent during normal operation. If, however, the level in the sample flask is allowed to reach the tip of the vacuum adapter throat, splashing of the sample water does create a minor carry-over problem well within the capacity of the water trap.

Post WCS Sampling: WCS validation required that a post oxidation furnace total hydrocarbon (HC) sample be taken. The HC analyzer (HCA) used has a low volumetric flow rate pump (HCA pump) which is designed to sample exhaust gas that is supplied at approximately atmospheric pressure. To obtain the WCS sample period required, WCS flow rates are high and the post oxidation furnace pressures are well below atmospheric. The first opportunity in the WCS flow path to effectively withdraw a HC sample is at the WCS pump discharge[53]. To get an accurate HC sample it was necessary to provide the system with an "oil-free" vacuum pump.

---

[53]Sampling at this point introduces a mole fraction error because the water vapor has been taken out of the exhaust gas. However, this effect can be accounted for stoichiometrically.

57

4.3 Test Matrices

The primary objectives of the project, as discussed in Chapter One, were broken down into the following test matrices:

Table 4-2: Objectives and Experimental Groups		
Objective	Test Matrices	Matrix Designation
a. OC Measurement Validation	Condenser Configuration Selection	A
	O_2 Flow rate Optimization	B
b. Direct Observation of the Effect of Ring Gap Azimuth (AZ) on Oil Consumption	Oil Consumption Map (Unpinned Rings)	C
	Radiotracer Measurement Azimuth Variation (Pinned Rings)	D
c. Correlation of Actual and Predicted OC	Hot Ring Gap Measurement	E
	LIF/DAS Measurement of Cylinder Film Thickness and Pressure	F

To reduce experimental set up time, matrix A was conducted concurrently with C, and matrix D was conducted concurrently with F (combined designation: AZ).

Condenser Configuration Selection: The WCS was provided with cooling (circulating) water connections to the condenser

58

assembly to accommodate **two** glass condensers. Test Matrix A
was designed to select the condenser configuration that gave
the highest sample collection rate. The parameters on which
the condenser assembly has an impact are:

   a.   the sample gas flow rate (head loss) and

   b.   the total heat transfer surface.

Three condenser types were evaluated both singly and in
combination:

   a.   coiled,

   b.   Allihn bulb and

   c.   Friedrichs.

Matrix A is shown in Table 3-3:

Table 4-3: Test Matrix A	
Parameter	Value or Condition
Engine Speed	2000 and 3000 rpm
BMEP	345 kPa
Condenser Configurations	
A	Friedrichs
B	Allihn bulb
C	Coiled
D	Friedrichs and Allihn Bulb
E	Friedrichs and Coiled

Each configuration was evaluated on the following points:

   a.   steady-state sample rate (ml/min),

   b.   initial sample response time (min) and

   c.   purge time.

59

Optimum O$_2$ Flow Rate: Typical catalyst HC oxidation efficiency in an automobile exhaust system is about 95%.[54] To improve the efficiency of the catalyst bed of the WCS, supplemental oxygen is introduced to the exhaust gas sample just prior to the oxidation furnace. The supplemental oxygen also has undesirable effects on the sampling process, though. For the purposes of this discussion, the WCS has a constant volume flow rate; any oxygen introduced to the system displaces exhaust gas sample. Furthermore, because of safety and geometry consideration, there is only a certain amount of preheat that can be applied to the oxygen prior to introduction, so it tends to cool the sample thus reducing the efficiency of the catalyst as discussed above. To evaluate the optimum oxygen flow rate, the catalytic efficiency was evaluated using a HC analyzer at several O$_2$ rates. Table 3-4 shows the test matrix used.

Table 4-4: Test Matrix B	
Parameter	Value or Condition
Engine Speed (rpm)	2500
BMEP (kPa)	480
Lubricant Condition	SAE 30W / Untritiated
O$_2$ Flow Rate (cc/min)	0, 40, 80, 120 and 160
Furnace Conditions*	Bypass and Non-bypass

* The two furnace conditions allow measuring the catalyst efficiency.

---

[54]Reference 1, pg. 651.

Test Engine Oil Consumption Map: It was desirable to establish the normal (test stand) oil consumption characteristics of the test engine prior to beginning alterations of the piston ring configurations. In addition, this test matrix provided an opportunity to meet two other operational objectives concurrently:

   a.   to evaluate the radiotracer sampling and measurement processes for systemic errors and effect corrections and

   b.   to allow the engine operators to gain experience with engine and dynamometer parametric response in a broad range of operating conditions.

Table 4-5 shows Test Matrix C:

Table 4-5: Test Matrix C	
Parameter	Value or Condition
Engine Speed (rpm)	1500[55], 2000, 2500, 3000, 3500[56]
BMEP (kPa)	345, 520, 760
Lubricant Condition	SAE 30W / Tritiated
Ring Tensions (N)	
Top	22.24 (diametral)
Second	20.90 (diametral)

---

[55]Operation at this speed was considered unsatisfactory because of large load cell oscillation that could not be filtered out with the loadcell conditioner; this engine speed was subsequently deleted from the test matrix.

[56]The first test point at 3500 rpm (bmep = 400kPa) caused the dynamometer motor-generator set output breaker to trip; the exact cause of the fault was not determined, but the engine operating speed was deleted from the test matrix.

Table 4-5: Test Matrix C	
Parameter	Value or Condition
Oil Control	40.47 (tangential)

Direct Observation of Ring Gap AZ Effect on OC: This test matrix pinned the top and second piston rings in cylinder number four. The second ring was pinned with the gap in the manufacturer's recommended position. The top piston ring was
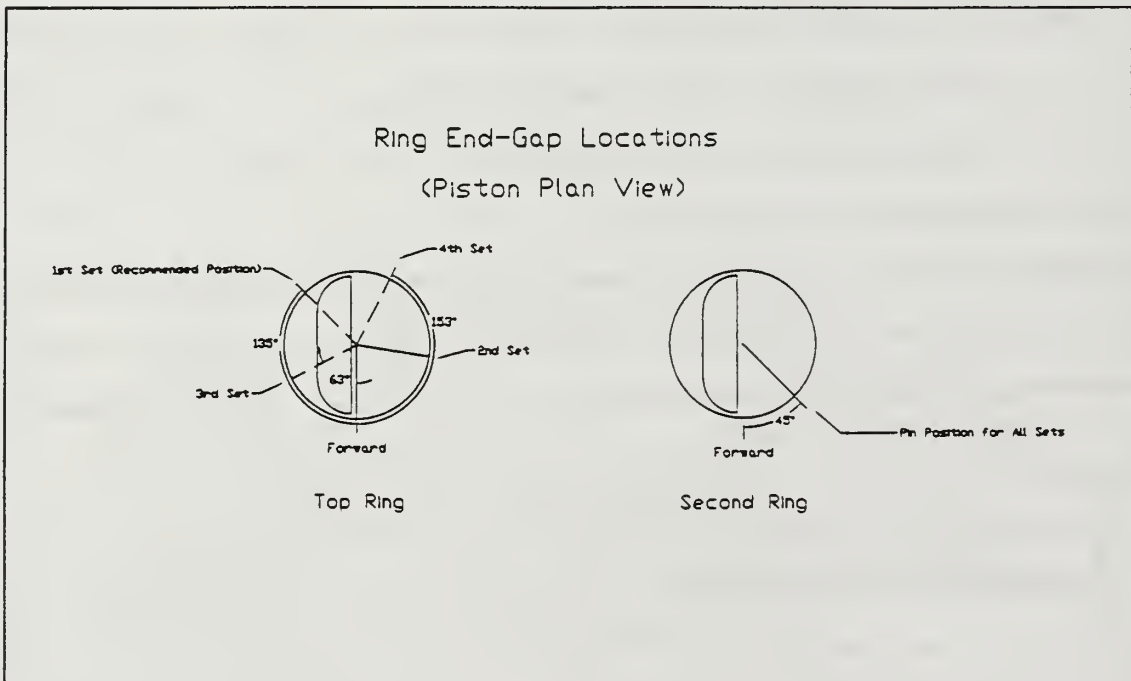
Figure 4-1: Top Ring Gap Locations

pinned with the gap in four different locations. Figure 4-1 shows schematically the location of the cylinder four compression rings in the four configurations used. To reduce piston-change times, four different pistons/connecting rod sets were used, one for each configuration. The **disadvantage**

62

of this approach is the slight variations in piston/connecting rod dimensions that may be introduced.

Table 4-6: Test Matrix D				
Parameter	Value or Condition			
Engine Speed (rpm)	2000, 2500, 3000			
BMEP (kPa)	400 (Not used for control)[57]			
Intake Manifold Vacuum (inches of Hg)	10			
Lubricant Condition	SAE 30w / Tritiated			
Piston Ring Data				
Ring	Gap θ coordinate (degrees)			
Top	225	81	297	153
Second	45	45	45	45
Data Set Designation	AZ1/AZ5 * (Set 1)	AZ2/AZ6 * (Set 2)	AZ3 (Set 3)	AZ4 (Set 4)
Top Ring Tension (N)	26.6 (Diametral)			
Second Ring Tension (N)	29.4 (Diametral)			
Oil Control Ring Tension (N)	77.8 (Tangential)			

 * Due to inadequacies of the first set of data taken, AZ1 and AZ2 had to be repeated.

The initial intent of this matrix was to maintain the same engine hardware as that used in Test Matrix C so that the oil consumption numbers could be compared on a magnitude basis.

---

[57]It was found that it was easier to do one-man testing using manifold vacuum instead load cell readings because of indication stabilization times. Although this might appear a major departure from earlier testing, it was found that BMEP's varied little between speeds for a given manifold vacuum since all the engine operating conditions are below the speed for peak torque.

However, inadvertently piston ring packs with different tensions were used[58] making such a comparison impossible.
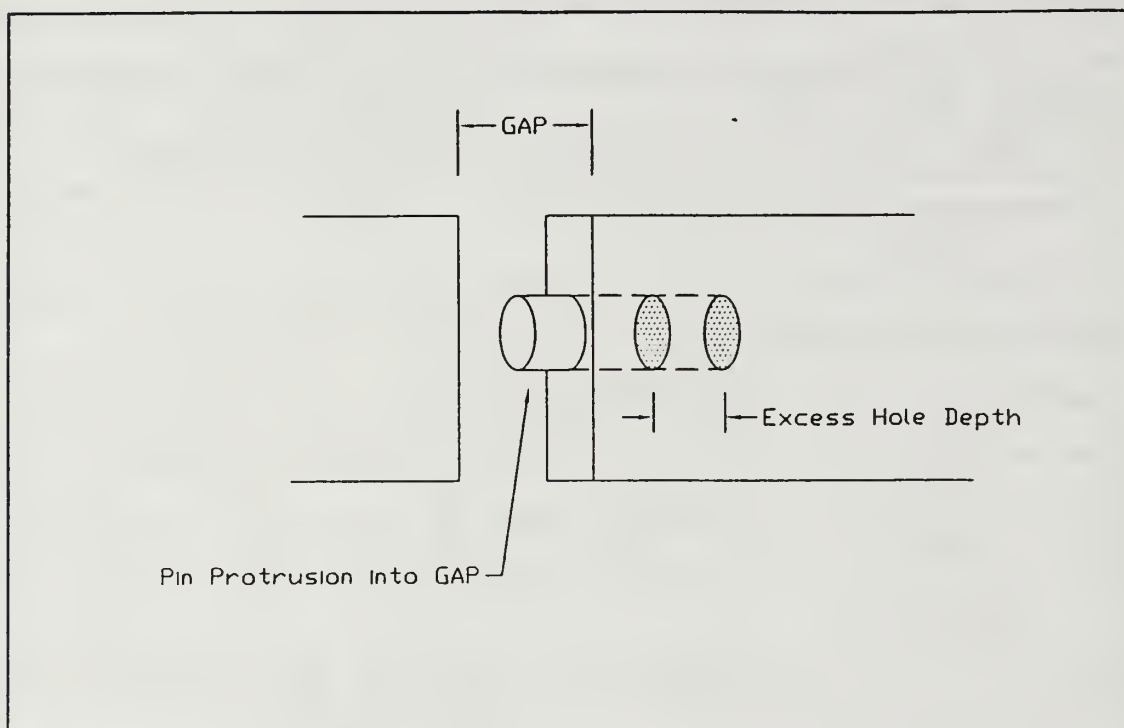
Figure 4-2: Hot Gap Roll-pin Configuration

Hot Ring Gap Measurement: As discussed in Chapter Two, to predict OC using GASFLOW and the Shaw Model, it is necessary to perform iterative calculations to obtain solution closure. Cherry discussed a method for calibrating GASFLOW to a given engine.[59] The method uses adjustments in compression ratio, second land dimensions (thermal effects) and ring gaps to match peak pressure, second land pressure and average blowby

---

[58]It should be noted that each test matrix is internally consistent, so oil consumption magnitudes can be compared within a test matrix.

[59]Reference 19, section 5.4.

to within five percent of measured values. Because of geometric constraints in access to the number four cylinder liner on the test engine, no measurement of second land pressure was possible. To overcome this difficulty, one of the geometric degrees of freedom was constrained by measuring the piston ring gap at operating conditions. This is done by drilling a hole into the end of the ring and inserting a roll-pin into the hole with the pin end protruding into the gap. The hole is deeper than the length of the pin. This allows the pin to be forced into the gap by the other end of the ring as the gap closes due to thermal expansion during engine operation. The geometry of this arrangement is shown in Figure 4-2. The hot ring gap matrix is shown in Table 4-7.

Table 4-7: Test Matrix E	
Parameter	Value or Condition
Engine Speed (rpm)	2500
BMEP (psi)	As necessary to achieve desired liner temperature
Liner Temperature (°C)	108, 115, 124
Lubricant Condition	SAE 30W / Untritiated

Cylinder Oil Film Thickness and Pressure Measurements: The dynamic inputs used by the Shaw Model to predict OC are average second land oil film thickness and cylinder pressure. These are measured for cylinder number four only using the Laser Induced Fluorescence System, the cylinder pressure transducer and Data Acquisition System described in the

previous chapter. The actual test conditions used for this matrix are the same as those for Test Matrix D making simultaneous measurement possible.[60]

4.4 Engine/Dynamometer Operating Procedures: The test engine and dynamometer were operated manually according to the test procedures included as Enclosures 1 and 2 to Appendix C. The safety procedures used were in accordance with applicable Sloan Automotive Engine Laboratory safety instructions. Where simultaneous radiotracer and DAS data was collected two operators were used.

4.5 Radiotracer Method Validation Procedures: Since no external standard could be used to independently measure the oil consumption of the test engine and thereby providing explicit validation of the Radiotracer Oil Consumption System (ROCS), it was necessary to validate the ROCS implicitly by showing that the system efficiently oxidized all hydrogenated compounds to water and by analyzing the system for other sources of error. This procedure used Test Matrix B (described above) and measured the HC in the WCS pump discharge. Concern that the laboratory's only HCA not become

---

[60]Initial matrix planning did not call for LIF data to be taken for in the ring gap azimuth matrices. However, preliminary results from ring configurations AZ1 and AZ2 indicated that film thickness measurements would be required. The LIF system was subsequently hooked up to the test engine and AZ1 and AZ2 configurations repeated under the designations of AZ5 and AZ6 respectively.

66

radioactively contaminated, required that the validation be completed prior to putting tritiated oil in the test engine.[61]

4.6 LIF/Data Collection System: The operating procedure for the LIF system is described in adequate detail by Deutch[62] and Lee[63].

4.7 Piston Replacement Procedures: This project required multiple piston replacements; most of the replacements were done on radiologically contaminated components. Each replacement procedure was carried out according to the test engine maintenance manual. To allow greater speed in completing the replacements, and to prevent errors a detailed procedure/check-off list was used. This procedure is included in Appendix C as Enclosure 3.

4.8 Radiotracer Oil Consumption Measurement Procedures: The procedures for determining oil consumption rates using the ROCS are included in Appendix C as Enclosures 4, 5, 6, and 7. It is important to note that volumetric measures are not used

---

[61]Revalidation may be performed in the future, but should only be accomplished after the engine oil system has been flushed adequately to produce exhaust water samples that fall below the RPO's limit for free release. If revalidation is accomplished, it is recommended that the operation of the catalyst be checked concurrently and fresh catalyst added as needed.

[62]Reference 20, section 2.4.

[63]Reference 16, pg. 24.

for quantities under 50 ml.. This is particularly critical in performing specific activity measurements on the tracer oil since the oil is viscous and provides poor volumetric measurement. The large volume dilutions used are specifically designed to allow solvation of the oil in a non-viscous, non-polar solvent in volumes that allow reasonably accurate volumetric measures to be made.

All water and oil samples have to be prepared for counting in the LSC by mixing approximately 1 ml of each sample with 10 ml of a fluorescing solution. Experience has shown that even the use of a micro-pipet introduces as much as four percent error; therefore, it recommended that LSC sample size be determined exclusively by gravimetric measurements done on an analytical balance.

4.9 Radiological Safety: Tritium ($^3H_1$) is a radioactive isotope of hydrogen with a 12.6 year half-life. It emits a low energy (18.6 keV) beta particle that poses a health threat only when inhaled, ingested or absorbed into the body. It is an ideal tracer isotope for organic compounds because it freely exchanges with $^1H_1$ in normal chemical equilibria and the difference between the isotopes is transparent to chemical processes. The normal equilibrium exchange of hydrogen isotopes can be accelerated through the use of catalysis to produce highly concentrated tracer liquids and gases. Although this project used such a tracer, it was in the form

68

of a viscous, non-polar liquid, that provided little potential
for absorption if handled with the appropriate precautions.
Of greater concern is the tritiated water exhausted by the
engine. Water vapor is readily absorbed through the skin and
lungs and therefore poses a much greater potential for
personnel internal contamination. To minimize the risk of
personnel contamination, the following radiological
precautions were taken:

Table 4-8: Radiological Precautions[1]	
Personnel Training	2 hour course given by RPO
Wipe Survey of Test Cell	Weekly
Personnel Urine Sample	Monthly
Protective Clothing	**During Operation**: Latex Gloves **During Maintenance**: Coveralls and Latex Gloves
Surface Decontamination	Spot decontamination based upon wipe surveys
Engine Internal Decontamination	Pre-maintenance flush procedure
Waste Disposal	Retained in test cell radwaste storage area for RPO pickup.

Prior to the initial introduction of tritium into the test
cell, the RPO evaluated the flow rate through the exhaust
trench as providing adequate dispersal of the tritiated
exhaust water based upon estimated oil consumption and
ventilation flow rates.

Chapter 5: Results and Discussion of Results

5.1 General

This chapter presents the results of the radiotracer measurement of oil consumption and the Laser Induced Fluorescence (LIF) and pressure data acquired during Test Matrix AZ (Test Matrices D and F combined). In addition, the LIF and pressure data are used to predict oil consumption using the Shaw Model; the oil consumption predicted by the model are compared to the radiotracer results. A preliminary discussion of data reduction is included to provide a background for the interpretation of the results included at the end of the chapter.

5.2 Radiotracer Oil Consumption System Evaluation

The details of the Radiotracer Oil Consumption System (ROCS) testing and evaluation are contained in Appendix D. Table 5-1 summarizes the performance evaluation of the system. The ROCS met all the design goals and was considered satisfactory for the continuation of the test matrices.

Table 5-1: ROCS Performance Evaluation		
Criteria	Goal	Actual
Sample Period (min)	9.4	7.7
Error (%)	15	5.4

5.3 Data Reduction

The data reduction can be divided into two major categories:

    a. oil consumption measurements, and

    b. Data Acquisition System (DAS) output.

The DAS output can be further broken down into cylinder pressure data and oil film thickness data.

Oil Consumption Measurements: The methodology used for computation of test engine oil consumption is discussed at length by Warrick and Dykehouse[64]. A detailed example of the calculation is included in Appendix A; this calculation corresponds to Sample 1 of the data reduction spreadsheet included as Appendix E. All the raw data used in the calculations has been transcribed into Appendix E. An archival copy of the original logs has been given to the supervisor of this thesis.

Data Acquisition System Output: The Data Acquisition System output files contain discretized cylinder pressure and film thickness signals in ASCII format. The DAS reads and digitizes voltages by allowing 4096 bits (2^{12}) for the range selected. The range used in this project was ± 10 volts; the size of a DAS output unit (OU) is therefore:

---

[64]Reference 14.

$$OU = \frac{20,000mV}{2^{12}} = 4.88mV \qquad (6.1)$$

The DAS samples data over a multi-cycle period (10 cycles in this case); this allows the creation of **intermediate files** containing either multi-cycle **averaged** data or single-cycle **raw** data. The multi-cycle data reduces random noise in the resulting pressure and LIF traces. The single-cycle data avoids the loss of resolution resulting from cycle averaging and can be used for the calibration of LIF traces. The intermediate files are created using DATAVG, an executable data averaging code written by Shaw.

After the creation of the intermediate files, the pressure and oil film thickness data are processed differently to provide data files that can be used in GASFLOW and the Shaw Model. All computer routines used in the following discussion were written by the author in BASIC. The text of these routines is included as Appendix F; the actual routines themselves can be found on the thesis data disc under the directory labeled "Basic".

Cylinder Pressure Data: The signal sent from the pressure transducer charge amplifier is a voltage proportional to the cylinder pressure. The calibration constant for the <u>entire</u>[65]

---

[65]It is critical that the pressure transducer, transducer lead and charge amplifier be used as a complete set after calibration is conducted. Substitution of a new component invalidates the calibration.

72

pressure signal path is determined by using a hydrostatic pressure calibration device as excitation and a high-input impedance voltmeter to read the charge amplifier output. Table 5-2 shows the specific calibration constants.

Table 5-2: Pressure Transducer Calibration Constants	
Units	Constant
psi/mV	0.14646
kPa/Mv	1.009854
bar/V	9.9718

All the output files in this project use the units of kilo-Pascals (kPa). The pressure profiles generated for GASFLOW supply pressure data at two crank angle degree increments. The pressure signal conditioning is done by the routine titled PRESSURE.

Because cylinder pressure is the driving force behind oil consumption in the Shaw Model, the raw pressure data was analyzed for the cycle-to-cycle variation in peak pressure magnitude. This analysis was performed using a simple maxima detector in the routine PRESPEAK.

Oil Film Thickness Data: The signal sent from the photomultiplier tube of the LIF system to the DAS is a voltage proportional to the volume[66] of the oil illuminated by the

---

[66]With a constant illumination beam geometry, this volume is proportional to film thickness as discussed in Chapter 2.

focusing probe.   For the reasons discussed in Chapter 2, it is not possible to determine a fixed calibration constant for the conversion of DAS output units to film thickness; instead, it necessary to conduct a calibration evaluation of each series[67] of LIF traces.

Film Thickness Calibration: The primary method of calibration was conducted by matching a piston skirt profile to portions of that profile observable in the LIF trace. The calibration constant for a given set of traces is the factor that must be applied to the LIF trace to match the amplitude of the skirt trace. For this project, the skirt profiles were measured on a Dektak 8000 surface profile measuring system. The linear resolution of this system far exceeds the requirements of this project (360 data points per millimeter) so it was possible to sample the raw profile data at the same linear spacing as the DAS output file[68] (a maximum resolution of about 72 data points per millimeter).   Theoretically, the portion of the piston skirt directly in front of the optical window (z=40) when the piston passes through top center should have given the best linear resolution because of the low

---

[67]A series of LIF data is considered to be all the data taken for a given piston ring configuration. As a practical matter, a calibration can be considered good for all data taken between the time the LIF system is completely warmed up (as indicated by a stable laser output power) and when the system is powered down. Ensuring that the focusing probe is tightened sufficiently in its mount to prevent a shift in focus is <u>critical</u>.

[68]The linear (z dimension) spacing of individual data points in the DAS output file is a cosine function since the data are obtained at a constant crank angle spacing.

piston speed. In practice, the portion of the LIF profile immediately under the oil control ring (z = 27 mm) provided the best features for profile matching because the piston is fully flooded with oil at that point and because this tends to be the lowest wear part of the skirt.

In the set of data designated AZ3 the LIF system was not properly focused.[69] .

Typical LIF Trace (Compression and Power Strokes)
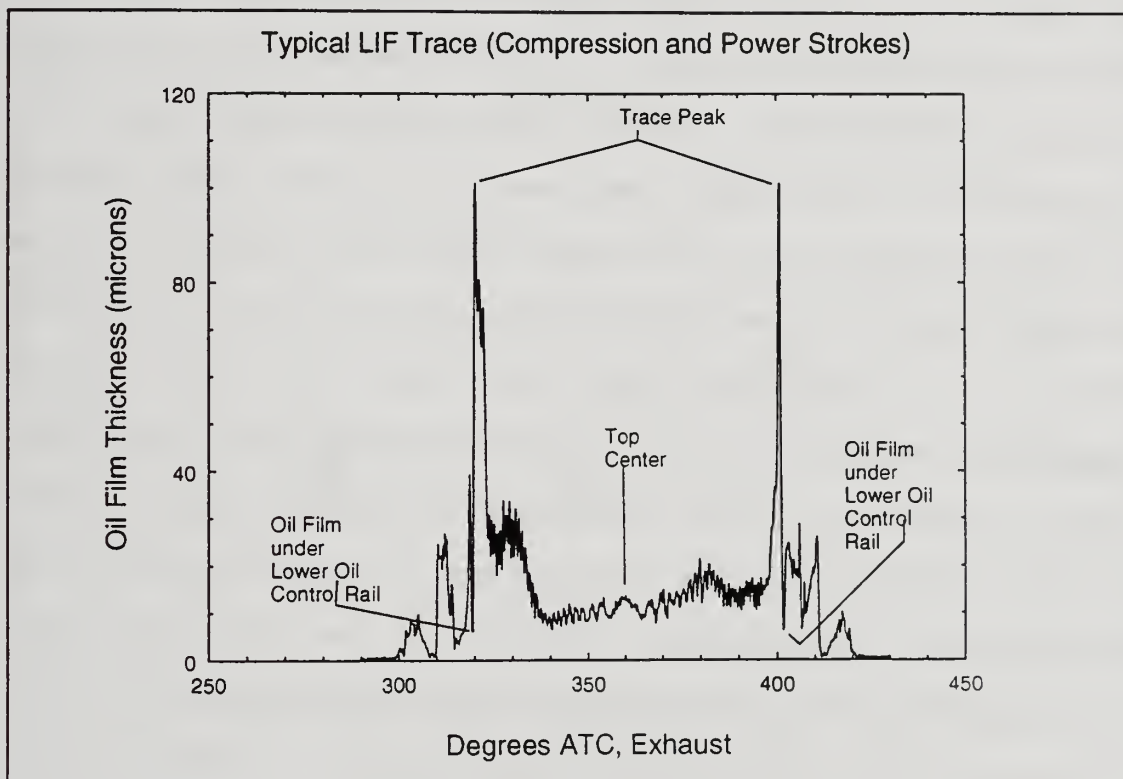
Figure 5-1: Typical LIF Trace

The result was a low resolution trace that provided

---

[69]Proper focusing consists of adjusting the focusing probe's location in its threaded mounting hole to achieve the maximum PMT output voltage for a motoring engine. It was discovered after the completion of AZ3 that this had not been done properly. Time limitations on pinned ring operation (2 hrs per set of rings) had already been exceeded on the AZ3 rings so no further tests were possible; it was hoped that normal calibration would correct the problem.

insufficient skirt features for accurate profile matching calibration. An alternative method was used for the calibration of AZ3 traces. Figure 5-1 shows a typical LIF trace for ±60° of Top Center (TC) of the power stroke. Several salient features are visible in each trace; two features were of special interest in finding an alternative means of trace calibration. The first was the oil film under the lower oil control rail; the second was the trace peak under the oil control ring. It was observed on the three properly focused data series (AZ4, AZ5 and AZ6) that the calibrated oil film under the lower oil control rail was of the same thickness for data sets that were obtained at the same speed (the load was held constant for all sets in the AZ Matrix). It was also noted that the trace peak was of roughly the same size in all the traces performed at the same speed. Since the only difference in the traces was the azimuthal location of the top ring gap, the above observation made physical sense also. Therefore, the AZ3 series was calibrated by matching the oil film thickness under the lower oil control rail for the data sets taken at 2000 rpm; the trace peak size was used as a second check on the validity of the method.

The combined surface profile and LIF trace files used for calibration were created with a routine called PROMATCH; the calibrated traces used for further analysis were created with the routine called LIF.

5.4 Test Matrix C (Unpinned Rings) Results

Test Matrix C was conducted with <u>unpinned</u> piston rings in all cylinders. It resulted in an oil consumption map for the test engine. Figure 5-2 is a scatter plot of the Matrix C data taken at a bmep of 345 kPa. The most noteworthy feature of this graph is the large amount of scatter at 2000 rpm. The
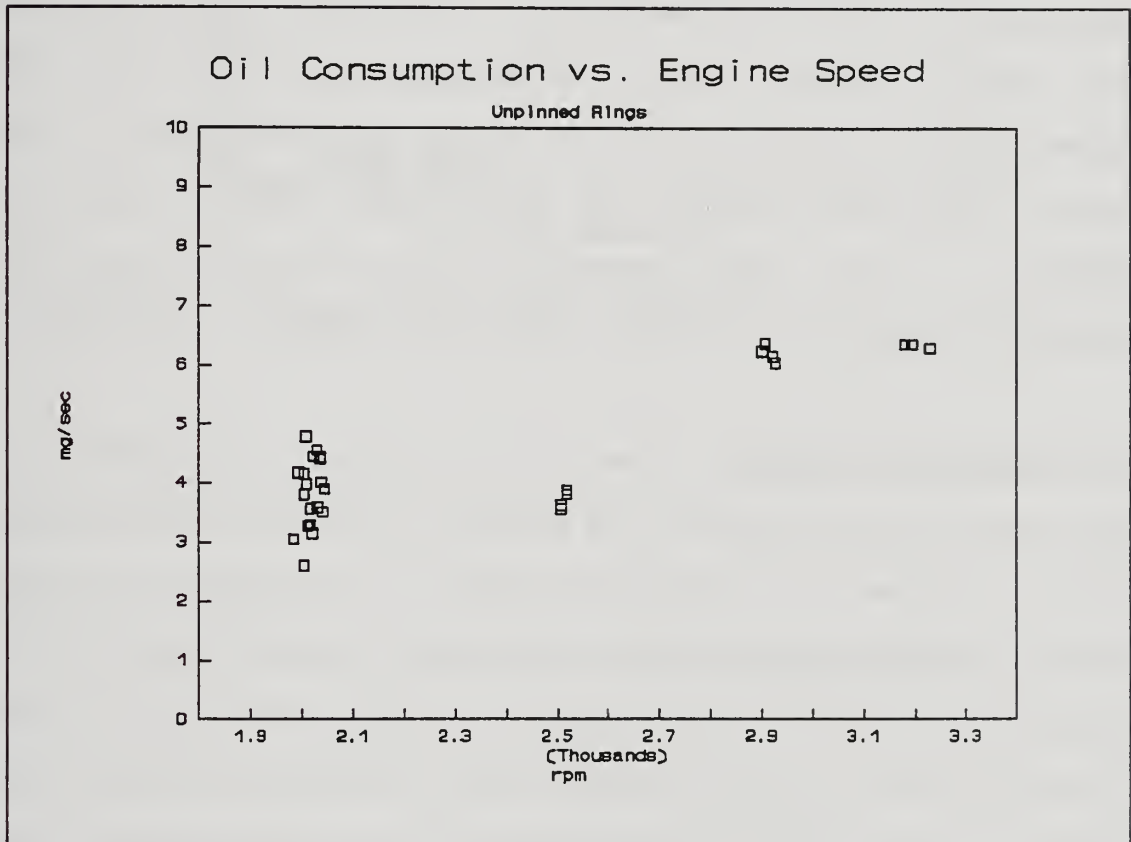
Figure 5-2: Matrix C Scatter Plot (bmep = 50 psi)

increased number of data points at 2000 rpm was the result of an effort to determine if the scatter was due to experimental error; review of the procedures indicates that the data is accurate.

77

5.5 Test Matrix AZ (Azimuthally[70] Pinned Rings) Results

Test Matrix AZ measured oil consumption, oil film thickness and pressure simultaneously. The matrix was originally designed without the use of LIF and with only the first four series planned. However, prior to conducting AZ3, the results of AZ1 became available and indicated that AZ1 and AZ2 should be rerun with LIF installed. Therefore, AZ1 and AZ2 lack oil film thickness data; but the ring configurations were rerun with LIF under the designation of AZ5 and AZ6 respectively. The raw DAS data files are contained on the thesis data disk under the directories titled AZ1DATA, AZ2DATA, ... etc. The intermediate data files are contained under the directories titled 1DATOUT, 2DATOUT, ... etc.[71]

Oil Consumption Results: The oil consumption measurements in Test Matrix AZ were taken with strict accounting of the sample times. Figures 5-3 through 5-8 show oil consumption plotted against _median sample time_ referenced to engine start time; engine speed for each datapoint is indicated above the point. In most cases the first sample after changing engine speed appears to be a _transition sample_ with an oil consumption rate between the values of the two operating conditions.

---

[70]Referenced to the front of the engine and measured counter-clockwise around the circumference.

[71]The data locations are listed here so that should questions arise as to the validity of a given analysis, the data is available for re-analysis.
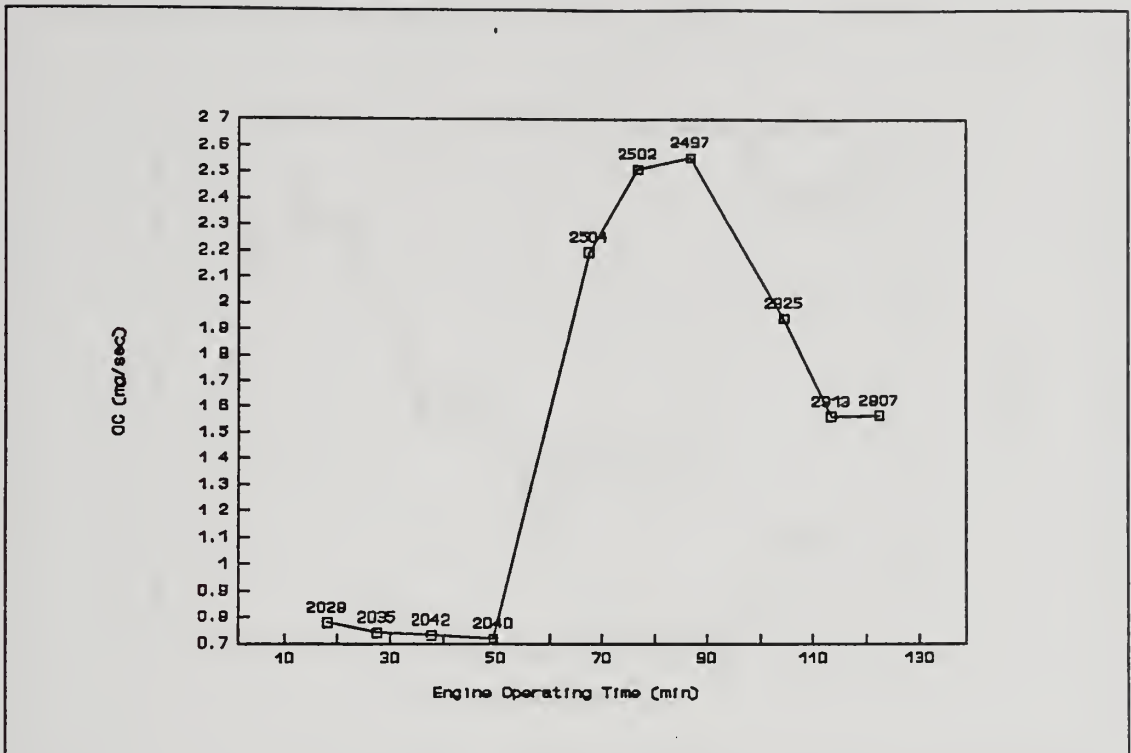
Figure 5-3:   OC vs. Time: AZ1 (θ=225)
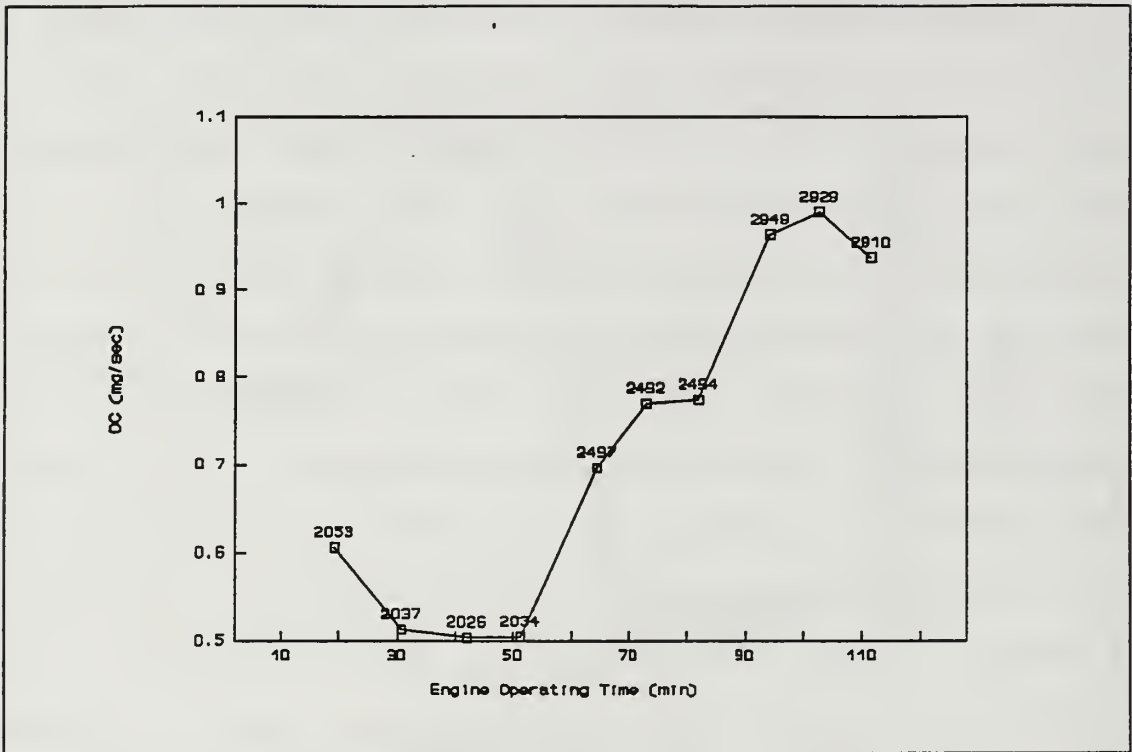
Figure 5-4:   OC vs. Time: AZ2
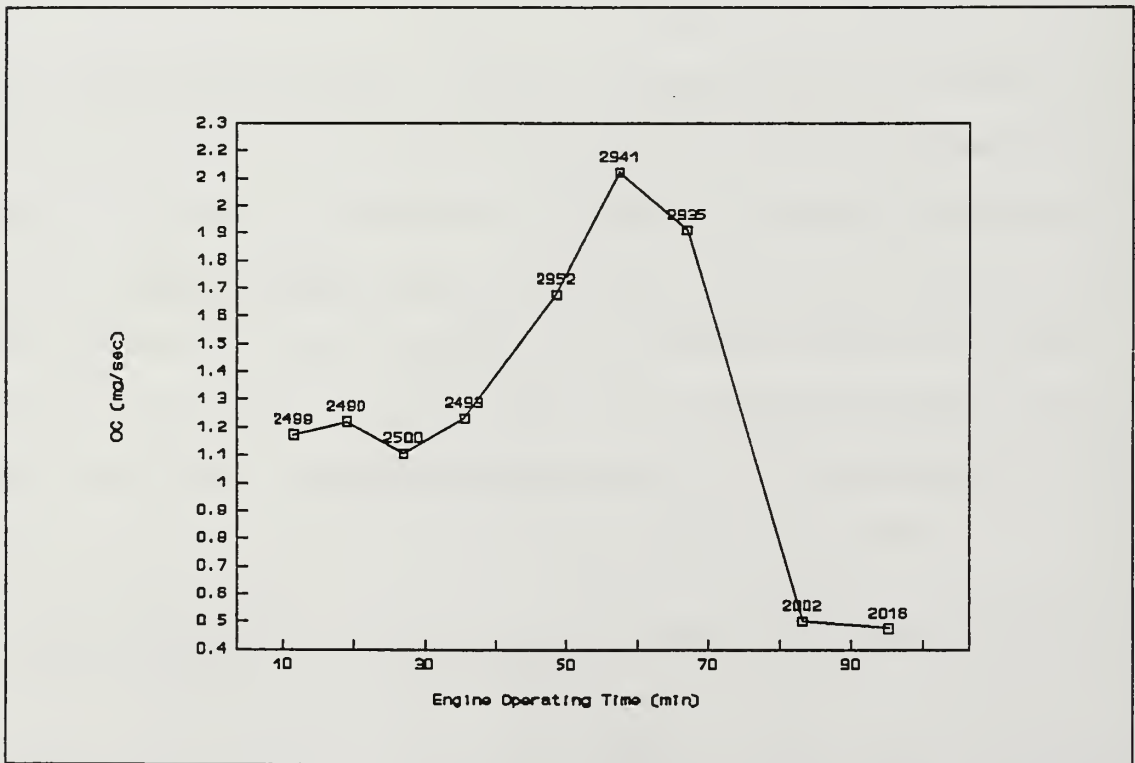
Figure 5-5:   OC vs. Time: AZ3
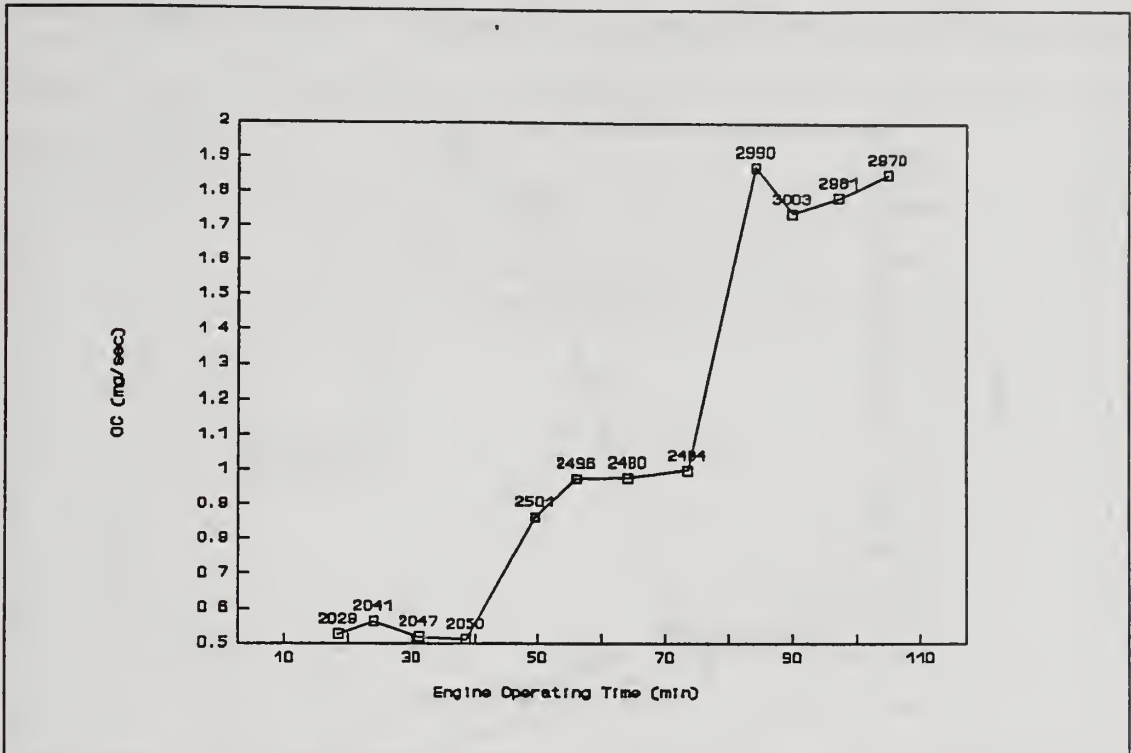
Figure 5-6: OC vs Time: AZ4
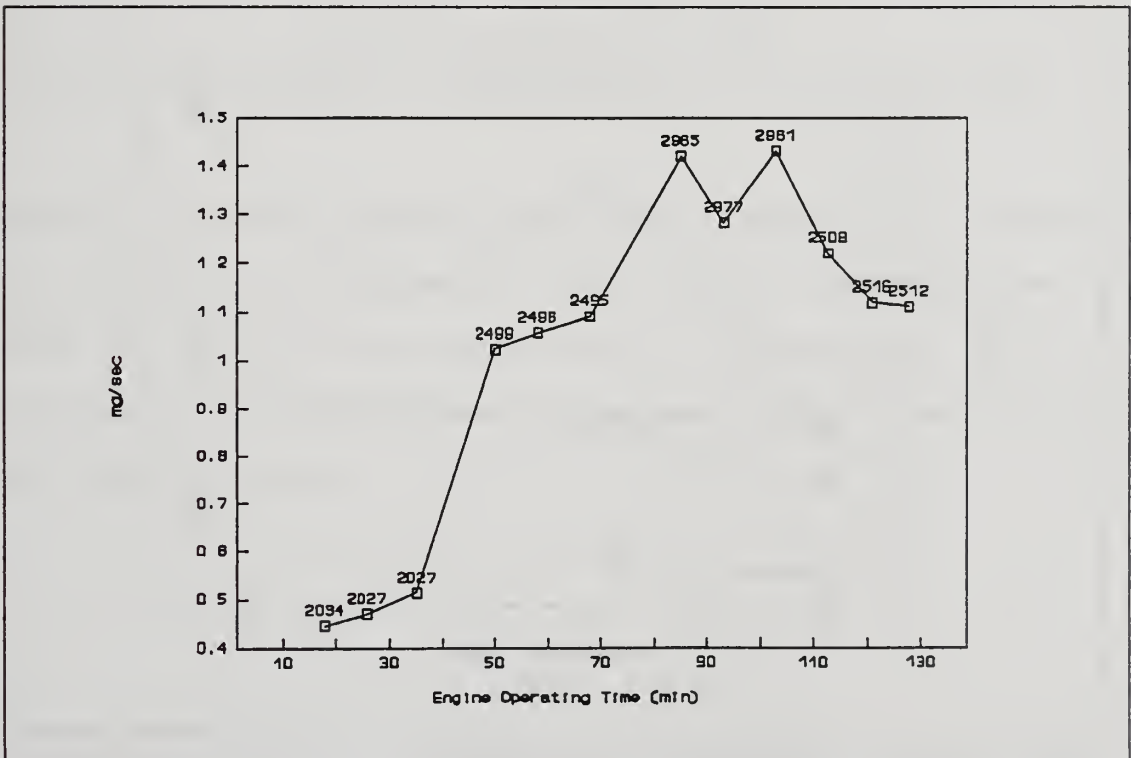
Figure 5-7: OC vs. Time: AZ5

81
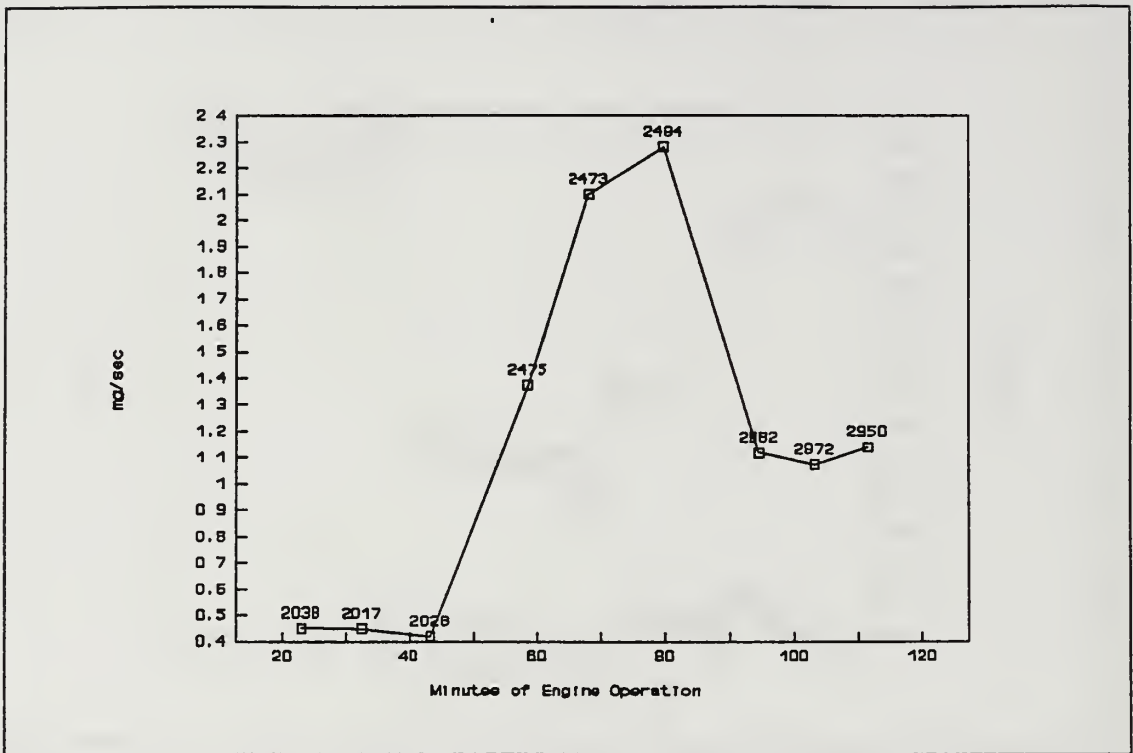
Figure 5-8: OC vs. Time: AZ6
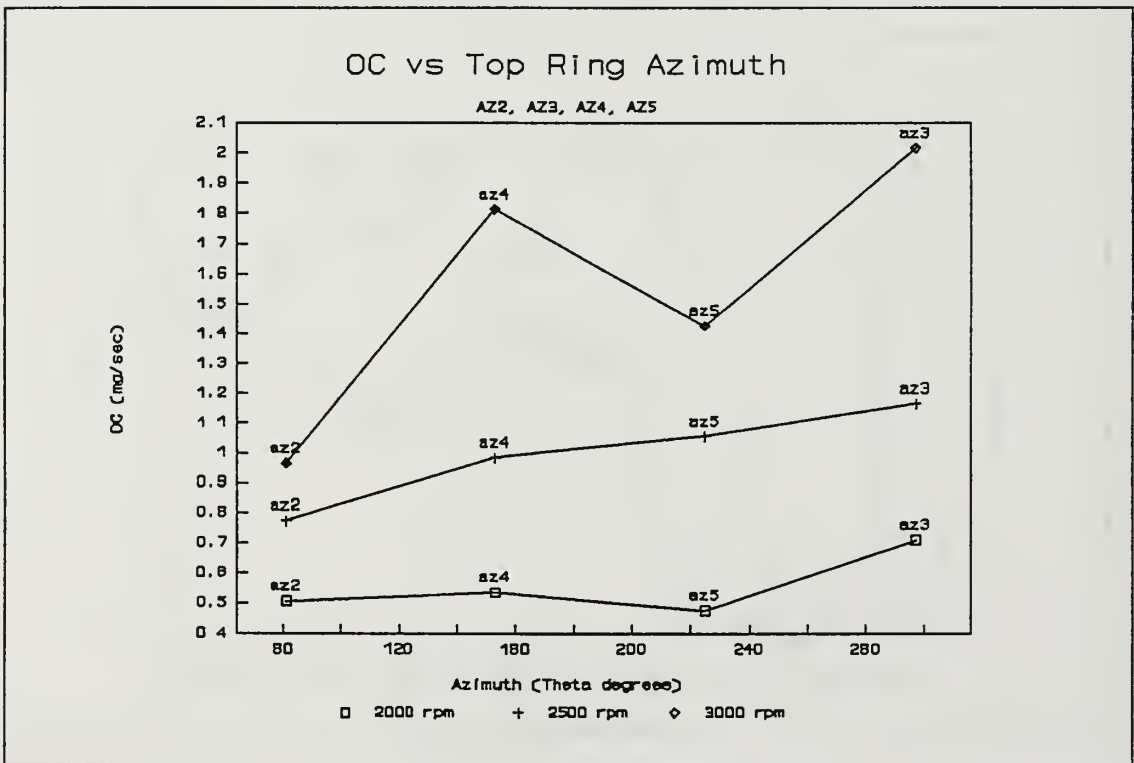
Figure 5-9: Average OC vs. Azimuth

The average oil consumption[72] dependence on top ring gap
azimuth and on speed is shown in Figures 5-9 and 5-10
respectively.
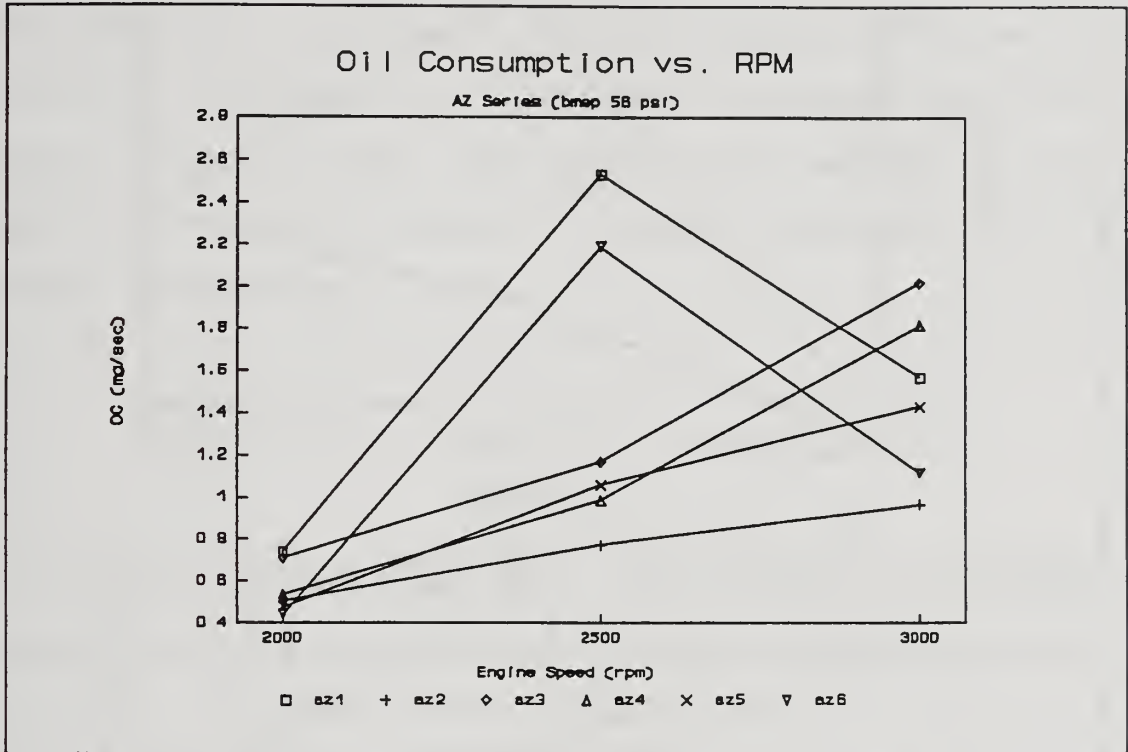
Figure 5-10:   Average Oil Consumption vs. Engine Speed

Series AZ1 and AZ6 demonstrated unusual behavior at 2500 rpm;
the ring configurations for these series were the same as
those for AZ5 and AZ2 respectively.   Figures 5-11 and 5-12
show the oil consumption plotted against engine speed for both
ring configurations.

---

[72]Average computed without the "transition" points.
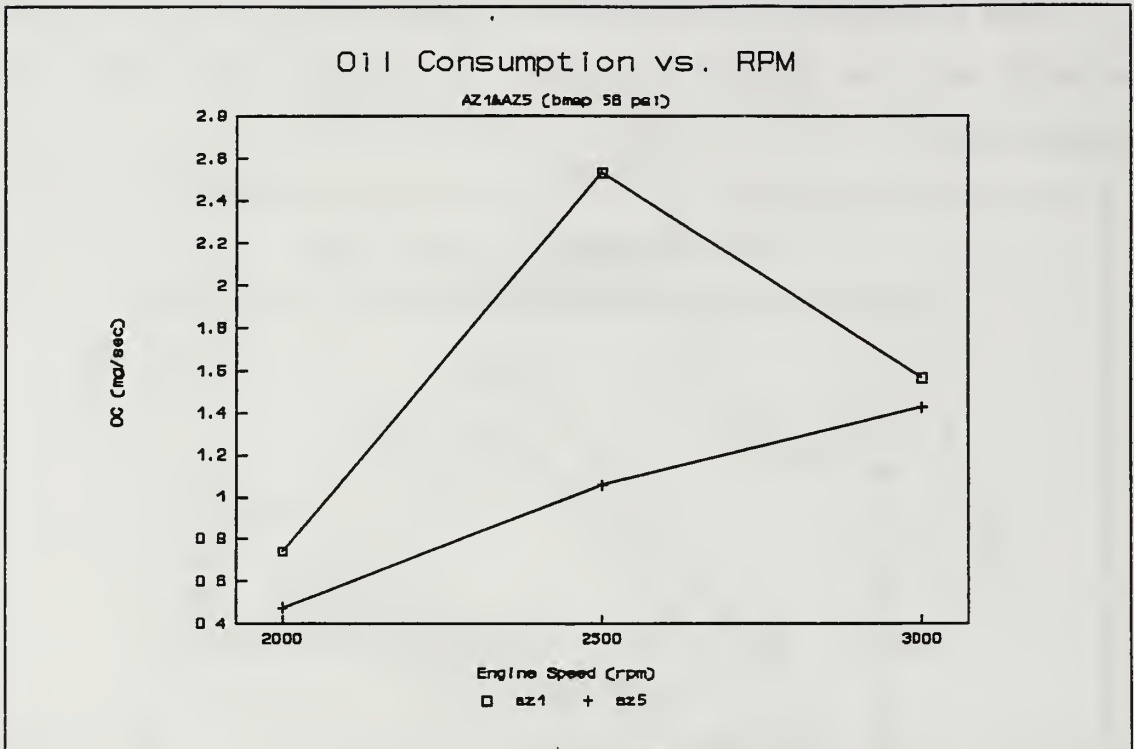
Figure 5-11: OC vs. Time: Ring Gap @ Θ=225°)
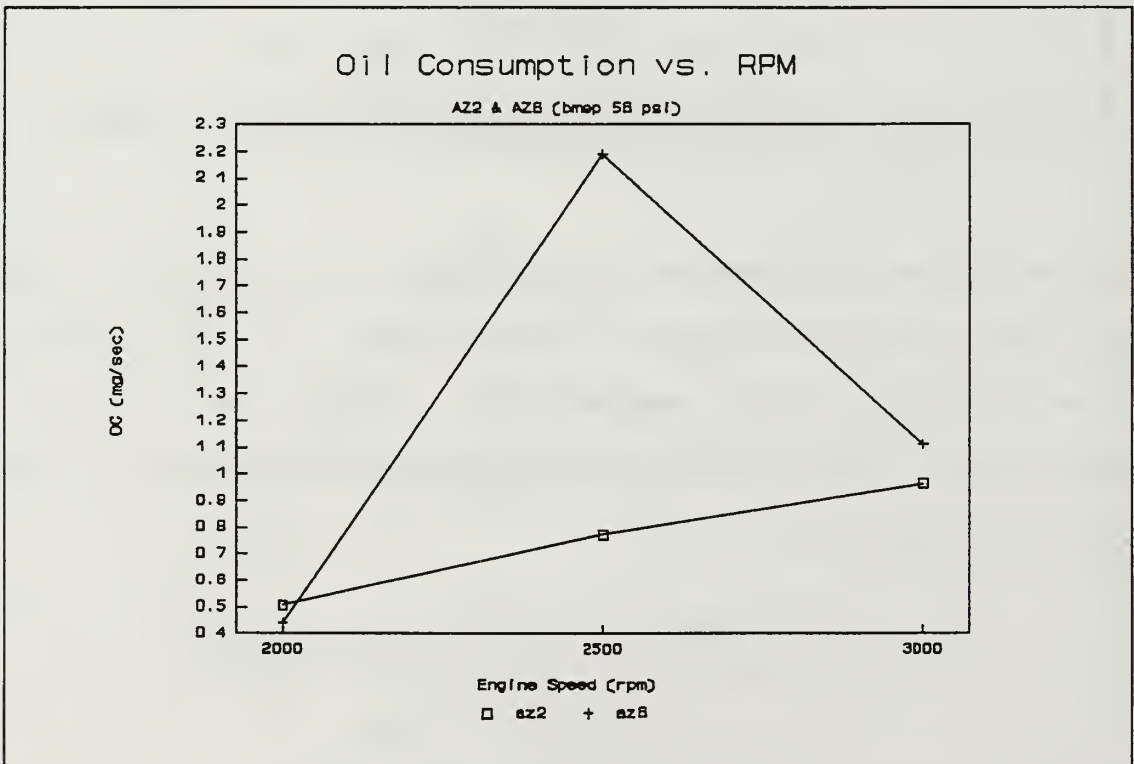
Figure 5-12: OC vs. Engine Speed (Top Gap @ Θ=81°)

Pressure Results: The raw cylinder pressure data was analyzed over nine cycles for pressure peaks. Each data set analyzed was then evaluated for the standard deviation of the peak pressures; the results of this analysis are shown with error bars in Figure 5-13. The peak pressures appear well behaved except at AZ5, 2500 rpm. This appears to be a significant outlier, although no unusual results were noted in the oil consumption.
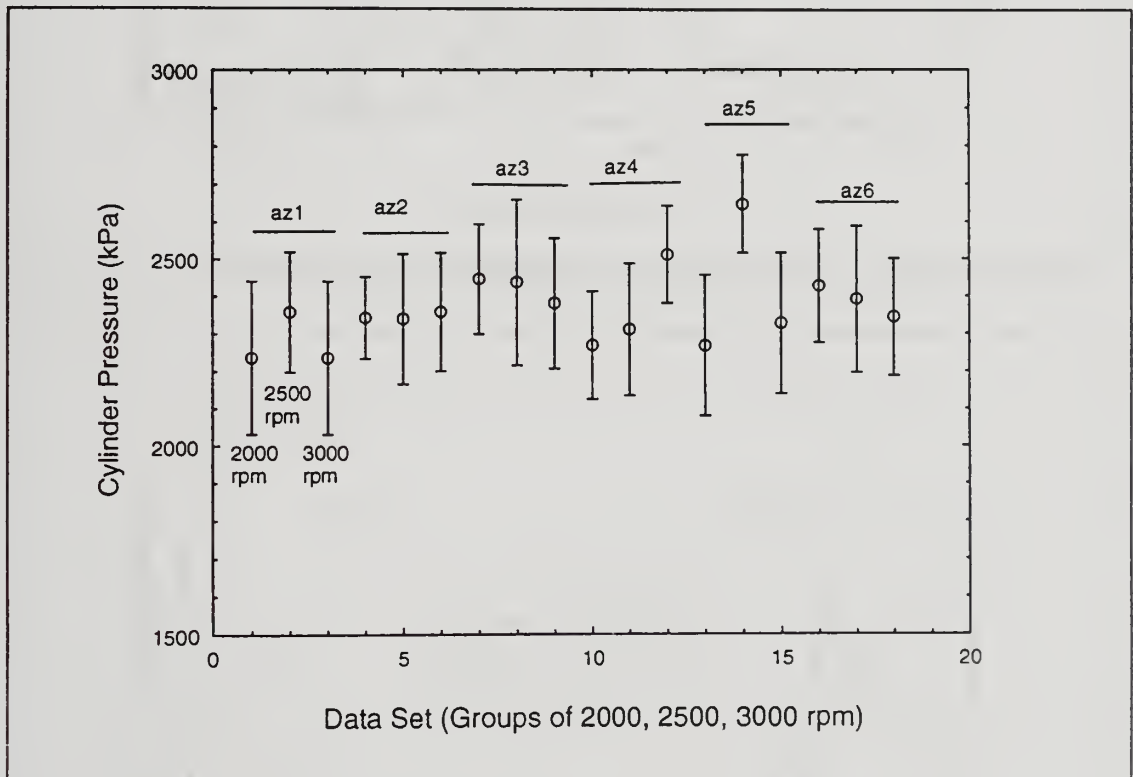
Figure 5-13: Cycle Averaged Peak Pressures.

Oil Film Thickness Results: Figures 5-14 through 5-17 show the results of the oil film thickness analysis for the second land on the power stroke. Figure 5-14 is an expanded view (from 10° ATC (Power) to 60° ATC (Power) to show the second land traces in perspective.

85
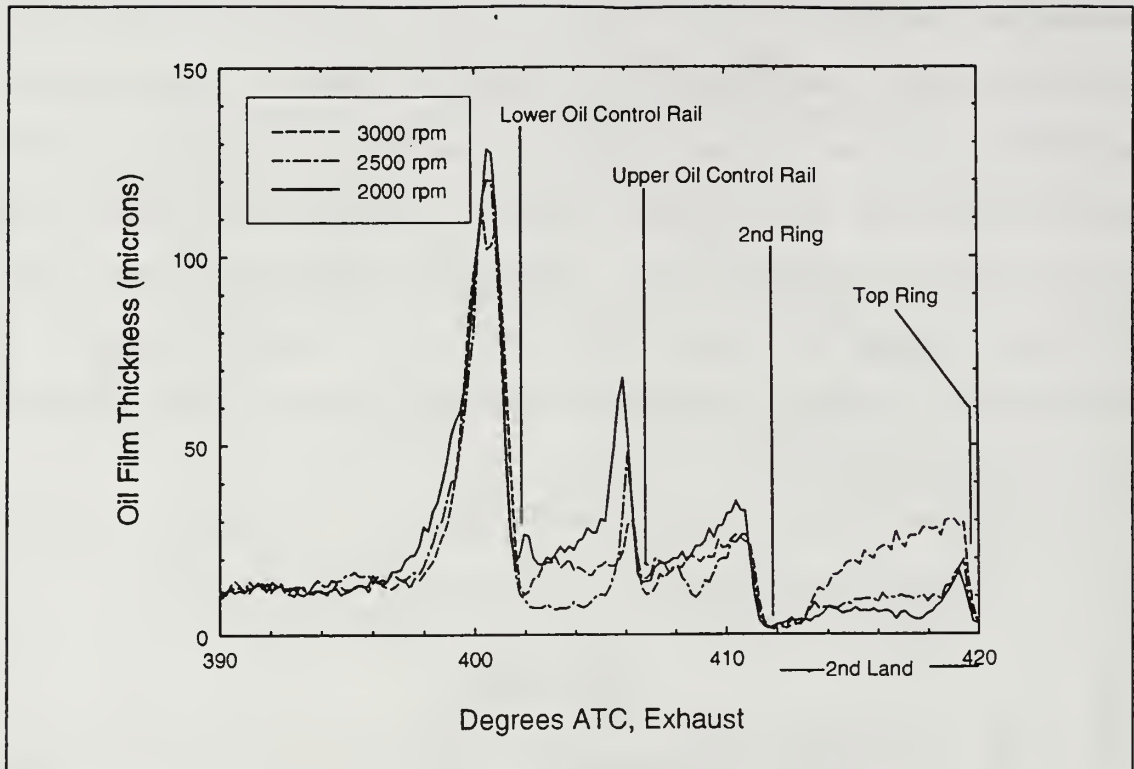
Figure 5-14: Oil Film Thicknesses, AZ3(θ=297°)
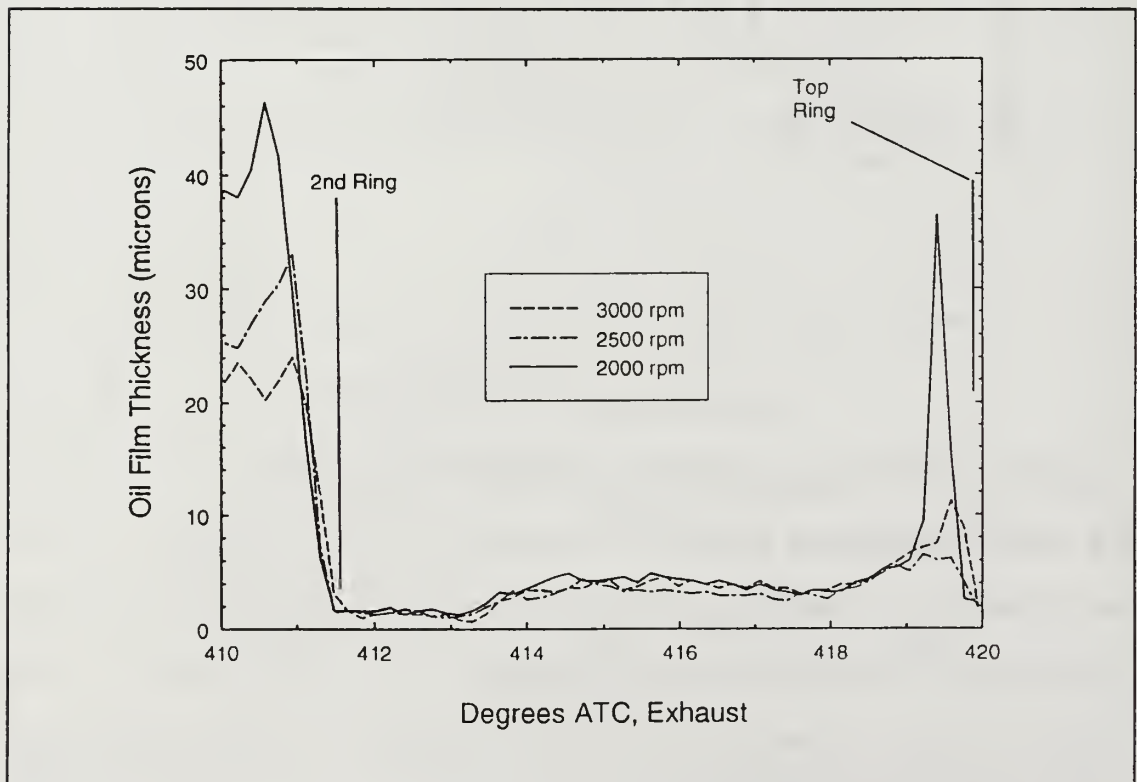
Figure 5-15: 2nd Land Oil Film Thickness, AZ4(θ=153°)

86
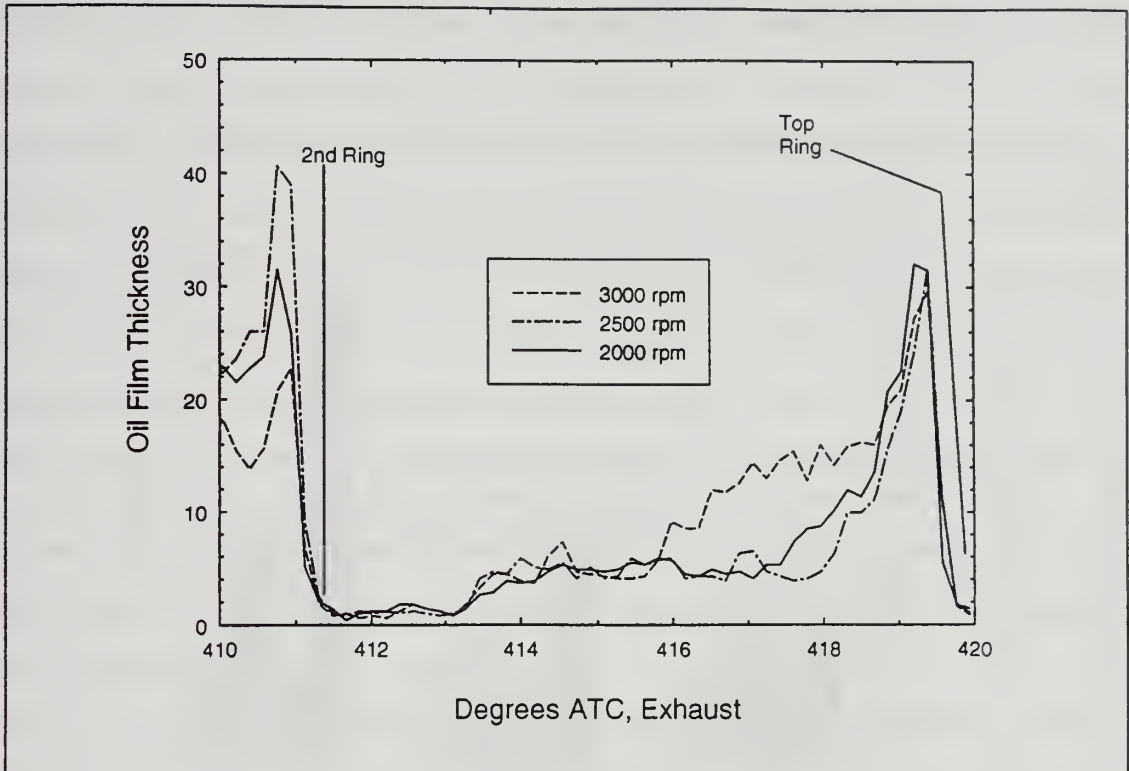
Figure 5-16:   2nd Land Oil Film Thickness, AZ5(θ=225°)
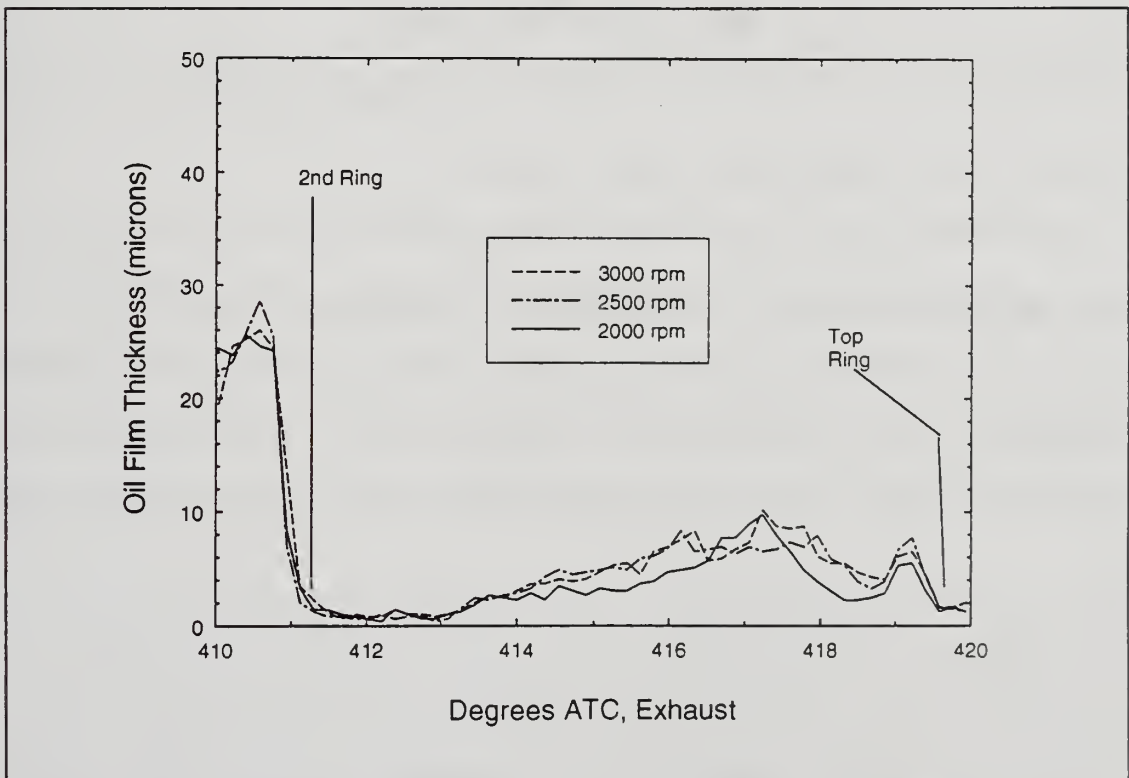
Figure 5-17:   2nd Land Oil Film Thickness, AZ6(θ=81°)

The oil film thicknesses was averaged over the second land.
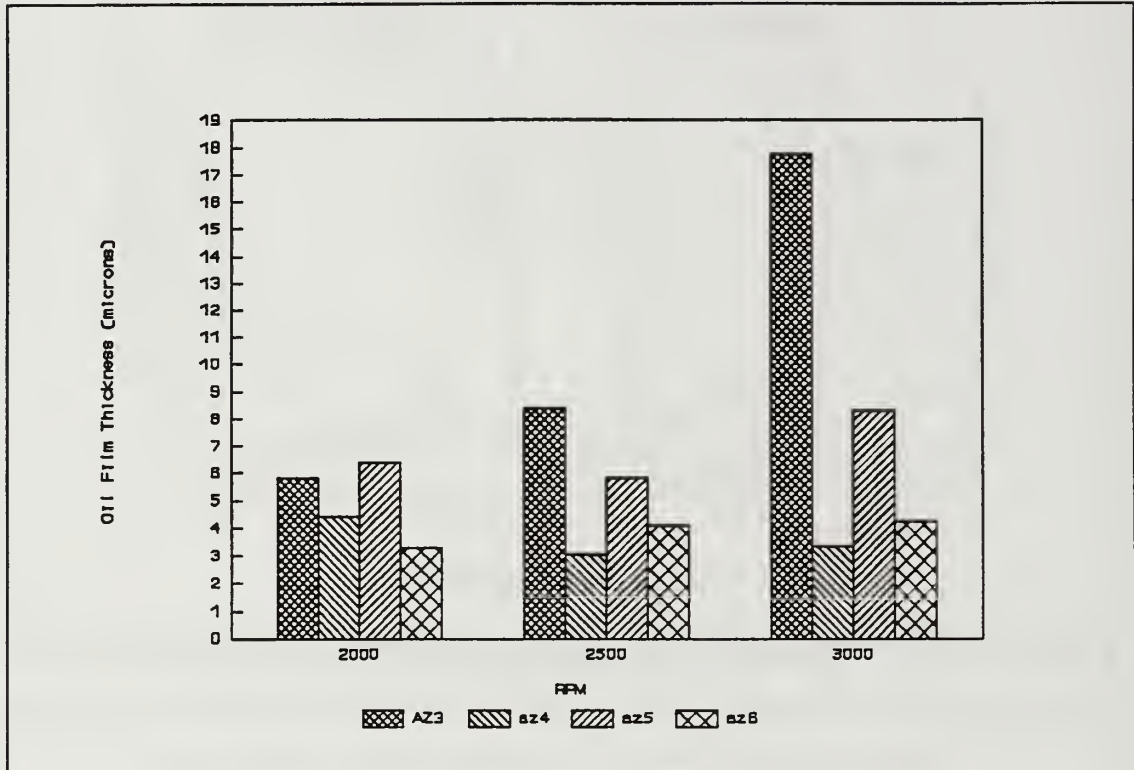
Figure 5-18:   Average 2nd Land Oil Film Thickness

Figure 5-18 summarizes these results.

Test Matrix E Results: The piston ring end-gap that exists at operating temperatures was measured using rings specially prepared[73] as described in Chapter 3.   The rings were installed under controlled conditions to prevent impacting the

---

[73]The rings were prepared by the Perfect Circle division of the Dana Corporation.

roll-pin during the use of a ring compressor.[74] After ring installation, the engine was operated at sufficient load to bring the temperatures into the operating band. After temperatures had stabilized, the rings were removed and the exposed length of roll-pin measured using a traveling microscope calibrated to 0.0001 inches. Table 5-4 shows the change in the gap size from hot to cold.

Table 5-4: Gap Size Change During Engine Operation (Nominal Liner Temperature: 116°C)	
Ring	Change (mm)
Top	0.20
2nd	0.16

This information allows a reasonable estimate of the hot ring gap of any set of rings used in the test engine if the cold gap of those rings is known.

5.6 Application of the Shaw Puddle Theory of Oil Consumption

General: The Shaw Puddle Theory of Oil Consumption has two distinct parts. The first is the gas flow prediction using the Namazian/Heywood Model as implemented in the program GASFLOW; the second part uses the reverse blowby (RBB)[75] with

---

[74]It was determined that 25 lb-in. was sufficient torque on the ring compressor to allow piston installation with out compressing the pin. This was done by incrementally tightening the compressor until the piston would go into the cylinder, and then removing the piston to check the pin length. The piston was then re-installed using the same torque on the ring compressor.

[75]Calculated in GASFLOW.

the film thickness measured experimentally to compute a predicted oil consumption.

Calibration of GASFLOW: One of the difficulties in employing the Shaw Model is "calibrating" the Namazian/Heywood Model to the particular test engine to which it is applied. Shaw extended Cherry's work on the calibration of GASFLOW with a detailed procedure that included the use of the cylinder pressure, second land pressure and blowby to allow "tuning" the hot engine geometry in the model to produce correct results.[76] This project did not provide second land pressures because of the geometric limitations of the test engine; blowby was only measured on test series AZ1 (θ=225°) and AZ6 (θ=81°) because of equipment and scheduling limitations. However, the Test Matrix E measured the hot piston gap, so some of the pertinent hot engine geometry was available to limit the number of geometric variables to the piston-cylinder clearance.

The initially, piston-cylinder clearance (clearance) was adjusted in an attempt to match the AZ1 blowby. It was not possible to match blowby without opening the ring gaps and then the volume flowrates produced oil consumption rates two orders of magnitude larger than those measured. Finally, GASFLOW was "calibrated" to the measured OC in AZ5 at 2000 rpm; the calculation necessary for this procedure is included in Appendix A. The rationale behind such a "back-calibration"

---

[76]Reference 19, pg. 61.

is that Shaw derived several relationships that were empirically based. It might reasonably be assumed that there were perhaps some engine-specific relationships impacting his relationships for A^* and h^* (Equations 2.15 and 2.16). It should be noted when reviewing the results that the final blowby rate achieved through the manipulation of GASFLOW was only 50% of that measured in AZ1 and approximately 25% of that measured in AZ6. In addition, to achieve the required velocity, it was necessary to open the second ring gap to several times the gap actually existing in the engine; the top ring end-gap was maintained at the size measured in Test Matrix E.

Shaw Model Results: Each data set was analyzed with GASFLOW using the peak pressures reported above and the geometry obtained in the GASFLOW calibration. The output geometries were then input into the Shaw Model. The resulting oil consumption predictions are shown in Figure 5-19 with the corresponding measured results.

Equation 2.21 states that oil consumption is proportional to engine speed. If oil consumption is discussed on a "per unit time" basis, the engine speed effect tends to mask other relationships like initial film thickness and Taylor number dependency. Therefore it is useful to discuss oil consumption on a "per cycle" basis; this tends to unmask the other relationships. The discussion of oil consumption will be

shifted to the per cycle basis for the remainder of the chapter for this reason.
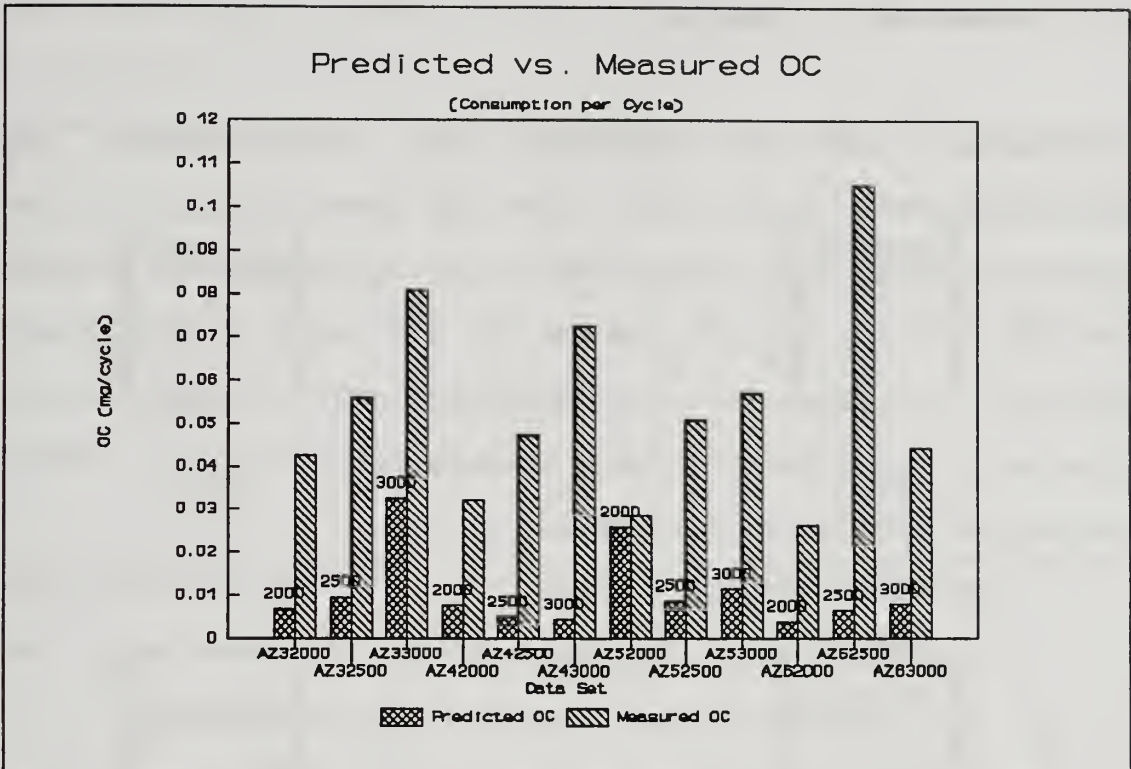
Figure 5-19:   Shaw Model Predictions of Oil Consumption
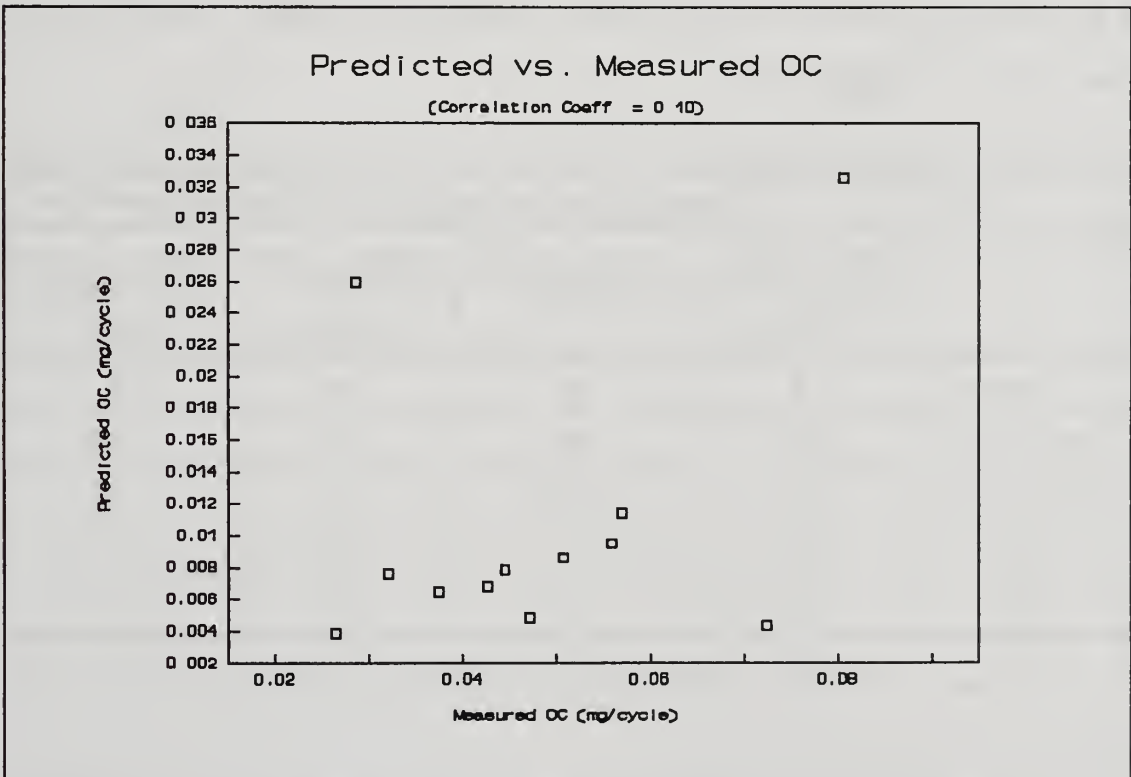
Figure 5-20:   Predicted vs. Measured Oil Consumption

5.7 Discussion of Results

Correlation between Predicted and Experimental Oil Consumption: Figure 5-20 shows the predicted OC plotted against the actual OC. The coefficient of correlation between the two is only 0.10.[77] Review of Figure 5-19 for trends indicates that while the measured oil consumption is relatively well behaved, the predicted values are not. There are several possible explanations for this.

    a. Piston Secondary Motion,

    b. increased flow resistance along the second land, and

    c. oil film thickness azimuthal variation.

To allow evaluation of these effects, it is useful to consider different azimuthal references. Table 5-5 shows three sets of translated coordinates:

Table 5-5: Alternative Azimuthal Coordinates				
	Ref. to: Front of Engine	Ref. to: $\theta=270°$	Ref. to: LIF Window	Ref. to: 2nd Ring Gap
Coord:	θ	θ_t	θ_w	θ_2
AZ1/AZ5	225	45	135	180
AZ2/AZ6	81	189	9	36
AZ3	297	27	153	108
AZ4	153	117	63	108

θ is drawn through 360 degrees counter-clockwise, all the

---

[77]Post analysis of Shaw's results indicates that he obtained approximately an 84% correlation.

other coordinate systems are drawn through 180 degrees of arc in the shortest direction.
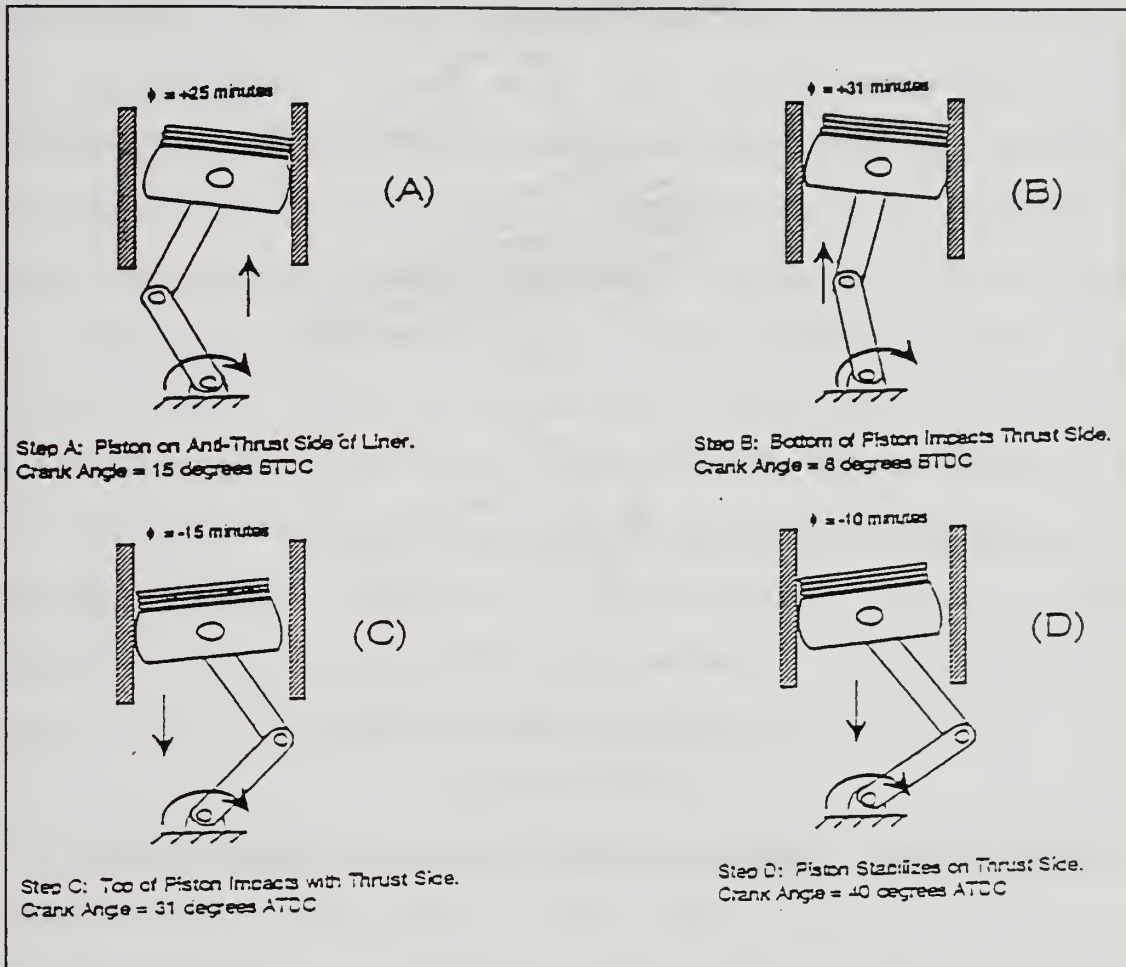
Figure 5-21: Conceptual Sequence of Piston Slap
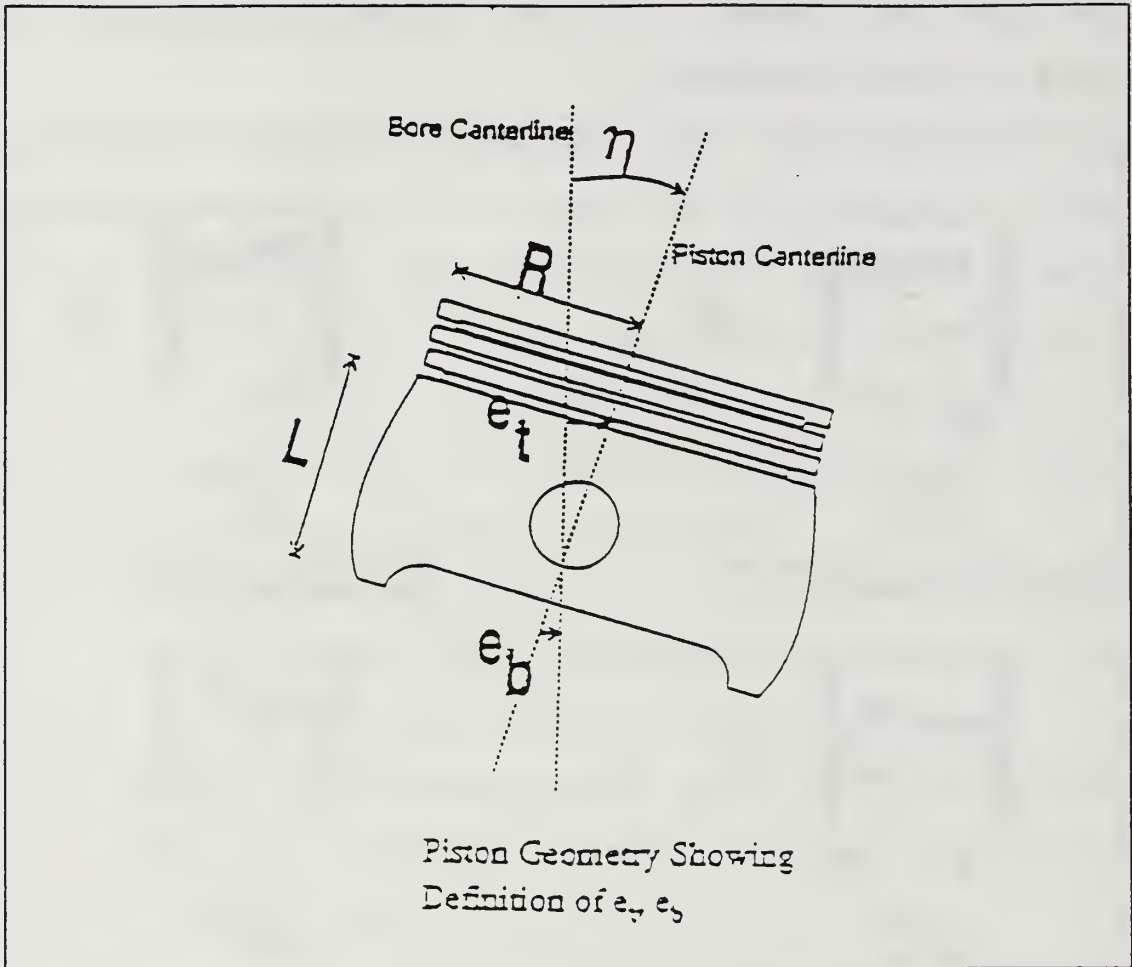
Figure 5-22: Piston Secondary Motion Geometry

Piston Secondary Motion: As the piston travels up and down the liner, a certain amount of rotational freedom is allowed about the wrist-pin axis by the piston-to-cylinder clearance. Figure 5-21 shows the secondary motion conceptually[78] and Figure 5-22 shows the geometry of that motion.[79] The geometry that has the largest effect on oil consumption is the clearance between the piston and the

---

[78]Reference 11, Figure 14.

[79]Reference 21, Figure 2.

cylinder <u>during reverse blowby</u>. It may be seen that if the piston is inclined away from the top ring gap, the effective area of that gap will be greater and the gas flow geometry will be altered.   Intuitively, one would assume that the reverse blowby would be increased, but experience with GASFLOW indicates that the actual effect will depend on the relative magnitudes of the specific geometries involved. Figure 5-23 plot the measured oil consumption against the Cosine(θ_t)[80] or "thrust factor" since the amount that the ring gap is opened or closed by piston secondary motion can be **approximated by** a cosine function <u>when the gap azimuth angle is referenced to a θ angle of 270°</u>.   There is a definite effect on OC as the absolute value of the cosine approaches 1.   However, there seems to be little effect in the intermediate region.

Relative Gap Azimuth: The second land region may be thought of as a small pipe or duct with the piston ring gaps acting as orifices at either end.   The greater the angle between the two gaps, the greater the effective "length" of the land for providing flow resistance.   Figure 5-24 shows measured oil consumption plotted against θ_2, the angle between the top and second ring gaps.   Any effect of the relative position of the two gaps is not clear from the results, although AZ2 (θ_2 = 36) is the lowest oil consumption and has

---

[80]A positive cos(θ_t) corresponds to the "thrust" side of the engine.

the smallest angular distance from the second ring gap; AZ5 (θ_2 = 180) has only slightly greater cyclic oil consumption indicating that the flow resistance effect is <u>not</u> dominant.

Oil Film Azimuthal Variation: Using the LIF system to observe the second land oil film thickness while making simultaneous oil consumption measurements has the potential to provide a useful correlation. In the case of this project,
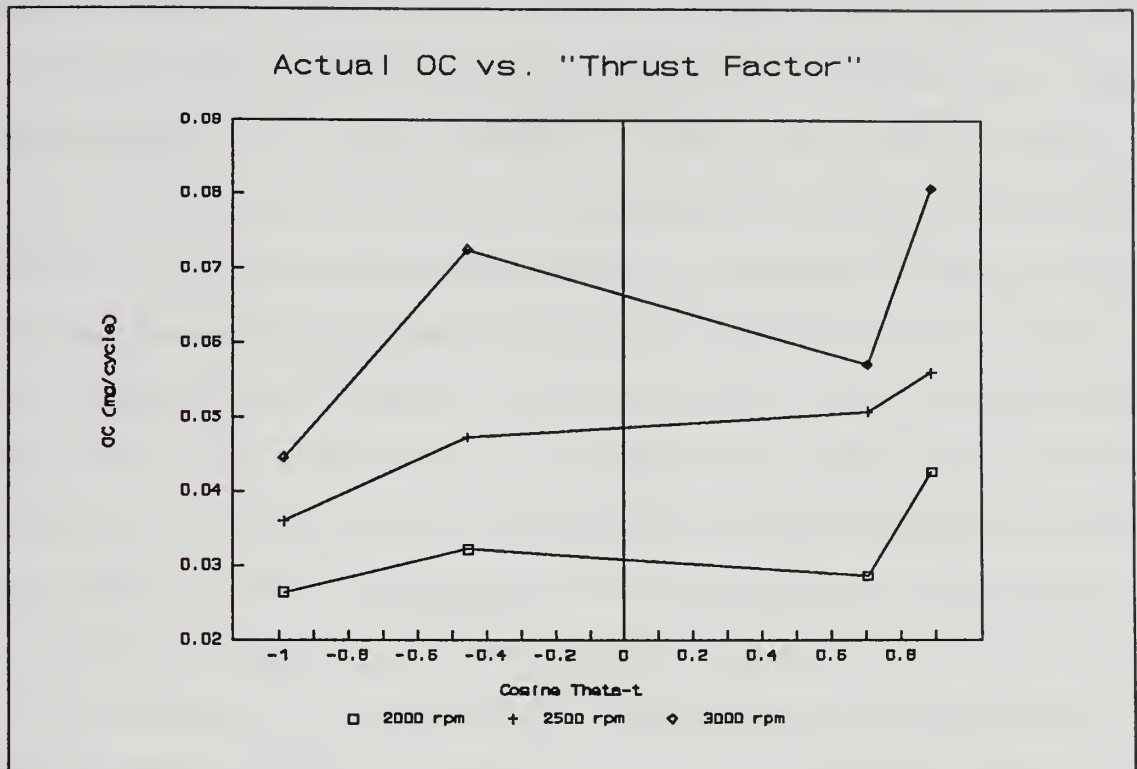
Figure 5-23:   Actual OC vs. θ_t

the assumption was made that the oil film was constant around the circumference of the second land; this led to the altering of the top ring gap azimuth. Figure 5-25 shows the average observed oil film thickness plotted against θ_w, the relative angle to the LIF window. Comparing the series AZ6 LIF trace in Figure 5-17 to those of the other data series shows marked differences in oil film profiles. Figure 5-26 presents the 2000 rpm AZ6 trace with that of AZ4 (72° from AZ6). The AZ4 trace shows the typical peak under the top ring; this feature is deformed or missing entirely on the AZ6 trace. Since the AZ6 peaks are the only ones that demonstrated this behavior, it is reasonable to infer that the proximity of the gap to the LIF window allows the observation of the oil film deformation caused by the gas flowing through the gap. It has the practical effect of disallowing comparison of the AZ6 traces with those of other series. As a direct consequence of this problem, the Shaw Model predictions will be in error if the second land oil film thicknesses measured are not the same as those under the top ring gap.
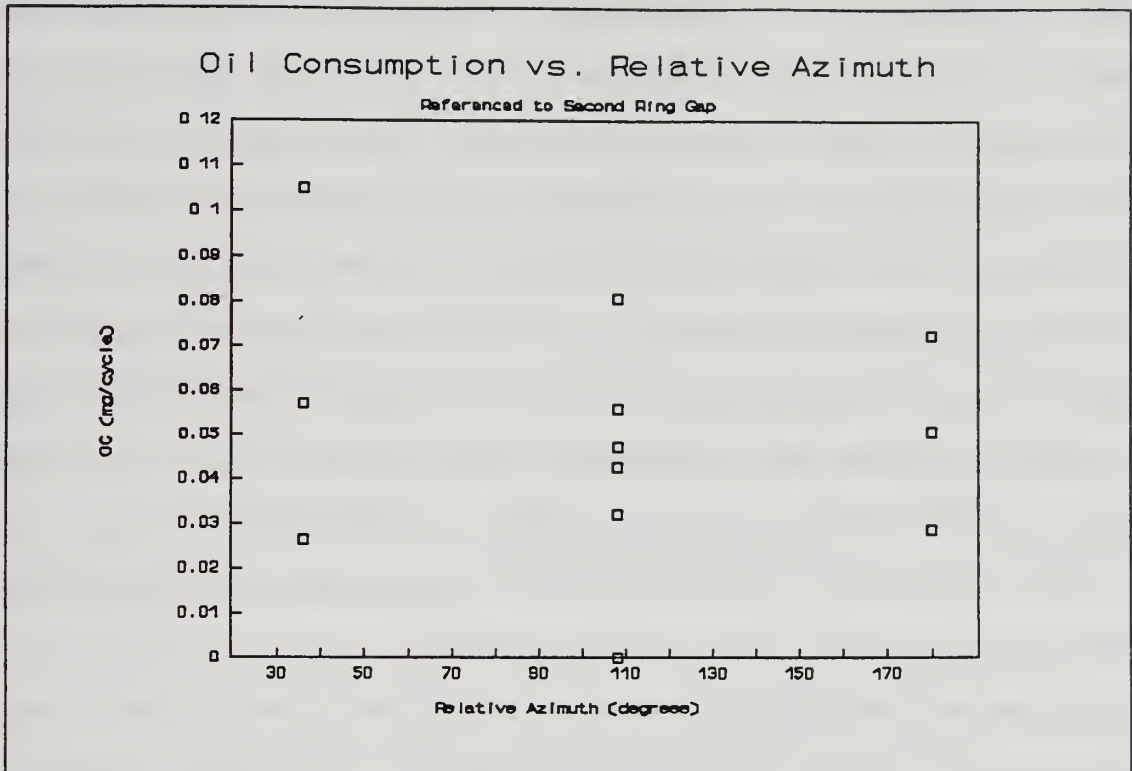
Figure 5-24: OC vs. θ_2
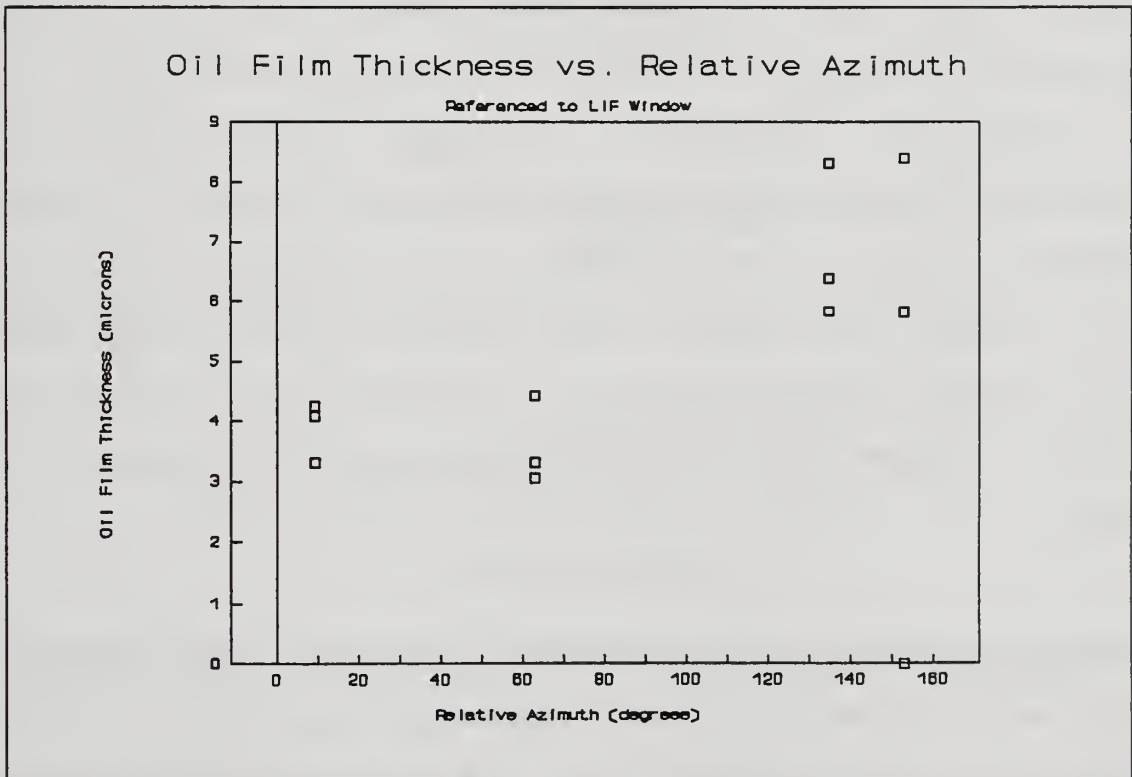
Figure 5-25: Oil Film Thickness vs. θ_2

Post-operation Piston Appearance: Each pinned piston, except the AZ3 piston, was limited to two hours of operation to prevent scoring the cylinder wall with the ring ends; the AZ3 piston was operated 3.5 hours due to an equipment malfunction. During operation the pistons developed a set of deposits that provide interesting insight into the top ring gap gas flow. Included as Figures G-1 through G-5 of Appendix G, photographs of these pistons show dramatic differences between pistons used for different AZ series tests; in these photographs the a small black dot has been made on the second land marking the position in which the ring was pinned. The density of the deposits on the AZ1 and AZ3 pistons (thrust-side top gap) tend to be heavier than the deposits present on AZ2 and AZ4 (anti-thrust-side gap) increasing confidence that the piston secondary motion plays a major role in oil consumption.

There also appears to have been a large amount of interaction between the reverse blowby and the swirl. This interaction was the most pronounced in the AZ1 piston where the reverse blowby gasses left deposits on the second land only in the clockwise direction. It might be that the reverse blowby is exacerbated by the dynamic pressure effects of swirl.

Anomalous Behavior of AZ1 and AZ6: Figures 5-11 and 5-12 show an unusual increase in the oil consumption for the AZ1 and AZ6 data sets measured at 2500 rpm. The experimental conditions

were identical to AZ5 and AZ2 respectively. Unfortunately, no oil film thickness measurements were taken during the AZ1 and AZ2 data sets. However, the film thickness traces (Figure 5-17) for the AZ6 data series were reviewed for trends and nothing unusual was found; the pressure traces were similarly reviewed with negative results for both AZ1 and AZ6. Another possible source of error is the OC measurement itself. The original logs of the ROCS were reviewed and nothing unusual was found. As of the writing of this thesis, no plausible explanation has been found.
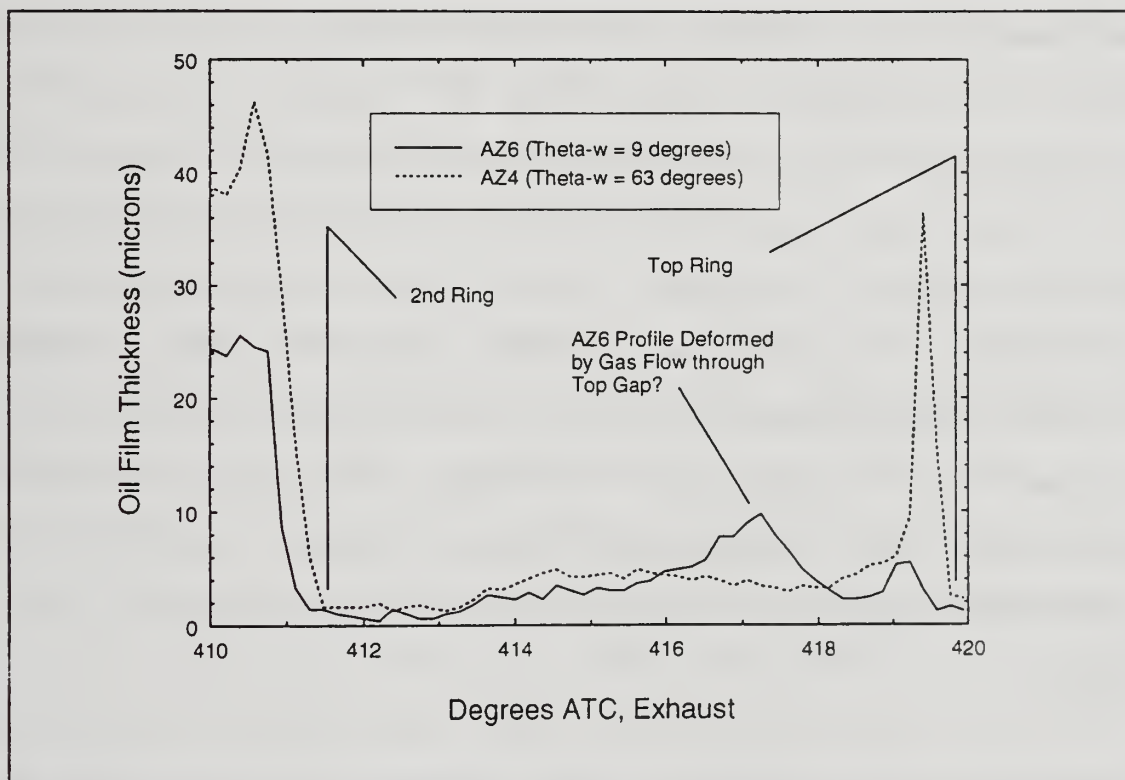
Figure 5-26:   AZ4 and AZ6; 2nd Land LIF Traces @2000 rpm

Chapter 6: Conclusions and Recommendations

6.1 General

This chapter presents a summary of both the technical conclusions and practical lessons garnered during the course of this project. It also presents recommendations in several areas, both theoretical and practical, that the author feels have the potential to impact future studies in internal combustion engine oil consumption.

6.2 Conclusions

Radiotracer Oil Consumption System Performance: Measured test engine oil consumption varied over the range 0.3 g/bhp-hr to 0.9 g/bhp-hr. This is within the expected band for engines of this size indicating that the Radiotracer Oil Consumption System produces reasonable results on an absolute scale. Evaluation of the pinned ring results indicates that consumption measurements have approximately 8% variability for a given set of operating conditions, indicating that the Radiotracer Oil Consumption System produces sufficiently consistent results to support the test matrices of the project.

Oil Consumption versus Engine Speed: Results of oil consumption measurements conducted with the piston rings unpinned indicate a modest speed dependence, but a large

amount of data scatter. The results for pinned rings show two differences. First, the variability is greatly reduced. Second, the slope of the linear speed dependence of the oil consumption varied by a factor of three as the ring gap azimuth was changed. These differences indicate that piston ring rotation is responsible for the variability of the data in the unpinned case, and that the azimuth of the top ring gap plays a major role in determining oil consumption rates.

Relative Ring Gap Azimuth: There is no clear relationship between measured oil consumption and the angular separation between the top ring gap and the second ring gap. This indicates that the reverse blowby flow through the top ring gap is not significantly influenced by the length of the annular space between the two ring gaps.

Absolute Top Ring Gap Azimuth: There is a definite relationship between the top ring gap absolute azimuth (measured from the forward wrist-pin axis) and oil consumption. If the gap is located near the center of the thrust side, oil consumption is maximized, and if the gap is located near the center of the anti-thrust side, oil consumption is minimized. This relationship implies that the tilt and lateral displacement associated with piston secondary motion effect the oil consumption by varying the "effective ring gap area."

Shaw Puddle Theory of Oil Consumption: There was no quantitative agreement between measured oil consumption and that predicted by the mathematical correlation for oil consumption proposed by Shaw. This was due, at least in part, to uncertainty in determining the effective gap area during reverse blowby and in determining the oil film thickness on the second land in the vicinity of the top ring gap. These difficulties arose due to piston secondary motion and azimuthal variations in average second land oil film thickness.

However, qualitative analysis shows that the Shaw Puddle Theory of Oil Consumption _is_ plausible because variation of gap parameters causes a significant variation in oil consumption.

Anomalous Behavior: In two instances measured oil consumption at 2500 rpm (and only 2500 rpm) was a factor of two greater than expected based upon engine speed and load. The oil consumption in these conditions may be governed by mechanisms which may be important but are, as yet, undetermined.

6.3 Further Study and Analysis

The following areas are suggested for further investigation and analysis:

106

Analysis of Existing Data: Data taken in this and other projects might be analyzed for the following information:

1. The impact of secondary piston motion on top ring gap gas velocities.

2. The exact dependence of second land oil film thickness on ring gap azimuth. Existing data might provide the basis for this, but it is likely that the accumulation of more data will be necessary.

New Areas of Investigation: The following areas are suggested for future experimentation:

1. Dual steadystate oil consumption rate. Future investigations of oil consumption, especially on the Chrysler 2.2 test engine, should provide a provision for observation of the dual steadystate oil consumption rate observed in this project at 2500 rpm during this project.

2. Second land oil film thickness dependence on cylinder azimuth. This will require the ability to monitor the oil film thickness at several azimuthal locations around the cylinder. This capability will soon exist in Sloan Engine Laboratory when the multi-optical window modification is complete to an existing Kohler Engine.

6.4 Recommendations and Observations for Continuing Investigations

The following recommendations are based upon the above conclusions and upon the experience gained in conducting this experiment.

Radiotracer Oil Consumption System (ROCS): The Radiotacer Oil Consumption System (ROCS) designed and built for this project provides adequate accuracy (94.6%) for steadystate and pseudo-steadystate measurements of engine oil consumption (OC). There are several design improvements that might be made to improve system accuracy should that be required; those actions are discussed below. The system's purge time, initial sample time and sampling period give the system a time constant that is between one and two orders of magnitudes higher than that necessary to achieve transient and non-steadystate measurements of oil consumption.

The following changes are made concerning the configuration and operation of the ROCS:

1. The largest impact on the accuracy of the system is the efficiency of the catalyst. Should it become necessary to improve the accuracy of the system, the following steps will help:

   a. Substitute higher temperature heating tapes for the sample line heaters. This will allow better pre-heating of the sample gases.

   b. Replace the manual heater controls with an automatic thermal controller. This will

reduce response and warmup times.

c. Reduce the length of connecting piping in the Water Collection System (WCS). This will reduce thermal losses and reduce the preheating requirements.

2. One of the most time consuming and inaccurate operations involved in taking ROCS data is determining the fuel consumption rate by subtractive weighing.[81] The time involved in taking the data might be reduced by providing an realtime fuel flow measurement device. If the existing scale <u>must</u> be used, the accuracy can be improved at the expense of sample period by measuring fuel consumption over a long period of time.

3. The ROCS in its current configuration produces "transition"[82] samples when the engine operating conditions are changed because the system purge path only purges the condenser assembly. If the system isolation valve is replaced with a three-way valve it will allow the entire flow path to be purged. However, using air at ambient temperatures to purge the system will cool the components; this

---

[81]This particular operation was also the single source of experimental error causing the invalidation of results.

[82]Discussed in Chapter 5.

configuration change should only be made in conjunction with the line heating changes discussed above.

4. System modifications to allow other than steadystate measurements would be difficult. If transient oil consumption measurement becomes necessary, it is recommended that an on-line sulfur dioxide system similar to that reported on by Ariga et al be created or procured.[83]

5. The ROCS may be used to measure the OC in combustion-ignition engines as well as spark-ignition engines. **However, a soot filter assembly must be added** as described by Hartman. The use of such an assembly requires some assumptions about exhaust content; the researcher using such a system should first satisfy himself/herself that those assumptions are true for the specific test engine.

Employment of the Shaw Model:

An attempt was made to calibrate the program GASFLOW using "hot" gap measurements and a reduced set of state measurements. This effort did not yield results that correlated with either blowby or oil consumption measurements. It is concluded that the only proven method for calibrating

---

[83]Reference 22.

110

GASFLOW is the iterative approach used by Shaw.[84]

If it is necessary to provide the optimum predictive results from the model, the experimental equipment should be set up so that the top ring gap is directly illuminated by the LIF optical window and provisions made for measuring second land pressure and blowby. These parameters will allow use of Shaw's method of calibrating GASFLOW.

Test Engine Operation with Pinned Rings: The test engine was operated for up to 3.5 hours with number four cylinder piston rings pinned in the fashion described in Chapter 3. After each set of data, the cylinder liner was examined in detail for adverse effects; none were noted. The conclusion drawn is that the 2 hour limit originally imposed on engine operation with pinned rings is a conservative limit and, as long as the rings are properly installed may be exceeded by 75% with little chance of engine damage.

Engine Decontamination: At the completion of this project, the standard three phase flush (found in Appendix C) was performed on the test engine. The only modification to the flush procedure was that fresh oil and a fresh filter were used for each phase. The dilution factor for the complete

---

[84]Shaw's method uses a sequential adjustment to the engine, piston and ring geometries to iteratively match peak cylinder pressure, second land pressure and blowby volume flow rate. (Reference 9, pg. 61).

flush process was 0.008 (the final specific activity was 0.8% of the original activity). This indicates that dilution factor for each phase (one drain and fill) is about 0.20; this can be used for planning purposes with the Radiation Protection Office.

This Page Intentionally Blank

References

1. Heywood, J. B.: <u>Internal Combustion Engine Fundamentals</u>, McGraw Hill, 1988.

2. Johnson, J. H., Bagley, S. T., Gratz, L. D. and Leddy, D. G.: "A Review of Diesel Particulate Control Technology and Emissions Effects - 1992 Horning Memorial Award Lectrue," SAE Paper 940233, 1994.

3. Wentworth, J. T.: "Effects of Top Compression Ring Profile on Oil Consumption and Blowby with Sealed Ring-Orfice Design," SAE Paper 820089, 1982.

4. Hill, S. H. and Sytsma, S. J.: "A Systems Approach to Oil Consumption," SAE Paper 910743, 1991.

5. Wahiduzzaman et al.: "A Model for Evaporative Consumption of Lubricating Oil in Reciprocating Engines," SAE Paper 922202, 1992.

6. Hoult, D. P. and Shaw, B. T. II: "The Puddle Theory of Oil Consumption," <u>Tribology Transactions</u>, Vol. 37, 1994, pp. 75-82.

7. Namazian, M. and Heywood, J.: "Flow in the Piston-Cylinder-Ring Crevices of a Spark-Ignition Engine: Effect on Hydrocarbon Emissions, Efficiency and Power," SAE Paper 820088, 1982.

8. Hartman, R. M.: "Tritium Method Oil Consumption and its Relation to Oil Film Thickness in a Production Diesel Engine," S. M. Thesis, Department of Ocean Engineering, Massachusetts Institute of Technology, 1990.

9. Shaw, B. T. II: "Direct Observation of the Oil Consumption Mechanism of a Production Single-cylinder Diesel Engine," S. M. Thesis, Department of Mechanical Engineering, Massachusetts Institute of Technology, 1992.

10. Schneider, E. W. and Blossfeld, D. H.: "Method for Measurement of Piston Ring Rotation in an Operating Engine," SAE Paper 900224, 1990.

11. Ryan et al.: "Engine Experiments on the Effects of Design and Operational Parameters on Piston Secondary Motion and Piston Slap," SAE Paper 940695, 1994.

12. Taylor, G. I.: "Deposition of a Viscous Fluid on the Wall of a Tube," Journal of Fluid Mechanics, Volume X, 1961.

13. Wu, C., Melodick, T., Lin, S., Duda, J. and Klaus, E.: "The Viscous Behavior of Polymer Modified Lubricanting Oils Over a Broad Range of Temperature and Shear Rate," Transactions of the ASME, Journal of Tribology, Vol. 112, July 1990, pp. 417-425.

14. Warrick, F. and Dykehouse, R.: "An Advanced Radiotracer Technique for Assessing and Plotting Oil Consumption in Diesel and Gasoline Engines," SAE Paper 700052.

15. Peters, D. G., Hayes, J. M. and Hieftje, G. M.: <u>Chemical Separations and Measurements: Theory and Practice of Analytical Chemistry</u>, W. B. Saunders Co., 1974.

16. Lee, J. M.: "Film Thickness Measurements in a Production Spark Ignition Engine," S. B. Thesis, Department of Mechanical Engineering, Massachusetts Institute of Technology, 1993.

17. Shaw, B. T. II, Hoult, D. P., Wong, V. W.: "Development of Engine Lubricant Film Thickness Diagnostics Using Fiber Optics and Laser Fluorescence," SAE Paper 920651, 1992.

18. Hoult, D. P., Lux, J. P., Wong, V. W. and Billian, S. A.: "Calibration of Laser Fluorescence Measurements of Lubricant Film Thickness in Engines," SAE Paper 881587, 1988.

19. Cherry, T. A.: "Gasflow Computer Code Calibration Using a Single Cylinder Diesel Engine," S. M. Thesis, Department of Ocean Engineering, Massachusetts Institute of Technology, 1991.

20. Deutsch, E. J.: "Piston Ring Friction Analysis from Oil Film Thickness Measurements," S. M. Thesis, Department of Mechanical Engineering, Massachusetts Institute of Technology, 1994.

21. Wong, V. W., Tian, T., Lang, H. and Ryan, J. P.: "A Numerical Model of Piston Secondary Motion and Piston Slap in Partially Flooded Elastohydrodynamic Skirt Lubrication," SAE Paper 940696, 1994.

22. Ariga, S., Sui, P. C. and Shahed, S. M.: "Instantaneous Unburned Oil Consumption Measurement in a Diesel Engine using SO_2 Tracer Technique," SAE Paper 922196, 1992.

Appendix A: Calculations

This appendix contains calculations in support of various parts of this thesis; each calculation is provided as a separate enclosure.

List of Enclosures

I. Unit Definitions

$cm \equiv 1L$ $g \equiv 1M$ $sec \equiv 1T$ $dpm \equiv 1Q$

$lb \equiv g \cdot 453.6$

$min \equiv sec \cdot 60$

$ml \equiv cm^3$

II. Input Data

Ambient Temperature:	$T_a = 23$	(All temperatures are in Celsius.)
Ambient Pressure:	$P_a = 769.3$	(All pressures are in Torr.)
Relative Humidity:	$H_r = 60.0$ %	
Engine Speed:	$RPM = 2033$	
Load Cell:	$Load = 22.2 \cdot lb$	
Initial Fuel Weight:	$FW_i = 62.7 \cdot lb$	
Final Fuel Weight:	$FW_f = 61.5 \cdot lb$	
Fuel Measure Time:	$T_f = 6.75 \cdot min$	
Activity, Oil Sample:	$A_o = 66236 \cdot dpm$	
Vol, Oil Sample:	$V_o = 0.009019 \cdot ml$	
Activity, Water Samp:	$A_w = 38132 \cdot dpm$	
Vol, Water Sample:	$V_w = 1 \cdot ml$	
H/C Ratio, fuel:	$HC_f = 1.88$	
H/C Ratio, oil:	$HC_o = 1.89$	
Oil Density:	$D_o = 0.888 \cdot \dfrac{g}{ml}$	
Water Density:	$D_w = 1.000 \cdot \dfrac{g}{ml}$	

III. Assumptions

This set of calculations assumes the following:

a. The engine is operating at an equivalence ratio of 1,
b. Linear interpolation for the saturation vapor pressure of water; this is based upon the assumption that temperature will stay within 5 degrees of 20 degrees Celsius.

IV.   Specific Humidity Calculations

Saturation pressure of water vapor in air at the ambient temperature:

$$SP_w = \frac{T_a - 20}{5} \cdot 4.6 + 17.4$$

$$SP_w = 20.16 \qquad \text{Torr}$$

Partial Pressure of Water:

$$PP_w := SP_w \cdot \frac{H_r}{100}$$

$$PP_w = 12.096$$

Ambient Pressure as read from the barometer, must be correct for temperature effects on the mercury. The appropriate correction are instrument specific. For the instrument used in this experiment, the corrections from 15 to 25 degrees Celsius range from approximately -2.0 to -2.25 Torr; correction in all cases of -Torr has been applied.

Corrected ambient pressure:

$$P_{ac} := P_a - 2$$

$$P_{ac} = 767.3 \qquad \text{Torr}$$

The average molar weight of dry air (approximately 20% oxygen and 80%) nitrogen is 28.8, and the molar weight of water is 18.0. For a given volume of a gas mixture, the individual gases will occupy the fraction of the volume corresponding to their partial pressures.

$$MW_w = 18.0$$

$$MW_{air} = .2 \cdot 32 + .8 \cdot 28 \qquad\qquad MW_{air} = 28.8$$

Specific Humidity (lb H2O/lb dry Air):

$$H_s := \frac{PP_w \cdot MW_w}{\left(P_{ac} - PP_w\right) \cdot MW_{air}}$$

$$H_s = 0.01$$

V. Fuel Rate

$$R_f := \frac{FW_i - FW_f}{T_f}$$

$$R_f = 1.344 \cdot mass \cdot time^{-1}$$

VI. Water Formation Constants

The water formation constants for fuel and oil (Kf and Ko) express the number of pounds of water produced for every pound of hydrocarbon burned. They are calculated from the stoichiometry of the combustion equation. In each case the single variable is the H/C ratio.

$$K_f := \frac{9 \cdot HC_f}{12 + HC_f}$$

$$K_f = 1.219$$

$$K_o = \frac{9 \cdot HC_o}{12 + HC_o}$$

$$K_o = 1.2246$$

VII. Air to Fuel Mass Ratio

To simplify the experimental apparatus, no air flow measurement was taken. It is therefore necessary to establish the air to fuel mass ratio (Kaf) in stoichiometric burning.

$$K_{af} = \frac{34.4 \cdot HC_f}{12 + HC_f}$$

$$K_{af} = 4.6594$$

VIII. Air Rate

$$R_a := R_f K_{af}$$

$$R_a = 6.2622 \cdot mass \cdot time^{-1}$$

119   Encl. 1

IX. Specific Activities

Specific Activity, Water:

$$SA_W := \frac{A_W}{V_W} \cdot D_W^{-1}$$

$$SA_W = 3.8132 \cdot 10^4 \cdot mass^{-1} \cdot charge$$

$$SA_o := \frac{A_o}{V_o} \cdot D_o^{-1}$$

$$SA_o = 8.2703 \cdot 10^6 \cdot mass^{-1} \cdot charge$$

X. Oil Consumption Rate

The oil consumption rate is calculated from the equations given in SAE paper #700052.

$$R_o := \frac{R_f \cdot K_f + R_a \cdot H_s}{\left(\dfrac{SA_o}{SA_W}\right) - K_o}$$

$$R_o = 0.0079 \cdot mass \cdot time^{-1}$$

I. Catalyst Efficiency Calculation

Conc. of Cl in exhaust, furnaced bypassed: $HC_{bp} = 715.4$ ppm

Conc. of Cl in exhaust, w/ furnace flow: $HC_{fum} = 11.4$ ppm

Catalyst Efficiency: $Eff_{cat} = 1 - \dfrac{HC_{fum}}{HC_{bp}}$

$$Eff_{cat} = 0.984$$

II. Unit Definitions:

$g \equiv 1M$

$cm \equiv 1L$

$mole \equiv 1T$

$dpm \equiv 1Q$

$ml \equiv cm^3$

For the purposes of tracking units in this derivation, dpm is called a unit of charge and a mole is called a unit of time. These definitions make it possible to use the software for a chemistry problem instead an engineering one.

III. Inputs for Error Calculation

H/C ratio for oil: $n = 1.87$

Density of oil (20 C): $\rho_o = 0.888 \cdot \dfrac{g}{ml}$

Density of water (20 C): $\rho_w = 0.999 \cdot \dfrac{g}{ml}$

Typical Spec. Act., oil: $SA_o = 7343346 \cdot \dfrac{dpm}{ml}$

Typical Spec. Act., sample: $SA_{sample} = 24312 \cdot \dfrac{dpm}{ml}$

121

IV. Unitized Molecular Wt of Oil

For the purpose of this calculation a quantity called the "unitized oil molecule" is defined as a single carbon atom with a fractional hydrogen atom equal in number to the H/C ratio.

$$UMW_O := (12 + n) \cdot \frac{g}{mole}$$

$$UMW_O = 13.87 \cdot mass \cdot time^{-1}$$

V. Weight Specific Activities

Weight Specific Activity of Oil: $WSA_O := \dfrac{SA_O}{\rho_O}$

Weight Specific Activity of Sample: $WSA_{sample} := \dfrac{SA_{sample}}{\rho_W}$

$$WSA_O = 8.27 \cdot 10^6 \cdot mass^{-1} \cdot charge$$

$$WSA_{sample} = 2.434 \cdot 10^4 \cdot mass^{-1} \cdot charge$$

VI. Molar Specific Activities

Molar Specific Activity of Oil: $MSA_O := WSA_O \cdot UMW_O$

Molar Specific Activity of Sample:
$$MSA_{sample} = WSA_{sample} \cdot 18 \frac{g}{mole}$$

$$MSA_O = 1.147 \cdot 10^8 \cdot time^{-1} \cdot charge$$

$$MSA_{sample} = 4.381 \cdot 10^5 \cdot time^{-1} \cdot charge$$

VII. Molar Water Formation Constant of Oil:

$$K_O = \frac{n}{2}$$

Moles of H2O per Mole of Oil:

$$K_O = 0.935$$

VIII. Specific Activity (dpm/mole) of Water from Combustion of Oil

$$MSA_{ow} := \frac{MSA_O}{K_O}$$

$$MSA_{ow} = 1.227 \cdot 10^8 \cdot time^{-1} \cdot charge$$

IX. Mole Fraction of Water from Oil in Sample

$$MF_{ow} := \frac{MSA_{sample}}{MSA_{ow}}$$

$$MF_{ow} = 0.004$$

X. Mole Fraction of Water from Oil in Exhaust Gases

Total number of moles of gas from combustion of one unitized mole of oil (since H/C ratio is close to that of fuel):

$$N_{tm} := 1 + 3.773 \left(1 + \frac{n}{4}\right) + \frac{n}{2}$$

$$N_{tm} = 7.472$$

Molar fraction of exhaust gas water: $EMF_w := \dfrac{\dfrac{n}{2}}{N_{tm}}$

$$EMF_w = 0.125$$

(The preceeding calculation assumes stoichiometric burning.)

$$EMF_{ow} := EMF_w \cdot MF_{ow}$$

$$EMF_{ow} = 4.469 \cdot 10^{-4}$$

or

$$ppm_{ow} := EMF_{ow} \cdot 10^6$$

$$ppm_{ow} = 446.852$$

XI. Resolving ppm C1 to ppm H2O

The actual concentration of unburned hydrocarbons in the oxidation furnace effluent (given in ppm C1) can be resolved into the ppm of H2O that would have been experienced if the hydrocarbons had been burned. This is done by correcting the ppm C1 by the molar water formation constant. The potential water thus described is called "error water".

$$ppm_{ew} := HC_{furn} \cdot K_o$$

$$ppm_{ew} = 10.659$$

XII. Figuring the Error from Inefficiencies in the Catalyst

The upper bound on the error generated because the catalyst does not fully oxidize the unburned hydrocarbons in the exhaust gases is evaluated by assuming that all the unoxidized hydrocarbons in the furnace effluent are from the oil.

$$\text{Error}_{\text{catalyst}} := \frac{\text{ppm}_{ew}}{\text{ppm}_{ow}}$$

$$\text{Error}_{\text{catalyst}} = 0.024$$

Given typical numbers, the maximum error given by catalyst inefficiency is 2.4%

I. Unit Definitions

$$cm \equiv 1L \qquad g \equiv 1M \qquad sec \equiv 1T \qquad dpm \equiv 1Q$$

$$lb \equiv g \cdot 453.6$$

$$min \equiv sec \cdot 60$$

$$ml \equiv cm^3$$

II. Input Data

Ambient Temperature:	$T_a = 23$	(All temperatures are in Celsius.)
Ambient Pressure:	$P_a = 769.3$	(All pressures are in Torr.)
Relative Humidity:	$H_r = 60.0$ %	
Engine Speed:	$RPM = 2033$	
Load Cell:	$Load = 22.2 \cdot lb$	
Initial Fuel Weight:	$FW_i = 62.7 \cdot lb$	
Final Fuel Weight:	$FW_f = 61.5 \cdot lb$	
Fuel Measure Time:	$T_f = 6.75 \, min$	
Activity, Oil Sample:	$A_o = 66236 \cdot dpm$	
Vol, Oil Sample:	$V_o = 0.009019 \cdot ml$	
Activity, Water Samp:	$A_w = 38132 \cdot dpm$	
Vol, Water Sample:	$V_w = 1 \cdot ml$	
H/C Ratio, fuel:	$HC_f = 1.88$	
H/C Ratio, oil:	$HC_o = 1.89$	
Oil Density:	$D_o = 0.888 \cdot \dfrac{g}{ml}$	
Water Density:	$D_w = 1.000 \cdot \dfrac{g}{ml}$	

III. Assumptions

This set of calculations assumes the following:

a. The engine is operating at an equivalence ratio of 1,

b. Linear interpolation for the saturation vapor pressure of water; this is based upon the assumption that temperature will stay within 5 degrees of 20 degrees Celsius.

126

IV. Specific Humidity Calculations

Saturation pressure of water vapor in air at the ambient temperature:

$$SP_w = \frac{T_a - 20}{5} \cdot 4.6 + 17.4$$

$$SP_w = 20.16 \qquad \text{Torr}$$

Partial Pressure of Water:

$$PP_w = SP_w \cdot \frac{H_r}{100}$$

$$PP_w = 12.096$$

Ambient Pressure as read from the barometer, must be correct for temperature effects on the mercury. The appropriate correction are instrument specific. For the instrument used in this experiment, the corrections from 15 to 25 degrees Celsius range from approximately -2.0 to -2.25 Torr; correction in all cases of -Torr has been applied.

Corrected ambient pressure:

$$P_{ac} = P_a - 2$$

$$P_{ac} = 767.3 \qquad \text{Torr}$$

The average molar weight of dry air (approximately 20% oxygen and 80%) nitrogen is 28.8, and the molar weight of water is 18.0. For a given volume of a gas mixture, the individual gases will occupy the fraction of the volume corresponding to their partial pressures.

$$MW_w = 18.0$$

$$MW_{air} = .2 \cdot 32 + .8 \cdot 28 \qquad\qquad MW_{air} = 28.8$$

Specific Humidity (lb H2O/lb dry Air):

$$H_s = \frac{PP_w \cdot MW_w}{\left(P_{ac} - PP_w\right) \cdot MW_{air}}$$

$$H_s = 0.01$$

V. Fuel Rate

$$R_f = \frac{FW_i - FW_f}{T_f}$$

$$R_f = 1.344 \cdot mass \cdot time^{-1}$$

VI. Water Formation Constants

The water formation constants for fuel and oil (Kf and Ko) express the number of pounds of water produced for every pound of hydrocarbon burned. They are calculated from the stoichiometry of the combustion equation. In each case the single variable is the H/C ratio.

$$K_f := \frac{9 \cdot HC_f}{12 + HC_f}$$

$$K_f = 1.219$$

$$K_o = \frac{9 \cdot HC_o}{12 + HC_o}$$

$$K_o = 1.2246$$

VII. Air to Fuel Mass Ratio

To simplify the experimental apparatus, no air flow measurement was taken. It is therefore necessary to establish the air to fuel mass ratio (Kaf) in stoichiometric burning.

$$K_{af} = \frac{34.4 \cdot HC_f}{12 + HC_f}$$

$$K_{af} = 4.6594$$

VIII. Air Rate

$$R_a = R_f K_{af}$$

$$R_a = 6.2622 \cdot mass \cdot time^{-1}$$

IX. Specific Activities
Specific Activity, Water:

$$SA_w = \frac{A_w}{V_w} \cdot D_w^{-1}$$

$$SA_w = 3.8132 \cdot 10^4 \cdot mass^{-1} \cdot charge$$

128

$$SA_o = \frac{A_o}{V_o} \cdot D_o^{-1}$$

$$SA_o = 8.2703 \cdot 10^6 \cdot mass^{-1} \cdot charge$$

X. Oil Consumption Rate

The oil consumption rate is calculated from the equations given in SAE paper #700052.

$$R_o = \frac{R_f K_f + R_a \cdot H_s}{\left(\dfrac{SA_o}{SA_w}\right) - K_o}$$

$$R_o = 0.0079 \cdot mass \cdot time^{-1}$$

XI. Error Analysis

Fuel Rate Error Factor:　　　　$E_{fr} = 1.011628$

Air Rate Error Factor:　　　　$E_{ar} = 1.011628$

Water Pipeting Error:　　　　$E_{wp} = 1 + 10 \cdot 10^{-5}$

Catalyst Inefficiency Error Factor:　$E_{cat} = 1.024$

Oil Pipeting Error:　　　　$E_{op} = 1 + 15 \cdot 10^{-5}$

Counting Error Factor:　　　　$E_c = 1.002$

Oil Dilution Error:　　　　$E_{od} = 1.012$

Oil Activity Error:　　　　$E_{oa} = E_{od} \cdot E_{op} \cdot E_c$

　　　　　　　　　　　　　　　　　　$E_{op} \cdot E_c$

　　　　　　　　　　$E_{oa} = 1.0142$

Water Activity Error Factor:　$E_{wa} = E_{wp} \cdot E_{cat} \cdot E_c$

　　　　　　　　　　$E_{wa} = 1.0262$

Activity Ratio Error Factor:　$E_{ar} = E_{wa} \cdot E_{oa}$

129 　$E_{ar} = 1.0407$

$$R_o := \frac{R_f K_f + R_a H_s}{\left(\dfrac{SA_o}{SA_w}\right) - K_o}$$

Total Error:
$$E_t := \frac{R_f K_f E_{fr} + R_a E_{ar} H_s}{\dfrac{SA_o}{SA_w} \cdot \dfrac{1}{E_{ar}} - K_o} \cdot \frac{1}{R_o} - 1$$

$$E_t = 0.0542$$

$$R_o := \frac{R_f K_f + R_a H_s}{\left(\dfrac{SA_o}{SA_w}\right) - K_o}$$

Encl. 3

I.   Input Data

    A.   Lubricant Specific Data
           Density at Reference Coditions (g/ml):

$$\rho_0 = 0.888$$

                  unit conversion (kg/m^3): $\rho_0 = \rho_0 \cdot 1000$

$$\rho_0 = 888$$

           Walter's Equation Constants:

$$m = 1$$
$$N := 1$$

           Surface Tension @ Reference Conditions (N/m):

$$\sigma_0 = .0266$$

           Temp., Reference for σ (Degrees K): $T_\sigma = 373$

           Temp., Reference for ρ (Degrees K): $T_\rho = 293$

           Surface Tension Proportionality Constant:

$$k = 0$$

    B.   Geometric Data
           Clearance Between the 2nd Land and Liner:

$$D \equiv .312$$

           Top Ring End-gap (mm): $g \equiv 2.376$

           Length, 2nd Land (mm): $l \equiv 4.92$

C. State Data

Temperature, 2nd Land (Degrees K): $T := 450$

2nd Land Film Thickness, Initial (mm):
$$h_i := 0.008$$

Initial Assumption for Puddle Radius (mm):
$$R_i \equiv 3.298$$

Average End-gap Volumetric Flow Rate (l/min):
$$Q_{max} \equiv 59.5$$

$$Q := Q_{max} \cdot \frac{10^6}{60}$$

unit conversion (mm^3/sec):

$$Q = 9.917 \cdot 10^5$$

Time to Q.max (sec): $t_{max} \equiv .000555$

Engine Speed (RPM): $N_{rpm} \equiv 3000$

2. Calculated Data

A. Lubricant Data

Low Shear Kinematic Viscosity (m^2/sec):
$$v := 10^{T^{-m} + 10^N} - 0.6$$

$$v := .000013$$

Density: $\rho := \rho_0 - 0.63 \cdot \left(T - T_\rho\right)$

Low Shear Dynamic Viscosity (kg/(m*sec)):
$$\mu = v \cdot \rho$$

$$\mu = \sigma_0 \cdot 0.434$$

$$\mu_a = 2.294 \ 10^{-5}$$

Low Shear Surface Tension (N/m):
$$\sigma = k \cdot \left(T - T_\sigma\right) + \sigma_0$$

132   Encl. 4

B. Geometric Data

Reference Radius (mm): $R_o := \dfrac{g}{2}$

$R_o = 1.188$

Average Velocity over Puddle (mm/sec):

$$U := \frac{Q}{\pi \cdot D \cdot (R_i - R_o)} \cdot \ln\left(\frac{R_i}{R_o}\right)$$

$\dfrac{\mu}{\sigma} = 0.434$

$U := \dfrac{U}{1000}$

$U = 489.58$ m/sec

Taylor Number: $T_a := \dfrac{\mu \cdot U}{\sigma}$

$T_a = 212.478$

(Defined based upon Shaw numbers pending receipt of lubricant viscosity and surface tension data.)

Reference Area: $A_{ref} := \pi \dfrac{l^2}{2}$

Recalculation of Puddle Radius:
(This calculation is based upon the assumption that "R", the puddle radius, has the square root of the puddle area Taylor number dependence. "Ri" above should be iterated until it is equal to "R"; this method provides the correct solution to the simultaneous equations for puddle radius and average gas velocity, "U".)

$$R = \frac{4 \, l}{T_a^{\frac{1}{3}}}$$

C. Non-Dimensional Geometric Data

Film Thickness (eq. 22, ref 2):

$$h_{star} := 1.30 \cdot \left(U \cdot t_{max} \right) \cdot T_a^{\frac{1}{3}} \cdot \left(\frac{\mu_a}{\mu} \right) + 0.61$$

Puddle Area (eq. 21, ref 2): $A_{star} := \dfrac{15.28}{T_a^{\frac{2}{3}}}$

3. Oil Consumption Calculation
   (The equations used were adapted from equation 23 of reference 2 to adjust for input and output units.)

$$OC_{cycle} := \frac{\rho}{10^6} \cdot h_i \left(h_{star} \right) \cdot A_{ref} \cdot A_{star}$$

$$OC_{cycle} = 6.326 \cdot 10^{-5}$$
                                            g/cycle

Cycle per Second: $n := \dfrac{N_{rpm}}{2 \cdot 60}$

$$n = 25$$

$$OC_{cylinder} := OC_{cycle} \cdot n$$

$$OC_{cylinder} = 0.002$$
                                            (g/sec)/cylinder

$$OC_{engine} := OC_{cylinder} \cdot 4 \cdot 1000$$

$$OC_{engine} = 6.326$$
                                            mg/sec

134   Encl. 4

1. Unit definitions:

$mm \equiv 1L$

$mg \equiv 1M$

$sec \equiv 1T$

$m \equiv 1000 \cdot mm$

$dm \equiv 100 \cdot mm$

$g \equiv 1000 \cdot mg$

$kg \equiv 1000 \cdot g$

$min \equiv 60 \cdot sec$

$l \equiv 10^6 \cdot mm^3$

$$N \equiv kg \cdot \frac{m}{sec^2}$$

2. Given DATA:

Desired OC:	$OC = .028598 \cdot mg$
Density of Oil:	$\rho = 789 \dfrac{kg}{m^3}$
Initial Oil Film Thickness:	$h_i = .006 \cdot mm$
Reference Area:	$A_{ref} = 38 \cdot mm^2$
Dynamic Viscosity of Oil:	$\mu = 0.01155 \dfrac{kg}{m \cdot sec}$
Surface Tension of Oil:	$\sigma = 0.0266 \dfrac{N}{m}$
End-gap:	$g = .305 \cdot mm$

3. Non-dimensional Quantity Determination (h* and A* together).

$$hA = \frac{OC}{\rho \cdot h_i \cdot A_{ref} \cdot 4} \qquad hA = 0.04$$

4. **Taylor Number Determination**

$$Ta = \left(\frac{6 \cdot 15.28}{h\Lambda}\right)^{\frac{6}{7}}$$

$$Ta = 763.099$$

5. **Velocity Determination:** $b = 20$

$$U = Ta \cdot \frac{\sigma}{\mu}$$

$$rat = \frac{\mu}{\sigma} \qquad rat = 4.342 \cdot 10^{-4} \cdot length^{-1} \cdot time$$

$$U = 1.757 \cdot 10^3 \cdot \frac{m}{sec}$$

6. **Desired Puddle Radius:**

$$land := \left(2 \cdot \frac{\Lambda_{ref}}{\pi}\right)^{.5}$$

$$r := 4 \cdot \frac{land}{Ta^{.333}}$$

$$r = 2.158 \cdot mm$$

7. **Desired Q/D ratio:**

$$Ratio := U \cdot \frac{\pi \left(r - \frac{g}{2}\right)}{\ln\left(2 \cdot \frac{r}{g}\right)}$$

$$Ratio = 417.833 \cdot \frac{dm^2}{sec}$$

$$D \equiv 0.7 \text{ mm}$$

$$Q := Ratio \cdot D$$

$$Q = 175.49 \cdot \frac{1}{min}$$

136

This Page Intentionally Blank

Appendix B: Equipment

This appendix contains detailed lists of equipment used during the course of this project. It also contains detail photographs of three Water Collection System components.

Engine Specifications

TYPE	in-line 4 cylinder SOHC
DISPLACEMENT	2.2L
BORE	87.5 mm
STROKE	92 mm
FIRING ORDER	1-3-4-2
NUMBER OF CYLINDERS	4
CYLINDER BLOCK	cast iron
PISTONS	Al alloy
COOLING	water
COMPRESSION RATIO	9.5
RATED POWER	74kW (100hp) @ 5600 rpm
MAXIMUM TORQUE	149 Nm (110 lb-ft) @ 3200 rpm
LUBRICANT	Various
LUBRICANT SYSTEM	Pressure feed-full flow filtration
COOLING SYSTEM	forced circulation
FUEL	indolene

Water Collection System
Equipment and Specifications

Item	Equipment or Specification
Oxidation Furnace	220 VAC, Lindberg Hevi-Duty, Type 59344
Oxidation Tube	Quartz Glass, 1 inch
Catalyst	Pellet Type, Pt-Pd-Rh 3-way, AC Rochester Designation HN11024
Condenser	Fredrichs, 24/40
Sample Pump	115 VAC, Oilless Vacuum, Emerson Model SA55NXGTE-4870
Line Heaters	115 VAC, Tape Type, Thermolyne Heavy Insulated Fibrox
Temperature Sensor	K type (Chromel/Alumel) Thermocouple
Temperature Indication	Omega Engineering, Model 175 (4 channel)
Fuel Consumption Measurement	Balance Scale, Howard-Richardson, Model 5400
High Temp. Tubing	Pyrex Glass / Stainless Steel
Low Temp. Tubing	Rubber
Hydrocarbon Analyzer	Flame Ionization Detector, Rosemount Analytical Model 402
Heater Control	Manually Varied Voltage, Superior Electric "Powerstat"
Sample Flow Indication	Wet Test Meter, Precision Scientific Model 63111
Oxygen Flow Indication	Flowmeter, Matheson Type 603
Pressure Indication	Manometer, Arthur Thomas Co.
Temperatures	
Furnace	600° Celsius
Max. Heater Tape	482° Celsius
Min. Condenser-inlet	50° Celsius
Flow Rates	

Item	Equipment or Specification
Sample	14.2 l/min
Oxygen	1000 ml/min (optimum)
Sample Collection Rate	0.5 ml/min

141

Sample Preparation and Counting Equipment

Item	Equipment
Sample Weight Measurements	Analytical Balance, Mettler AE200
Micro Pipet	1000 ml, Medical Laboratory Automation, Inc.
Analyzer	Liquid Scintillation Analyzer, Packard Model 2500TR
Fluorescing Solution	OptiFluor, Packard Co.
Average Counting Efficiency	0.41
Sample to Solution Ratio	1:10

Figure B-1: Modified Vacuum Adapter
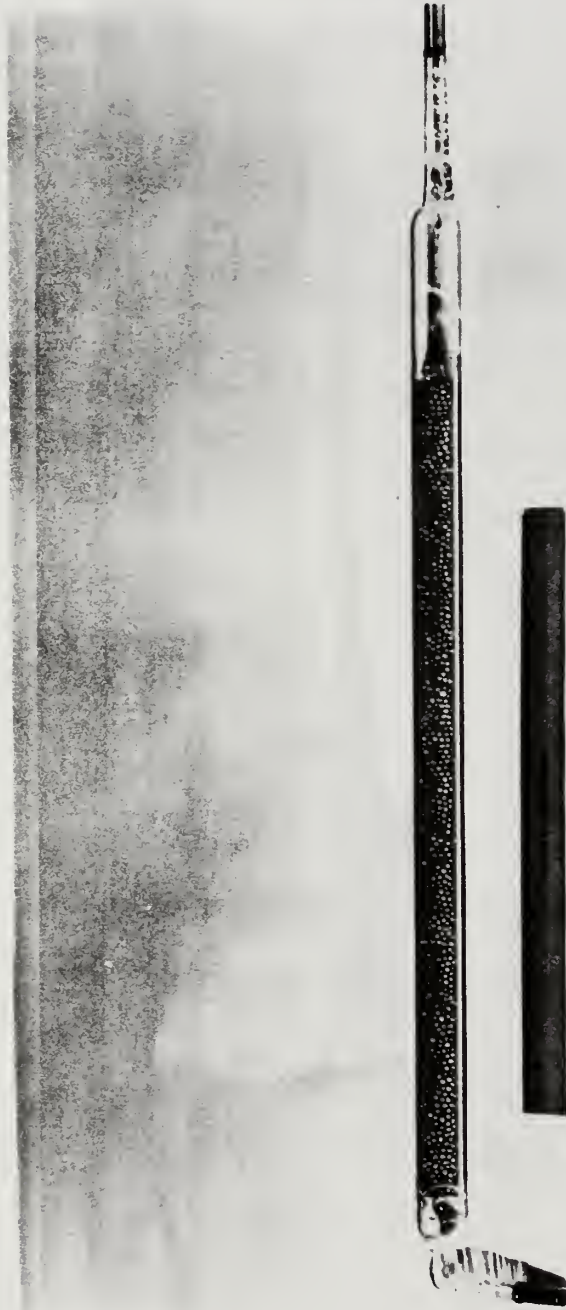
Figure B-2: Catalyst Tube

Figure B-3: Water Trap Arrangement

145

This Page Intentionally Blank

Appendix C: Operating Procedures and Logs

This appendix presents the final version of the operating procedures and logs used in this project. They are intended to be used in conjunction with a system "walk-through" as some of the terms are not self-explanatory.

Enclosure 1:   Engine Start-up, Normal Shut-down and Emergency Shut-down Procedures

Enclosure 2:   Engine Operating Log

Enclosure 3:   Piston Removal/Installation Procedure

Enclosure 4:   Oil Consumption Measurement Procedure Using Tritium Tracer Procedures

Enclosure 5:   WCS Sample Log

Enclosure 6:   Procedure for Drawing an Oil Sample

Enclosure 7:   Oil Sample Log Sheet

Step #	Component	Position or Action
*****	**Pre-Startup Checks**	*******
1	Engine Oil Dipstick	In operating range
2	Engine Coolant	In sight glass
3	Dyno Oil Sump	In sight glass
4	Dyno Foundation	Clear of fluid puddles, Drip pan in place
5	Engine Foundation	Clear of oil puddles
6	Fuel Can	Half Full Minimum
*****	Valve Line-up	*****
7	Circulating (Circ) Water Supply Valve (on south wall)	FULL OPEN; check supply pressure 40 to 60 psi on black scale.
8	Circ Water Supply Manifold	a. Oil Cooler Supply: Check OPEN b. Coolant HX Supply: Check OPEN c. Fuel Cooler Supply: Check OPEN (These are the red handled valves on the circ water supply manifold)
9	Circ Water Drain Manifold	Coolant Head Tank Vent Isolation: Check OPEN
10	Steam Supply Manifold	Check all valves SHUT
11	Coolant Head Tank Drain Valve	Check SHUT
12	Coolant Head Tank Isolation Quick-throw Valves	Check OPEN (in-line position)

148

Enc.

Step #	Component	Position or Action
13	@ Fuel Manifold	a. Pump Discharge Control Valve: Check TO ENGINE position b. Fuel Return Isolation: Check OPEN (both valves should be pointing at the 9:00 position.)

13a	Oil Cooler Recirculating Pump	Check:
		   a. Coupling is fully mated.
		   b. Three-way discharge valve is positioned to discharge to the sump.

19	Power Strips on back of Control Panel	Switch ON, light ON
15	Ignition/Fuel Power Strip	Switch ON, light OFF
16	Heat Exchanger Oil Out Setpoint	190 degrees F.
****	**Dyno Startup**	****
17	"Sloan-lab, GE Dyno" breaker in Rm 31-037C (Key #187)	ON position (indication light on breaker burned out) Check indication on Dyno Control Panel (Blue light)
18	Trench Fan Controller	ON, light ON.
19	MG-SET switch on Dyno control panel	ON
20	DYNO REV SWITCH @Dyno control panel	REV (starts dyno oil pump) (allow 5 minute warm-up from this point before performing step number 24)
21	Power Switch for Stepper Motor (rocker switch @bottom of Dyno control cabinet)	ON, light ON

Step #	Component	Position or Action
22	At Engine Control Panel	a. RPM display: ON, Light ON b. Temp Display: ON, Light ON c. Oil Recirc Pump: ON, Light OFF d. Load Cell Readout: ON (reading zero)
23	Dyno MANUAL RHEO	Check at "0" position by using the DYNO rocker switch in the "lower" direction until you hear the rheostat click.
24	Dyno START SWITCH	**********Critical Step************** START; <u>MANUAL RHEO</u> to increase speed to 1200 RPM as indicated by manual rheo indication of "10". (Electronic indication responds too slowly for this initial adjustment.)
25	Engine OIL Pressure	**********Critical Step*********** 70 to 80 psi, cold Idiot light off. **IF EITHER LOW PRESSURE OR IDIOT LIGHT CONDUCT IMMEDIATE DYNO SHUTDOWN** (Step 7 of Normal Shutdown Procedure)
29	Load Cell Readout	Positive (+) number [indicates that the engine is motoring]
27	@ Dyno	a. Oil Pressure: approx. 10 psi b. Drip-o-lators: atleast 1drip/5sec. c. Fan: Positive Air Flow.
28	Wall Fan	ON Point fan at engine exhaust manifold.
29	Thermocouple Readouts	Check for proper operation; "EEE" means an open thermocouple
****	**Engine Startup**	****
30	Throttle manometer	*********Critical Step*********** 10 inches of mercury
31	Ignition Switch	ON Verify 12 to 14 VDC indicated.
32	Load Cell Readout	Check negative (-) number; indicating that the engine is firing.

Engine Normal Shutdown Procedure

Step#	Component	Position or action
1	THROTTLE Rocker	10 inches of mercury
2	MANUAL RHEO	1200 RPM
3	THROTTLE Rocker	10 inches of mercury
4	OIL OUT Temp	Maintain light load until less than 95 degrees Celsius.
5	IGNITION Switch	OFF
6	Load Cell Readout	Check Load (+)
7	OIL OUT Temp	70-80 degrees C for proper cooldown
****	**Secure Dyno**	****
8	MANUAL RHEO	*********Critical Step*********** Slew to "0" and <u>immediately</u>:
3	Dyno START SWITCH	STOP **(Counter Clockwise)**
10	Dyno REV SWITCH	OFF **(Counter Clockwise)**
11	MG-SET SWITCH	STOP **(Counter Clockwise)**
12	@ Engine Control Panel	Take all remaining switches to OFF.
13	Power Strips of back of Engine Control Panel	OFF, light OFF
14	Circ Water Supply Valve	Shut
15	Dyno Oil Sump	In sight glass
16	"Sloan-lab, GE Dyno" Breaker in Rm 31-037C (key# 187)	OFF
17	Vent Fan Controller	After visually verifying that no other lab engines are running, OFF

Emergency Shutdown Procedure
(Oil Trouble Light On)

Step#	Component	Position or Action
1	IGNITION Switch	OFF
2	MANUAL RHEO	Rapidly to "0" and <u>immediately</u>
3	Dyno START SWITCH	STOP
****	Continue normal shutdown procedure	****

Chrysler 2.2L Engine Operating Log

Item	Min	Norm	Max					
Engine Hours								
RPM								
Throttle								
Load Cell								
Engine Temperatures								
1								
2	85		95					
9								
4	85		105					
5								
8			40					
7								
8								
9								
Oil Press.		70						
Ignit. Volts		13						
Fuel Press.		20						
Coolant Pres.		0						
Dyno Oil Press.	2		10					
Dyno Sump Level		1/2						
Dripolators (1 drip/5 sec)								

*1: Coolant into engine   6: Fuel into engine
2: Coolant out of engine   7: Intake air
3: Oil out of cooler (OOC)   8: Coolant, Cylinder 2
4: Oil Sump   9: Liner, Cylinder 4
5: Exhaust Gas (OOC)

Piston Removal/Installation Procedure
for Chrysler 2.2 Liter Engine

Tool List:
    a. Bundle of Rags
    b. Bundle of Paper-towels
    c. Head Gasket
    d. Manifold Gasket
    e. Rubber Bands
    f. Q-Tips
    g. Gasket Glue
    h. Box / open end wrenches:
        - 7/16"
        - 1/2"
        - 9/16"
        - 11/16"
        - 3/4"
        -
    i. Sockets (3/8" drive, 6 point):
        - 1/2"
        - 8mm
        - 10mm
        - 13mm
        - 13mm deep
        - 14mm
        - 15mm
    j. Coolant Drain Tank
    k. Oil Drain Tank
    l. 500ml beaker
    m. Pliers
    n. Set of slot screwdrivers
    o. Oil drain adapter
    p. Coolant drain adapter
    q. Pipe wrenches:
        - 14"
        - 24"
    r. Socket drives:
        - 3/8" ratchet
        - 1/2" ratchet
        - 1/2 to 3/8 adapter
        - 3/8" long extention
        - Two 3/8" short extentions
        - 3/8" speed wrench
    s. Electric Drill w/ small brush attachment   t   .
Acetone
    u. Engine oil
    v. Wire toothbush
    w. Channel-locks
    x. Nylon Hammer
    y. Ball-pien hammer
    z. Brass "chisel"
    aa. Ring Compressor

bb. Thread Protectors
        cc. Torque Wrench: required range 40 to 120 lbf-ft (1/2"
drive, calibrated in "lbf-ft")
        dd. Set of Cross-recessed (Philips) screwdrivers.
        ee. 12" Crescent Wrench
        ff. Special Tool for Cam Pulley alignment.
        gg. Anti-seize

Procedure:

#	Tools	Action
Engine Oil Flush		
1a	Oil Drain Adapter	Drain Tracer Oil, Hang "Do Not Operate" sign on Dyno Start Switch
1b	Crescent Wrench, 7/8"	Disconnect and cap Oil Cooling System connections. Be careful not to cross-thread the swage-lok fittings.
1c	Flush filter kit. 1st Flush Oil	Remove and store the Tracer Oil filter; install the 1st Flush filter. Fill engine with 1st Flush Oil.
1d		Operate Engine until oil is 50 degrees C.
1e	Flush filter kit, 2nd Flush Oil	Remove and store 1st Flush oil and filter. Install 2nd flush oil and filter.
1f		Operate engine until oil is 50 degrees C.
1g	Flush filter kit, 3rd Flush Oil	Remove and store 2nd Flush oil and filter. Install 3rd Flush oil and filter. 3rd Flush oil should be the same grade as the Tracer Oil.
1h		Operate the engine until the oil is atleast 50 degrees C.
1i		Drain and store 3rd Flush oil and filter. Install Tracer Oil filter.
Water Collection System		
2		Unplug 110 and 220 VAC.
3		Unplug heaters on sample line.

#	Tools	Action
4	9/16"	Disconnect O2 line from sample line, <u>bag end</u>.
5	9/16"	Disconnect Sample line from furnace tube; <u>bag ends.</u>
6		Remove sample line bracket from cart.
7		Remove sample line from exhaust line bracket.
8	11/16"	Remove sample line from exhaust line. Cap exhaust line and bag end of sample line.
9		Disconnect water supply
10		Remove WCS cart. Set up parts cart on starboard side of engine.
Engine		
11		Isolate coolant head tank.
12		Unplug all thermocouples on engine.
13		Remove air cleaner. Set on work bench (WB).
14		Unplug pressure sensor.
15		Unplug wire from O2 sensor.
16		Unplug sensing lines #6 and #7.
17		Disconnect wiring harness from throttle block. (4 numbered connections)
19		Disconnect sparkplug wires.
19		Remove coolant sensor (#5).
20	15mm socket	Remove 2 ground connections.
21		Hook up coolant drain adapter under engine.
22		Disconnect headtank-to-thermostat hose at thermostat.
23	Coolant Drain Tank	Drain Coolant.

#	Tools	Action
24	Coolant Drain Tank	Disconnect coolant by-pass hose at the thermostat. Drain coolant in line.
25	Pliers	Disconnect coolant lines to throttle block.
26		Remove adapter.
27		Disconnect fuel tank and remove.
28	Slot Screwdriver (SS)	Remove fuel lines from intake manifold. Retighten hose clamps to prevent loss.
29	500 ml beaker	Drain residual fuel.
30		
31		
32		Remove dipstick; place on parts cart.
33		Shut oil drain valve; remove and bag adapter.
34	14" Pipewrench (PW), 24"PW, 7/16"	Disconnect #4 cylinder exhaust line. Disconnect #4 exhaust line from mounting bracket.
35	1/2", 1/2"socket	Disconnect main exhaust line. Put exhaust donut on parts cart.
36	10mm socket	Remove timing belt cover. Place cover on workbench.
37	15mm socket, long extention.	Loosen timing belt idler pulley.
38		Slide timing belt off cam pulley.
39	10mm socket, 13mm socket, long ext.	Remove valve cover. Place on parts cart.
40	13mm socket	Remove EGR line. Place EGR line on parts cart place gaskets and bolts in throttle block.
41		Disconnect stepper motor.

#	Tools	Action
42	10mm socket, short ext., long ext.	Disconnect intake manifold; place manifold on parts cart.
43	10mm socket, short ext., long ext.	Remove exhaust manifold; place on parts cart.
44		
45		Loosen head bolts according to loosening sequence diagram.
46	15mm socket	Remove cylinder head; place on parts cart <u>on rags</u>.
47	10mm socket, 8mm socket, 2 short ext., long ext.	Remove oil pan. Place on parts cart.
49	Rag	Wipe coolant out of cylinders.
49	Q-Tip	Swab headbolt holes in block dry.
50	Elec.Drill, 1" drill attachment, Small handheld steel brushes, rags, acetone, engine oil	Clean cylinder walls.
51	Channel-locks, Nylon hammer, Ball-pien hammer, Brass "chisel" 14mm socket w/extension.	Remove con-rod bearing caps. Place on parts cart. When pistons are available, put caps back on appropriate con-rods.
52	Hammer handle	Rotate piston to top of stroke. Then rotate crank free of piston. Use hammer handle on bottom of piston to remove piston. <u>Place piston on parts cart; protect with rag.</u>
Piston Re-installation		
53		Bring crank to top of piston stroke.

#	Tools	Action
54		Install thread protectors made of rubber tubing.
55		Stagger compression rings by 180 degrees for design ring position. See manual for exact azimuthal position.
56	Oil, Rags	Smear side of piston with oil.
57	Ring Compressor, Large SS	Install compressor being careful to ensure that rings are seated in groove. Leave 1" protruding at bottom of skirt.
58	Oil	Put oil on bearing liner and oil channels.
59		Insert piston in cylinder with the numbers toward the distributor side.
60	Nylon hammer	Tap compressor level so that the bottom part is in complete contact with the top of the block.
61	Hammer handle	Drive piston into place.
62		Rotate crank to BDC for piston while pushing down on piston.
63		Check bearing liner did not rotate out of proper position.
64	Thread protectors.	Remove thread protectors. Place on parts cart.
65		Inspect bearing cap and liner for cleanliness and burrs.
66	Oil	Coat liner with oil.
67	14mm socket, Torque Wrench	Install bearing cap. Torque to 20 lbf-ft, then to 40 lbf-ft.
68	10mm socket, 8mm socket	Install oil pan. Install 8mm bolt first. Do not tighten until all bolts are in place.
Timing Setup		

159

#	Tools	Action
69		Rotate cam follower manually to purple-purple.
70	Crossed, recessed screwdriver(CRS) 3/4"	Rotate crank to zero degrees for #1 cylinder; check that distributor rotor is pointing to #1 wire.
Cylinder Head Installation		
71	Gasket glue, Q-Tips	Put thin film of glue around the oil supply hole of the head and the block (Aft, port side of block). Use Q-tip to remove the glue from the edge of the holes.
72		Install head gasket on block.
73		Install cylinder head on block using bolts for alignment.
74	15mm socket, Torque wrench	Torque bolts per torquing pattern in manual. Step 1: 45 lbf-ft. Step 2: 65 lbf-ft. Step 3: 65 lbf-ft. Step 4: 1/4 turn (> 90 lbf-ft)
Timing Completion		
75	Special Tool	Line up cam pulley per the picture in the manual.
78		Install timing belt. Ensure that the port side (distributor side) is under tension.
77	Crescent wrench	Tighten tensioning pulley (CCW) until timing belt is firm.
Final Installations and Connections		
78	13mm deep socket, 10mm socket, long ext.	Install valve cover. Place two studs in the front. (105 lb-in)
79		
80		Connect oil cooling system.
81		Install new manifold gasket.
82	10mm socket, short ext.	Install exhaust manifold. (200 lb-in)

#	Tools	Action
83	10mm socket, short and long ext.	Install intake manifold and throttle block. (200 lb-in)
84	13mm socket, short ext.	Install EGR line.
95	15mm socket	Connect 2 cylinderhead ground wires.
86		Re-install sensing lines #6 and #7.
87	SS	Install thermostat and thermostat by-pass hoses
8%	Anti-seize	Install Exhaust lines. Use anti-seize compound
89	Pliers	Install coolant lines to throttle block.
96		Install harness connections to throttle block.
91		Install thermocouples.
92		Connect O2 sensor.
93		Connect pressure sensor.
94		Connect sparkplug wires.
95		
96		Check the PVC line connections to the valve cover.
97		Check shut the following valves: -Fuel Drain Valve -Oil Drain Valve -Coolant Drain Valve
98		Open the following valves: - Coolant head-tank isolation. - Both oil cooling system isolations.
99		Refill oil system.
100		Refill coolant system at head tank.
101		Vent cooling system at thermostat thermocouple.
102		Conduct pre-operation line-up per the engine operating instructions.

#	Tools	Action
102a	Timing Light	Connect Timing Light and ensure coolant sensor (#5) is disconnected. Be careful to position the Timing Light pickup with the appropriate side toward the sparkplug.
102b		Remove fuel pump fuse.
102c		Motor engine at 850 RPM
102d	1/2"	Check timing at 12.5 degrees BTC as indicated on the harmonic balancer. Adjust timing if necessary by rotating distributor. If unable to attain the proper timing with the distributor, the cam follower must be readjusted per step 69.
102e		Secure engine. Remove Timing Light. Re-install fuse and coolant sensor (#5).
103		Conduct tightness check on fuel system by operating pump and throttling (to 50psi system pressure) the return line at the fuel manifold. Check particularly the connections to the throttle block.
104		Re-connect WCS. Ensure that O2 line is connected and O2 isolation valve is open.

Oil Consumption Measurement Procedure
Using Tritium Tracer Procedures

Step	Potential Radiologic Hazard	Action
1		Don Surgical Gloves
2		Unplug or switch "off" sample pump.
3		Turn on master power strip. - Ensure both the thermocouple (TC) reader and the line heater power strip are energized.
4		Set TC reader to monitor channel 1: Sample line temperature.
6		Set Variac at "80".
6		Set furnace at 600 C.
7		Shut Water Collection System (WCS) isolation valve.
8		Open: O$_2$ isolation valve, Sample Bypass Valve, Circulating Water (CW) throttle valves on WCS, CW Manifold Supply (on south wall) WCS CW isolation on CW manifold
9		Turn on furnace.
10		Bring Engine to operating temperature. This means that the following conditions exist for a given set of load conditions: a. Oil Temp Steady (recirc motor cycling on the thermostat). b. Liner Temp Steady.
11		Verify the following temperatures prior to initiating sample flow. a. 400 <Sample Line Temp<470 C. b. Furnace Temp > 550 C.
12		Set O$_2$ flow at 27mm on the 603 tube.
13		Start WCS sample pump.
14		Open WCS Isolation Valve
15		Shut slowly, the Sample Bypass Valve.

Step	Potential Radiologic Hazard	Action
16		Collect 5 minutes of purge water in a round bottom flask. This ensures that the tritium concentration in the condensers will reflect that concentration in the exhaust gas.
17	yes	Remove the purge flask and replace with a sample collection flask (Graduated flask).
18	yes	Empty the purge flask in the sink and flush sink. (Regulations allow the disposal of tritiated water up to the concentration of 100 micro-Curries/ml down a sink drain.)
19		Collect 10ml of sample: Ensure the following conditions exist during sampling: a. Constant Throttle Setting b. Constant Dyno Speed setting Minimum sample time is 5 minutes.
20		During sampling: a. Fill out sample log sheet. b. Ensure fuel rate is sampled over a minimum of a 5 minute period. c. Fill out a sample label on Radiation tape with the following information: H^3_1 Sample #____ Date:____ d. Place label on clean sample vial.
21	yes	Remove sample flask and replace with purge flask. (Care should be taken to avoid breaking the central extention on the vacuum adapter as this is custom made to prevent carry-over.)
22		Open Sample Bypass Valve.
23		Shut WCS Isolation Valve.
24		Secure WCS sample pump.
25	yes	Using a pipet bulb and a 10ml pipet, transfer 5 to 7 ml's of sample to a sample vial.

Step	Potential Radiologic Hazard	Action
26		Double check that the sample # is on the sample vial.
27	yes	Place pipet in contaminated pipet holder.
28	yes	Condensers should be flushed according to the following procedure prior to changing sample conditions: a. Remove condensers b. Flush with tap water c. Flush with 50ml of DI water d. Blow dry with compressed air
29		Secure the following: a. O_2 supply at the cylinder valve b. CW manifold supply and WCS isolation c. Furnace d. Master power strip.

WCS Sample Log

Parameter								
Sample #								
Date								
Ambient Temp								
Ambient Pressure								
Relative Humidity								
Engine Parameters								
RPM								
Throttle								
Load Cell								
Liner Temp								
Oil Sump Temp								
Air Inlet Temp								
WCS Parameters								
Line Temp								
Gas In Temp								
Furnace Temp								
Condenser In Temp								
Variac Setting								
Fuel Rate Calculations								
Initial Wt.								
Final Wt.								
Time Duration								
Sample Times								
Time Started								

Enc

Parameter									
Time Isolated									

Procedure
for
Drawing an Oil Sample

Step	Equipment	Action
1	Oil Adapter	Don latex gloves and attach adapter to the oil pan.
2	100 ml mixing cylinder and Mettler Balance	Remove the stopper to the cylinder and place it on the balance, re-zero the balance.
3	100 ml mixing cylinder	Draw <u>approximately</u> a 10 to 20 ml sample from the oil pan.
4	Mettler Balance	Weigh the oil sample; <u>record weight.</u>
5	----------------	Allow sample to cool to ambient temperature.
6	1000 ml buret	Ensure that the buret is full of heptane or some other non-polar solvent like toluene.
7	100 ml mixing cylinder	Dilute the oil sample to between 90 and 99 ml total volume with solvent from step 5. Record volume under 1st dilution volume. Mix thoroughly: this means that you cannot see any oil film on the side of the mixing cylinder.
8	10 ml graduated pipet, pipet bulb, 250	Pipet approximately 10 ml into the 250 ml mixing cylinder. Record volume transferred (read it off the pipet).
9	1000 ml buret	Dilute mixture in the 250 ml cylinder to about 150 ml; record the total volume.
10	Scintillation Vial (Glass), Clean 10 ml pipet, pipet bulb.	Transfer between 5 and 10 ml into the scintillation vial. Ensure that the cap of the vial is numbered.
11	------------	Dispose of rad waste properly and wash glassware.

Oil Sample Log Sheet

Sample #:	O-	O-	O-	O-	O-	O-	O-
Date:							
Oil Designation:							
Initial Volume:							
1st Dilution Vol:							
2nd Sample Vol:							
2nd Dilution Vol:							

Sample #:	O-	O-	O-	O-	O-	O-	O-
Date:							
Oil Designation:							
Initial Volume:							
1st Dilution Vol:							
2nd Sample Vol:							
2nd Dilution Vol:							

Sample #:	O-	O-	O-	O-	O-	O-	O-
Date:							
Oil Designation:							
Initial Volume:							
1st Dilution Vol:							
2nd Sample Vol:							
2nd Dilution Vol:							

Encl 7

169

This Page Intentionally Blank

Appendix D: ROCS Validation and Evaluation

D.1   General: This chapter evaluates the errors involved in the ROCS, discusses two areas where performance optimization was conducted and finally makes recommendations as to what future improvements might be considered.

D.2   Error Evaluation: A system error evaluation was conducted on the ROCS.   The accuracy of the system (A) is defined as:

$$A = 1 - E \qquad\qquad (D.1)$$

where: E is the aggregate system error.

This analysis was on-going during Test Matrix C.[85] Corrections were made to equipment and sampling techniques to correct problems encountered.   By the completion of Test Matrix C, the equipment and procedures were considered mature and no further modifications to either were made.   Table D-1 shows the initial and final evaluations of component errors.

Table D-1: ROCS Error Evaluation		
Measurement	Initial Error	Final Error
Oil Dilution	1.7%	1.2%
Fuel Weight	4.2%	1.2%
Oil Sample Preparation	2.0%	0.015%
Water Sample Preparation	1.0%	0.010%
Sample Counting	0.2%	1.2%
Catalyst Inefficiency	2.0%	2.4%
System	10.1%	5.4%

The errors were determined by the following methods:

---

[85]To avoid reducing the validity of that test matrix, the number of readings of a given measurement was increased so that those readings could be analyzed statistically; in such cases a normal distribution was assumed and the mean value was used for further calculations.

171

Single Measurements: Each measurement that is used as a single data point, like a volume measured in a graduated cylinder, is evaluated by assuming that the error in any careful measurement can be assumed to be one half of the finest scale gradation. The percentage error is taken to be the error divided by a typical measurement.[86]

Statistical Measurements: In the cases where there is no obvious way to evaluate the error (like the LSC or the micropipet volumes), multiple measurements of a standardized quantity were made. The measurements were analyzed for consistency and the standard deviation taken as the error. This is an admittedly simplistic approach, but gives a good indication of the relative magnitude of the system errors.

Catalyst Inefficiency: Obtaining an absolute measure of the systemic errors caused by the unoxidized hydrocarbons is difficult; separation of unburned hydrocarbons from the post catalyst gases is difficult because of the diverse nature of these compounds and because some are polar enough to be miscible in exhaust water. As an alternative to an involved chemical extraction, it was assumed that all the HC leaving the catalyst bed were derived from the lubricating oil. This assumption gives an upper bound on the error due to non-oxidation in the catalyst. Taking as given the geometric constraints of the catalyst tube, the largest source of catalyst inefficiency is sample gas entrance temperature. As part of initial assembly, this temperature was evaluated and found to be close to 140° Celsius (360° from the temperature required for efficient catalyst operation). Line heaters and insulation were added increasing entrance temperature to approximately 250° Celsius with the line heaters operating just below burnout temperature. No further thermal improvement to the catalyst efficiency was possible. The calculation of the catalyst inefficiency error is included as part of Appendix A.

Multiple Measurement Error: In the case where a parameter is derived from multiple measurements (such as multiple dilutions) the error was calculated from the following formula:

---

[86]For example, if 150 ml of liquid is measured in a 250 ml graduated cylinder with 1 ml gradations, the error is

$$E_{volume} = \frac{0.5}{150}$$

or 0.33 percent.

$$A_{total} = \prod_i A_i \qquad\qquad (\text{D}.2)$$

where: A_i is the accuracy of the ith component measurement.

System Error: The overall system error was calculated by applying the worst-case error to each measurement and performing a complete oil consumption calculation. The resulting flawed oil consumption rate was then compared to the results of the same calculation without the error. This calculation is included in Appendix A.

Error Reduction: It was found that the volumetric measurements involved in Oil Dilution, Oil Sample Preparation and Water Sample Preparation were the principle contributors to those errors; as many of the volumetric measurements as possible were changed to gravimetric determinations to reduce those errors. For example, micropipets were found to have an error of about 2%; if subtractive weighing on an analytical balance was used to measure the same quantity of liquid, the error was approximately 0.015%.

Originally, the largest error in the system was that of the fuel consumption measurement. This error was reduced by increasing the length of time over which fuel consumption rate was measured. The optimum appears to be between 8 and 10 minutes. Longer samples are not desirable because at least two samples should be taken at each set of engine operating conditions to provide a double check (concurrence between the samples).

D.3 Performance Optimization: The performance of the ROCS can be evaluated in two areas:
    a. sample rate and
    b. measurement accuracy.
Test Matrices A and B were specifically designed to provide data to aid in performance optimization.

Condenser Configuration: Test Matrix A evaluated the system performance using five different condenser configurations. Table D-2 presents the results of that evaluation.

Table D-2: Condenser Performance					
	Condenser Configuration (defined in Chapter 4)				
Criteria	A	B	C	D	E
Steady State Sample Rate (ml/min)	0.49	0.47	0.52	0.58	0.65

173

Table D-2: Condenser Performance					
	Condenser Configuration (defined in Chapter 4)				
Initial Sample Response Time[87] (sec)	90	55	58	117	125
Purge Time (sec)	312	55	20	>360	>360

The twin condenser improved in steady state sample rate, however, _all_ configurations met the 9.4 minute sample time criteria for a 4 ml sample. Experience showed that the minimum useful sample period is about 8.5 minutes for one-man operation of the system and the engine; all the ancillary tasks required in sampling (log keeping, etc.) are actually more time limiting than the sample period. More important are the Initial Sample Response and Purge times; these two times dictate how soon after a change in engine operating conditions valid samples can be obtained. _Configuration E, a single coiled condenser, is considered the optimum condenser configuration._ In the course of conducting Test Matrix A, it was discovered that applying vacuum grease to the fittings of the condenser assembly increased sampling rate by as much as 40%.[88]

Supplemental Oxygen Flow: To improve the catalyst efficiency within the constraints discussed above, supplemental oxygen is added to the sample gas upstream of the catalyst bed. Test Matrix B was designed to optimize the amount of oxygen added to the sample; as discussed in Chapter 4, excess supplemental oxygen slows sampling and can drive down catalyst efficiency by excess sample cooling. The system was operated in two configurations:
   a.   Bypass: the oxidation furnace bypassed, and
   b.   Non-bypass: the oxidation furnace in its normal mode of operation.
This allowed the measurement of non-catalyzed and catalyzed exhaust gases for varying oxygen flow rates. The resulting unburned hydrocarbon concentrations [HC] were used to calculate catalyst efficiencies (η_{cat}):

---

[87]Initial Sample Response Time is defined as the length of time from when sample gas flow is initiated until the first drop of condensate enters the sampling flask.

[88]This also indicates that without the grease, the system develops air leaks that are severe enough to cause noticeable inaccuracies in the system measurements.

$$\eta_{cat} = 1 - \frac{[HC]_{non\text{-}bypass}}{[HC]_{by\text{-}pass}} \qquad\qquad (D.3)$$

The results are shown in Figure D-1. Based on these results, the **ratio** of the oxygen volume flow rate to the sample volume flow rate is optimized at 0.074.[89]
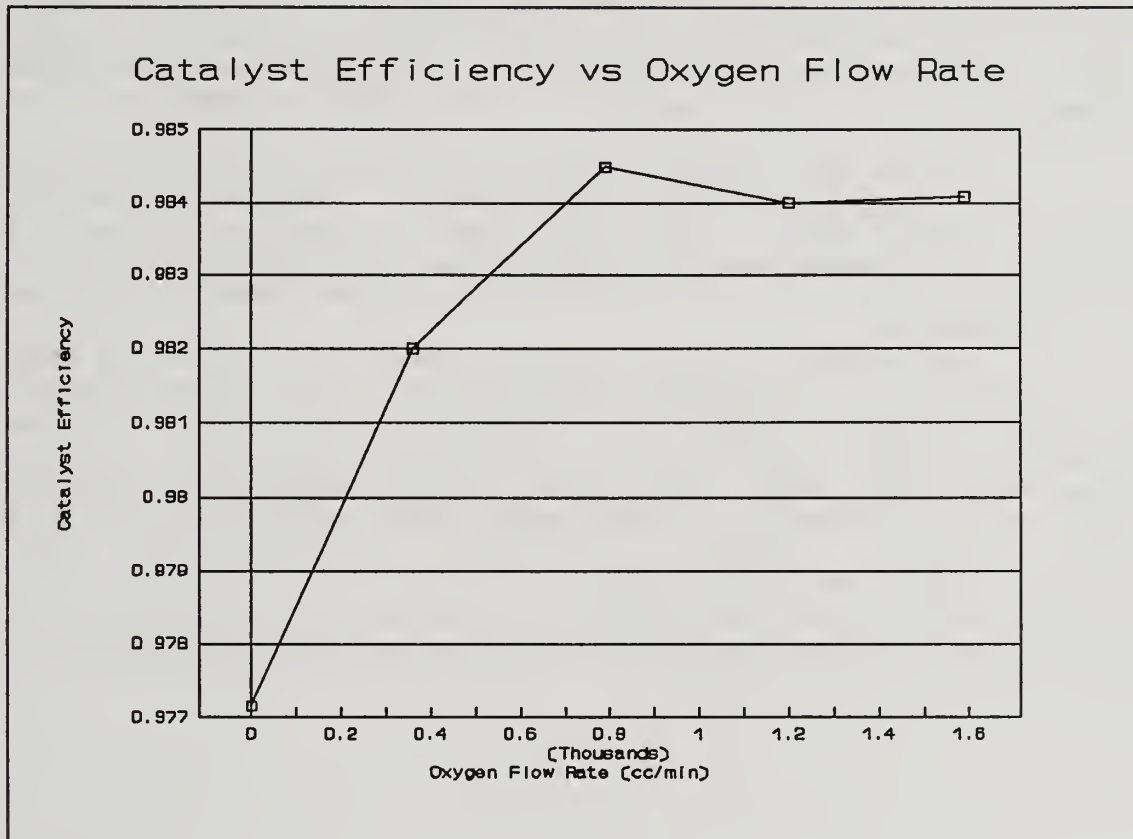
Figure 5-1:   Supplemental   Oxygen   Effect   on   Catalyst Efficiency.

D.4   System Summary and Future Modifications

The Radiotracer Oil Consumption System developed for this project has the following performance characteristics:

---

[89]In current configuration of the WCS, a stainless steel ball reading on the 602 flow tube will give this ratio; it should be checked frequently for approximately the first half hour of operation as the components in the oxygen flow path tend to cool and change the flow from the desired value.

Table D-3: ROCS Performance Summary		
Criteria	Goal	Actual
Sample Period (min)	9.4	7.7
Error (%)	15	5.4

As currently configured the system employs a single furnace, single condenser design. The line heaters are limited to 482° Celsius and are controlled manually. If future work requires increased system performance, the following recommendations are made.

    a. System response and sample rates might be improved by using two <u>parallel</u> coiled condensers. The two-condenser designs evaluated by this study were placed in series; a parallel arrangement would preserve the time response provided by single condensers, but provide the higher sample rate of dual condensers.

    b. The system currently takes about 30 minutes to heat up to operating line heater temperatures. The line heaters can only bring the sample gas to 250° Celsius, requiring an additional 250 degrees of heating internal to the furnace/catalyst bed. The use of higher temperature heating tapes and thermostatic line heater control would allow a faster thermal response in heatup situations and more efficient catalyst operation.

    c. Future construction of a similar ROCS should also shorten the internal connecting piping as much as possible to obviate some of the heaters.

This Page Intentionally Blank

Appendix E: Oil Consumption Spreadsheets

This appendix contains the data reduction spreadsheets for Test Matrices C and AZ. All the data from the data log sheets has been transcribed into this appendix. For the actual cell contents the original spreadsheets may be addressed on the thesis disk under the titles: OILCALC.wk1 and AZOC.wk1. These spreadsheets also contain the pertinent oil specific activity calculations.

Enclosure 1: Data Reduction Spreadsheet for Test Matrix C.

Enclosure 2: Data Reduction Spreadsheet for Test Matrix AZ.

Sample #:	1	2	4	6	7	8	9
Date:	9E+05	9E+05	9E+05	9E+05	9E+05	9E+05	9E+05

LOG DATA

Ambient Temp (deg. C):	23	23	21.5	19.5	19.5	19.5	19.5
Ambient Pressure (torr):	769.3	768.8	762.7	767	767	767	767
Relative Humidity (%):	60	60	61	60	60	60	60
Engine Speed (RPM):	2033	2027	2065	2004	2004	2016	2016
Throttle (indicated):	12.1	12.1	11.8	11.3	11.3	15.6	15.6
Load Cell (#):	22.2	22.5	21.8	20	20	29.8	29.8
Liner Temperature:	114	113	117	111	111	115	115
Oil Sump Temperature:	90	90	89	86	86	89	89
Air Inlet Temperature:	36	37	30	33	33	32	32
Line Temperature:	411	417	426	439	439	445	445
xh. Gas Into Furnace Temp:	208	244	242	244	244	249	249
Furnace Temperature:	645	653	604	631	631	619	619
Condenser Inlet Temp:	154	163	146	145	145	145	145
Variac Setting:	80	80	83	83	83	83	83
Initial Fuel Wt. (lb):	62.7	62.7	49	81.3	81.3	77.8	77.8
Final Fuel Wt. (lb):	61.5	61.5	47.7	80.45	80.45	76.6	76.6
Time Duration (min):	6.75	6.75	6.67	5.75	5.75	5.5	5.5
Sample Volume (ml):							
Sample Start Time:							
Sample Isolation Time:							
Duration Time:							
Median Sample Times:							

SPECIFIC HUMIDITY SECTION

Corrected Atm.Press.(torr)	767.3	766.8	760.7	765	765	765	765
Part.Press.H2O @100%Humid.	20.16	20.16	18.78	16.94	16.94	16.94	16.94
Specific Humidity (g H2O/g	0.01	0.01	0.01	0.008	0.008	0.008	0.008

STOICHIOMETRIC RATIO SECTION

Ko:	1.225	1.225	1.225	1.225	1.225	1.225	1.225
Kf:	1.219	1.219	1.219	1.219	1.219	1.219	1.219
Kaf:	4.659	4.659	4.659	4.659	4.659	4.659	4.659

FLOW RATE SECTION

H/C ratio, oil:	1.89	1.89	1.89	1.89	1.89	1.89	1.89
H/C ratio, fuel:	1.88	1.88	1.88	1.88	1.88	1.88	1.88
Equivalence Ratio:	1	1	1	1	1	1	1
Fuel Rate (g/sec):	1.344	1.344	1.473	1.118	1.118	1.649	1.649
Air Mass Flow Rate (g/sec)	6.262	6.262	6.865	5.207	5.207	7.685	7.685

ACTIVITY SECTION

Local Sample #:	1	2	4	6	7	8	9
RPO Sample #:	1	2	4	6	7	8	9
Date Analyzed:	8 Feb	8 Feb	8 Feb	8 Feb	8 Feb	8 Feb	8 Feb
Sample Activity(dpm):	38132	36593	22429	22301	24312	13096	14162
Sample Volume (ml):	1	1	1	1	1	1	1
Density of Water (g/ml):	0.999	0.999	0.999	0.999	0.999	0.999	0.999
SAw (dpm/g):	38170	36630	22451	22323	24336	13109	14176
SAo (dpm/ml)	7E+06	7E+06	7E+06	7E+06	7E+06	7E+06	7E+06
Oil Density (g/ml):	0.888	0.888	0.888	0.888	0.888	0.888	0.888
SAo (dpm/g):	8E+06	8E+06	8E+06	8E+06	8E+06	8E+06	8E+06

OIL CONSUMPTION SECTION

Rate of O/C (g/sec):	0.008	0.008	0.005	0.004	0.004	0.003	0.004
Rate of O/C (mg/sec)	7.899	7.579	5.073	3.81	4.154	3.297	3.566

Sample #:	10	11	12	13	14	15	16
Date:	9E+05	9E+05	9E+05	9E+05	9E+05	9E+05	9E+05

LOG DATA

Ambient Temp (deg. C):	19.5	18.5	18.5	18.5	18.5	18.5	18.5
Ambient Pressure (torr):	767	773	773	773	773	773	773
Relative Humidity (%):	60	58	58	58	58	58	58
Engine Speed (RPM):	2008	2006	2011	2506	2506	2518	2518
Throttle (indicated):	23.4	19.1	19.1	11.1	11.1	15.8	15.8
Load Cell (#):	44.3	45.5	45.5	19.7	19.7	30	30.1
Liner Temperature:	121	120	118	109	109	114	115
Oil Sump Temperature:	90	90	92	92	92	96	95
Air Inlet Temperature:	36	33	32	35	35	36	35
Line Temperature:	455	472	459	455	455	450	458
xh. Gas Into Furnace Temp:	255	249	245	250	250	250	252
Furnace Temperature:	633	531	548	577	577	608	617
Condenser Inlet Temp:	150	89	110	123	123	126	127
Variac Setting:	83	83	83	83	83	83	83
Initial Fuel Wt. (lb):	70.3	65	65	55.16	55.16	49	49
Final Fuel Wt. (lb):	68.1	58.5	58.5	53.56	53.56	47	47
Time Duration (min):	6	16.95	16.95	8.05	8.05	7.5	7.5
Sample Volume (ml):							
Sample Start Time:							
Sample Isolation Time:							
Duration Time:							
Median Sample Times:							

SPECIFIC HUMIDITY SECTION

Corrected Atm.Press.(torr)	765	771	771	771	771	771	771
Part.Press.H2O @100%Humid.	16.94	16.02	16.02	16.02	16.02	16.02	16.02
Specific Humidity (g H2O/g	0.008	0.008	0.008	0.008	0.008	0.008	0.008

STOICHIOMETRIC RATIO SECTI

Ko:	1.225	1.225	1.225	1.225	1.225	1.225	1.225
Kf:	1.219	1.219	1.219	1.219	1.219	1.219	1.219
Kaf:	4.659	4.659	4.659	4.659	4.659	4.659	4.659

FLOW RATE SECTION

H/C ratio, oil:	1.89	1.89	1.89	1.89	1.89	1.89	1.89
H/C ratio, fuel:	1.88	1.88	1.88	1.88	1.88	1.88	1.88
Equivalence Ratio:	1	1	1	1	1	1	1
Fuel Rate (g/sec):	2.772	2.899	2.899	1.5	1.5	2.016	2.016
Air Mass Flow Rate (g/sec)	12.92	13.51	13.51	6.99	6.99	9.393	9.393

ACTIVITY SECTION

Local Sample #:	10	11	12	13	14	15	16
RPO Sample #:	10	11	12	13	14	15	16
Date Analyzed:	8 Feb	8 Feb	8 Feb	8 Feb	8 Feb	8 Feb	8 Feb
Sample Activity(dpm):	9417	3137	7436	15598	15886	12640	12448
Sample Volume (ml):	1	1	1	1	1	1	1
Density of Water (g/ml):	0.999	0.999	0.999	0.999	0.999	0.999	0.999
SAw (dpm/g):	9427	3140	7444	15613	15902	12653	12461
SAo (dpm/ml)	7E+06	7E+06	7E+06	7E+06	7E+06	7E+06	7E+06
Oil Density (g/ml):	0.888	0.888	0.888	0.888	0.888	0.888	0.888
SAo (dpm/g):	8E+06	8E+06	8E+06	8E+06	8E+06	8E+06	8E+06

OIL CONSUMPTION SECTION

Rate of O/C (g/sec):	0.004	0.001	0.003	0.004	0.004	0.004	0.004
Rate of O/C (mg/sec)	3.983	1.382	3.278	3.563	3.629	3.878	3.819

Encl. 1

```
Sample #:                          17
Date:                          9E+05

LOG DATA
    Ambient Temp (deg. C):     18.5
  Ambient Pressure (torr):      773
    Relative Humidity (%):       58

       Engine Speed (RPM):     3679
      Throttle (indicated):    12.6
           Load Cell (#):      20.2
        Liner Temperature:
     Oil Sump Temperature:
     Air Inlet Temperature:

          Line Temperature:     465
xh. Gas Into Furnace Temp:      258
       Furnace Temperature:     628
      Condenser Inlet Temp:     127
            Variac Setting:      83

      Initial Fuel Wt. (lb):  37.81
        Final Fuel Wt. (lb):
        Time Duration (min):       1
        Sample Volume (ml):
          Sample Start Time:
     Sample Isolation Time:
              Duration Time:
       Median Sample Times:




SPECIFIC HUMIDITY SECTION
Corrected Atm.Press.(torr)     771
Part.Press.H2O @100%Humid.   16.02
Specific Humidity (g H2O/g   0.008

STOICHIOMETRIC RATIO SECTI
Ko:                          1.225
Kf:                          1.219
Kaf:                         4.659

FLOW RATE SECTION
H/C ratio, oil:               1.89
H/C ratio, fuel:              1.88
Equivalence Ratio:               1
Fuel Rate (g/sec):            2.22
Air Mass Flow Rate (g/sec)   10.34

ACTIVITY SECTION
Local Sample #:                 17
RPO Sample #:                   17
Date Analyzed:               8 Feb
Sample Activity(dpm):        12448
Sample Volume (ml):              1
Density of Water (g/ml):     0.999
SAw (dpm/g):                 12461
SAo (dpm/ml):                 7E+06
Oil Density (g/ml):          0.888
SAo (dpm/g):                  8E+06

OIL CONSUMPTION SECTION
Rate of O/C (g/sec):         0.004
Rate of O/C (mg/sec)         4.205
```

Sample #:	40	41	42	43
Date:	940315	940315	940315	940315
Series:	AZ1	AZ1	AZ1	AZ1

LOG DATA

	40	41	42	43
Ambient Temp (deg. C):	20.5	20.5	20.5	20.5
Ambient Pressure (torr):	752	752	752	752
Relative Humidity (%):	70	70	70	70
Engine Speed (RPM):	2029	2035	2042	2040
Throttle (indicated):	13.9	14	14	14
Load Cell (#):	21	21.4	21.2	21.2
Liner Temperature:	114	114	114	114
Oil Sump Temperature:	87	91	89	90
Air Inlet Temperature:	31	33	35	34
Initial Fuel Wt. (lb):	61.125	61.125	61.125	61.125
Final Fuel Wt. (lb):	58.5313	58.5313	58.5313	58.5313
Time Duration (min):	13.75	13.75	13.75	13.75
Engine Start Time:	5	5	5	5
Sample Start Time:	18	28	37	48.5
Sample Isolation Time:	28	37	48.5	60.5
Duration Time:	10	9	11.5	12
Sample Times (ref eng start time):	18	27.5	37.75	49.5

SPECIFIC HUMIDITY SECTION

	40	41	42	43
Corrected Atm.Press.(torr):	750	750	750	750
Part.Press.H2O @100%Humid.:	17.86	17.86	17.86	17.86
Specific Humidity (g H2O/g Air):	0.01067	0.01067	0.01067	0.01067

STOICHIOMETRIC RATIO SECTION

	40	41	42	43
Ko:	1.22462	1.22462	1.22462	1.22462
Kf:	1.21902	1.21902	1.21902	1.21902
Kaf:	4.65937	4.65937	4.65937	4.65937

FLOW RATE SECTION

	40	41	42	43
H/C ratio, oil:	1.89	1.89	1.89	1.89
H/C ratio, fuel:	1.88	1.88	1.88	1.88
Equivalence Ratio:	1	1	1	1
Fuel Rate (g/sec):	1.42609	1.42609	1.42609	1.42609
Air Mass Flow Rate (g/sec):	6.64468	6.64468	6.64468	6.64468

ACTIVITY SECTION

	40	41	42	43
Date Analyzed:	940316	940316	940316	940316
Sample Activity(dpm):	3615	3440	3266	3284
Sample Weight (g):	0.9810	0.9819	0.9445	0.9666
SAw (dpm/g):	3685.02	3503.41	3457.91	3397.48
SAo (dpm/g):	8554748	8554748	8554748	8554748

OIL CONSUMPTION SECTION

	40	41	42	43
Rate of O/C (g/sec):	0.00078	0.00074	0.00073	0.00072
Rate of O/C (mg/sec)	0.7798	0.74135	0.73172	0.71892

Sample #:	44	45	46	47
Date:	940315	940315	940315	940315
Series:	AZ1	AZ1	AZ1	AZ1

LOG DATA

	44	45	46	47
Ambient Temp (deg. C):	20.5	20.5	20.5	20.5
Ambient Pressure (torr):	752	752	752	752
Relative Humidity (%):	70	70	70	70
Engine Speed (RPM):	2504	2502	2497	2925
Throttle (indicated):	14	14	14	14
Load Cell (#):	21.4	21.4	21.4	21.4
Liner Temperature:	114	112.5	113	114
Oil Sump Temperature:	93	93	91	94
Air Inlet Temperature:	36	35	36	37
Initial Fuel Wt. (lb):	50	50	50	43.8125
Final Fuel Wt. (lb):	47.1875	47.1875	47.1875	39.75
Time Duration (min):	12.4333	12.4333	12.4333	15.7667
Engine Start Time:	5	5	5	5
Sample Start Time:	67.9	77	86.5	105.8
Sample Isolation Time:	77	86.5	97	113.1
Duration Time:	9.1	9.5	10.5	7.3
Sample Times (ref eng start time):	67.45	76.75	86.75	104.45

SPECIFIC HUMIDITY SECTION

	44	45	46	47
Corrected Atm.Press.(torr):	750	750	750	750
Part.Press.H20 @100%Humid.:	17.86	17.86	17.86	17.86
Specific Humidity (g H2O/g Air):	0.01067	0.01067	0.01067	0.01067

STOICHIOMETRIC RATIO SECTION

	44	45	46	47
Ko:	1.22462	1.22462	1.22462	1.22462
Kf:	1.21902	1.21902	1.21902	1.21902
Kaf:	4.65937	4.65937	4.65937	4.65937

FLOW RATE SECTION

	44	45	46	47
H/C ratio, oil:	1.89	1.89	1.89	1.89
H/C ratio, fuel:	1.88	1.88	1.88	1.88
Equivalence Ratio:	1	1	1	1
Fuel Rate (g/sec):	1.71012	1.71012	1.71012	1.94794
Air Mass Flow Rate (g/sec):	7.96808	7.96808	7.96808	9.07616

ACTIVITY SECTION

	44	45	46	47
Date Analyzed:	940316	940316	940316	940316
Sample Activity(dpm):	6705	9624	9682	6526
Sample Weight (g):	0.7757	0.9734	0.9626	0.9707
SAw (dpm/g):	8643.81	9886.99	10058.2	6722.98
SAo (dpm/g):	8554748	8554748	8554748	8554748

OIL CONSUMPTION SECTION

	44	45	46	47
Rate of O/C (g/sec):	0.0022	0.00251	0.00255	0.00194
Rate of O/C (mg/sec)	2.19501	2.51116	2.5547	1.94412

```
Sample #:                                48        49        50        51
Date:                                940315    940315    940318    940318
Series:                                 AZ1       AZ1       AZ2       AZ2
LOG DATA
                 Ambient Temp (deg. C):      20.5      20.5        20        20
              Ambient Pressure (torr):       752       752     750.9     750.9
                Relative Humidity (%):        70        70      63.5      63.5

                    Engine Speed (RPM):      2913      2907      2053      2037
                 Throttle (indicated):     14.05     14.07      13.4      13.4
                       Load Cell (#):       21.4      21.8      21.4      21.8
                   Liner Temperature:        114       113       115       115
               Oil Sump Temperature:          93        93        89        86
               Air Inlet Temperature:         36        36        31        34

              Initial Fuel Wt. (lb):     43.8125   43.8125    91.125    91.125
                Final Fuel Wt. (lb):       39.75     39.75   88.2188   88.2188
              Time Duration (min):       15.7667   15.7667   15.7333   15.7333

                    Engine Start Time:          5         5        38        38
                  Sample Start Time:        113.1     123.8        52      62.5
               Sample Isolation Time:       123.8       131      62.5        75
                        Duration Time:       10.7       7.2      10.5      12.5
Sample Times (ref eng start time):       113.45     122.4     19.25     30.75
```

SPECIFIC HUMIDITY SECTION
```
Corrected Atm.Press.(torr):                750       750     748.9     748.9
Part.Press.H2O @100%Humid.:              17.86     17.86      17.4      17.4
Specific Humidity (g H2O/g Air):       0.01067   0.01067   0.00944   0.00944
```

STOICHIOMETRIC RATIO SECTION
```
Ko:                                    1.22462   1.22462   1.22462   1.22462
Kf:                                    1.21902   1.21902   1.21902   1.21902
Kaf:                                   4.65937   4.65937   4.65937   4.65937
```

FLOW RATE SECTION
```
H/C ratio, oil:                           1.89      1.89      1.89      1.89
H/C ratio, fuel:                          1.88      1.88      1.88      1.88
Equivalence Ratio:                           1         1         1         1
Fuel Rate (g/sec):                     1.94794   1.94794   1.39648   1.39648
Air Mass Flow Rate (g/sec):            9.07616   9.07616    6.5067    6.5067
```

ACTIVITY SECTION
```
Date Analyzed:                        940316    940316    940318    940318
Sample Activity(dpm):                   5136      5249   2865.57      2127
Sample Weight (g):                    0.9493    0.9670    0.9756    0.8558
SAw (dpm/g):                          5410.3   5428.13   2937.24   2485.39
SAo (dpm/g):                         8554748   8554748   8554748   8554748
```

OIL CONSUMPTION SECTION
```
Rate of O/C (g/sec):                  0.00156   0.00157   0.00061   0.00051
Rate of O/C (mg/sec)                  1.56423   1.56939   0.60583    0.5126
```

Encl. 2

```
Sample #:                            52        53        54
Date:                            940318    940318    940318
Series:                             AZ2       AZ2       AZ2
LOG DATA
           Ambient Temp (deg. C):      20        20        20
        Ambient Pressure (torr):    750.9     750.9     750.9
         Relative Humidity (%):      63.5      63.5      63.5

             Engine Speed (RPM):     2026      2034      2497
           Throttle (indicated):     13.4      13.4     13.55
                Load Cell (#):        21.8      21.6      21.4
             Liner Temperature:       114       114       116
           Oil Sump Temperature:       85        89        92
           Air Inlet Temperature:      34        34        36

           Initial Fuel Wt. (lb):   91.125    91.125   83.5938
            Final Fuel Wt. (lb):    88.2188   88.2188  80.2188
            Time Duration (min):    15.7333   15.7333  15.8333

              Engine Start Time:       38        38        38
              Sample Start Time:       75        85      98.5
          Sample Isolation Time:       85      93.5     106.5
                 Duration Time:        10       8.5         8
 Sample Times (ref eng start time):     42     51.25      64.5




SPECIFIC HUMIDITY SECTION
Corrected Atm.Press.(torr):         748.9     748.9     748.9
Part.Press.H2O @100%Humid.:          17.4      17.4      17.4
Specific Humidity (g H2O/g Air):   0.00944   0.00944   0.00944

STOICHIOMETRIC RATIO SECTION
Ko:                               1.22462   1.22462   1.22462
Kf:                               1.21902   1.21902   1.21902
Kaf:                              4.65937   4.65937   4.65937

FLOW RATE SECTION
H/C ratio, oil:                      1.89      1.89      1.89
H/C ratio, fuel:                     1.88      1.88      1.88
Equivalence Ratio:                      1         1         1
Fuel Rate (g/sec):                1.39648   1.39648   1.61147
Air Mass Flow Rate (g/sec):        6.5067    6.5067   7.50845


ACTIVITY SECTION
Date Analyzed:                     940318    940318    940318
Sample Activity(dpm):                2364      2361      2818
Sample Weight (g):                 0.9682    0.9650    0.9629
SAw (dpm/g):                      2441.64   2446.63   2926.58
SAo (dpm/g):                      8554748   8554748   8554748

OIL CONSUMPTION SECTION
Rate of O/C (g/sec):               0.0005    0.0005    0.0007
Rate of O/C (mg/sec)               0.50358   0.50461   0.69657
```

185

This Page Intentionally Blank

This Page Intentionally Blank

Appendix F: Basic Routines

This appendix contains the BASIC routines used in this project. These routines can be run on BASIC interpreter. The routines are stored on the thesis disk (in the care of the thesis advisor) in the directory titled "BASIC".

Enclosure 1:   LIF.bas

Enclosure 2:   PRESPEAK.bas

Enclosure 3:   PRESSURE.bas

Enclosure 4:   PROMATCH.bas

This routine provides a calibrated LIF trace for the measurement of
film thicknesses. It requires the calibration constant be derived
manually using the traces derived by PROMATCH.

```
10 OPEN "i",1,"b:az42000b.out"
20 OPEN "o",2,"b:az42000b.lif"
30 LET K=0
40 LET N=0
44 '
45 'Set crank shaft radius
50 LET A=46
54 '
55 'set rough calibration constant for film thickness.
60 LET LS=1
64 '
65 'set conrod length (mm)
70 LET L=152.4
80 INPUT#1,D
90 LET N=N+1
100 IF N=1 THEN GOTO 80
105 IF N=3 THEN GOTO 40
110 LET DEGREE=K*360/2000
120 LET THETA=DEGREE*.017453
130 LET Z=A*COS(THETA)+(L^2-A^2*SIN(THETA)^2)^.5-196.5+38.1
140 LET V=D*.002441
150 LET FILM=V*LS
160 PRINT#2,DEGREE,Z,FILM
170 LET K=K+1
180 IF K<4000 GOTO 80
190 CLEAR
200 END
```

This routine calculates the cyclic peak pressures and the crank angle at which they occur. The routine assumes that the pressures are contained in a file with two columns in which the pressures are the first column.

```
10 OPEN "i", 1, "b:az42000b.dat"
11 LET R=0:LET K=0:LET L=0:LET P2=0:LET P1=0
12 LINE INPUT#1, A$
14 LET R=R+1
15 IF R<44 THEN GOTO 12
20 OPEN "o", 2, "b:az42000b.ppk"
24 CLS
25 INPUT; "Enter pressure test interval:     ", PINTERVAL
26 CLS
30 INPUT; "Enter rise slope trigger:      ", ST
31 CLS
32 INPUT; "Enter peak slope threshold:    ",PS
33 CLS
34 PRINT "Deg ATC","Pressure"
35 LET M=0
40 LET N=0
50 REM
59 IF L=2000 THEN LET L=0
60 INPUT#1,I
70 LET N=N+1
80 IF N=2 THEN GOTO 40
90 'IF N=3 THEN GOTO 40
95 K=K+1
96 L=L+1
100 LET M=M+1
110 IF M< PINTERVAL THEN GOTO 60
115 LET M=0
120 LET P1=P2:LET P2=I
130 LET DIFF=P2-P1
140 IF Q=1 THEN GOTO 160
145 IF DIFF>ST THEN LET Q=1
150 GOTO 60
160 IF DIFF>PS OR P2<580 THEN GOTO 60
170 LET DEGREE=L*360/2000
180 PRINT#2,DEGREE,P2
190 PRINT DEGREE,P2
200 LET Q=0
210 IF K<36000! THEN GOTO 60
220 CLEAR
230 END
```

```
5 REM "This program uses the cycle-averaged DAS output file as an
input.  It reads the data and uses a counter to determine which
data points are pressure data, and then writes the data to a
pressure output file with the corresponding     crank angle."
10 OPEN "i",1,"b:AZ42000B.OUT"
20 OPEN "o",2,"b:AZ42000B.P"
30 LET K=0:LET D=0
40 N=0
50 REM
60 INPUT#1,I
70 N=N+1
80 IF N=2 THEN GOTO 60
90 IF N=3 THEN GOTO 40
100 LET DEGREE=K*360/2000
110 LET DIFF=D-DEGREE
120 IF ABS(DIFF)>.1 THEN GOTO 150
130 D=D+2
140 PRINT#2,D,I
150 K=K+1
160 IF K<4000 THEN GOTO 60
170 IF D<358 THEN PRINT "Less than full cycle data!!!!"ELSE
PRINT"pressure file complete."
180 CLEAR
190 END
```

This routine prepares matched surface files for calibration purposes. The surfaces can then be manipulated in a spreadsheet program.

```
10 REM open input & output files
20 INPUT; "Enter name of LIF data file path:   ",LIF$
30 CLS
40  INPUT;"Enter name of surface profile data file path:   ",
PROFDAT$
50 CLS
60 INPUT; "Enter name of matched profile ouput path:   ",MATCHFILE$
70 CLS
80 OPEN"i",1,LIF$
90 OPEN "i",2,PROFDAT$
100 OPEN"o",3,MATCHFILE$
110 REM initialize constants
120 LET Z1=26.797: LET SWITCH=0
130 REM
140 REM
150 REM
160 REM initialize data identifiers:  m=profile, n=lif
170 LET M=0
180 LET N=0
190 REM routine to find first z.
200 INPUT#1, LIF
210 LET N=N+1
220 IF N=1 THEN GOTO 200
230 IF N=3 AND SWITCH=0 THEN GOTO 180
240 IF N=3 GOTO 262
250 IF LIF<Z1 THEN GOTO 259
255 GOTO 200
259 LET LIFZ=LIF
260 LET SWITCH = 1
261 GOTO 200
262 N=0
263 GOTO 280
270 REM routine to build a matched profile file.  Initial z point
is stored in Lifz, n=0, lif contains a voltage.
280 INPUT #2, PROF
290 LET M=M+1
300 IF M=2 THEN GOTO 360
304 REM convert prof from cm to mm.
305 PROF=PROF*10
308 PRINT PROF,M
310 IF PROF<LIFZ THEN GOTO 400
320 PRINT#3, LIFZ, PROF1
325 PRINT LIFZ,PROF1
330 IF EOF(2) THEN GOTO 370
340 GOSUB 500
350 GOTO 280
360 LET PROF1=PROF
365 GOTO 280
```

```
370 CLEAR
380 PRINT"end of profile data"
390 END
400 M=0
405 GOTO 280
500 INPUT#1, LIF
510 LET N=N+1
520 IF N=1 THEN GOTO 500
530 IF N=3 THEN GOTO 560
540 LET LIFZ=LIF
545 GOTO 500
550 PRINT"subroutine is not working"
560 N=0
570 RETURN
```

This Page Intentionally Blank

Appendix G: Photographs of Piston Deposit Patterns

This appendix presents photographs of the pistons removed from the number four cylinder after operation. The principal feature depicted is the deposit pattern on the side of the piston above the gap pin (designated by a small black dot on the second land).

Enclosure 1:   AZ Test Pistons; Comparative View

Enclosure 2:   AZ1 Close-up

Enclosure 3:   AZ2 Close-up

Enclosure 4:   AZ3 Close-up

Enclosure 5:   AZ4 Close-up

Figure G-1

Figure G-1
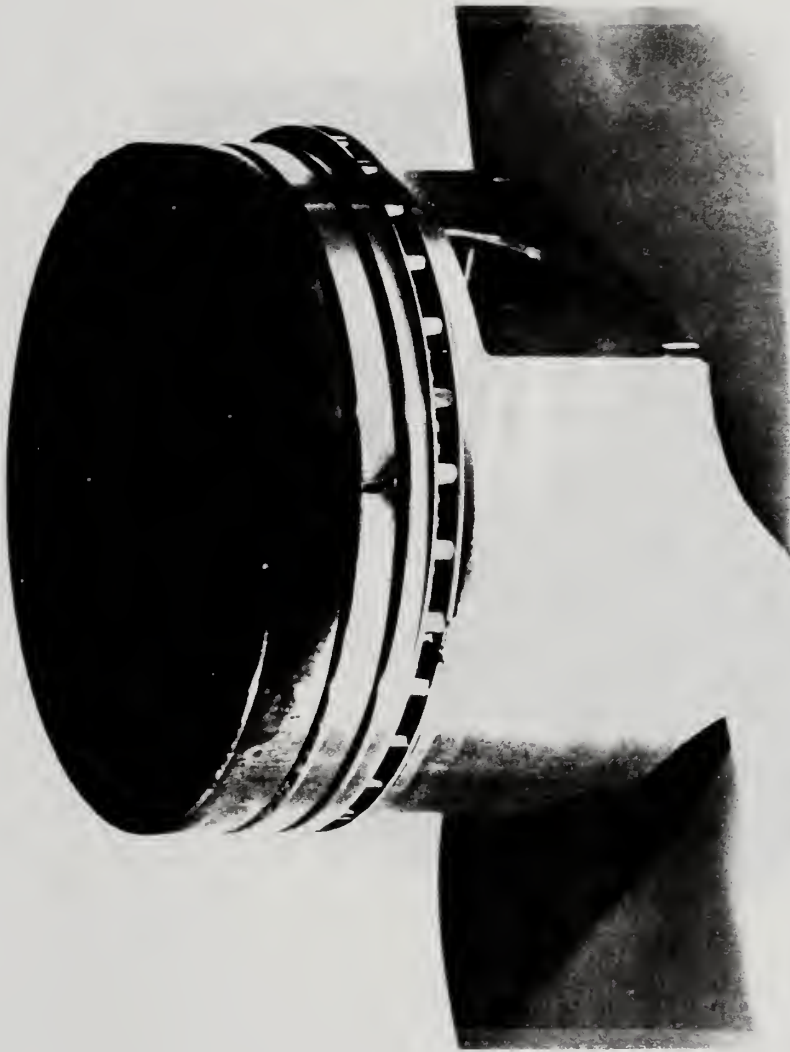
Figure G-2

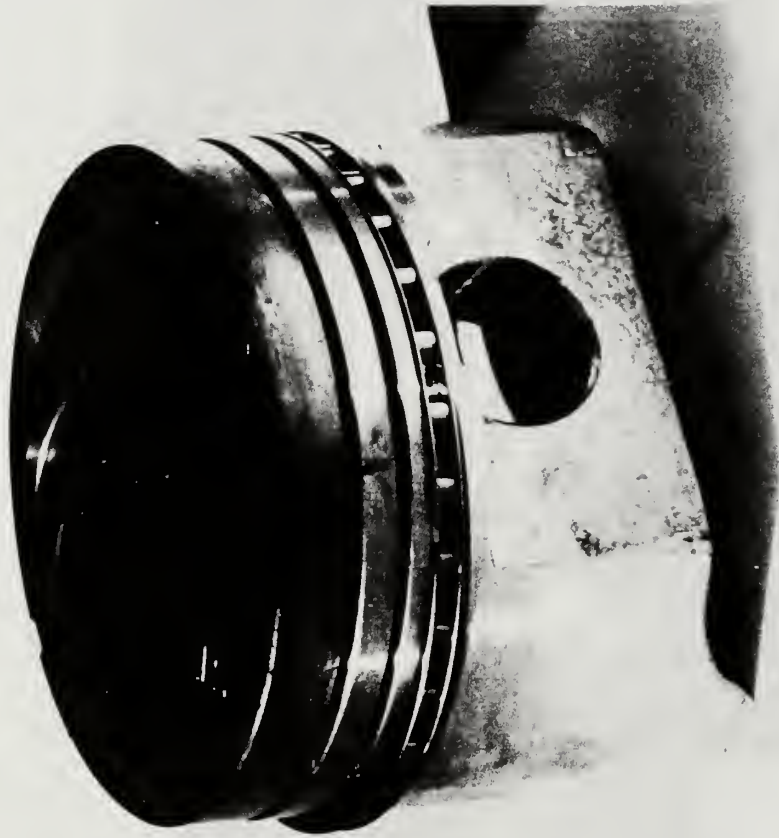Figure G-3

198

AZ3

Figure G-4

AZ4

Figure G-5

GAYLORD S